Cell Fusion Studied in Yeast Mating

by

Maxwell G. Heiman

DISSERTATION

Submitted in partial satisfaction of the requirements for the degree of

DOCTOR OF PHILOSOPHY

in

Biochemistry & Molecular Biology

in the

GRADUATE DIVISIONS

of the

UNIVERSITY OF CALIFORNIA SAN FRANCISCO

and

UNIVERSITY OF CALIFORNIA BERKELEY

Date University Librarian

Degree Conferred: .....

For Mimi

ACKNOWLEDGMENTS

I thank Peter Walter, my adviser and colleague, for his support in developing this project from first-principle notions and for providing me so many opportunities to learn and to learn from. I also thank Peter for his friendship, especially that friendship that persisted as our ambitions diverged, that shows itself in the fun I find in talking to him.

I thank Ira Herskowitz, my thesis committee member and fellow mentor, for inspiring me. In his intelligence, clear thinking, appreciation of biology and biological diversity, joy of teaching, love of learning, position of respect and authority in the community, approachability and ability to communicate, and as a blues guitar player, Ira has served as a model of what I would hope to achieve.

I thank Cynthia Kenyon, my fellow thesis committee member, for listening carefully and thoughtfully and providing a balanced outside view to my work. I asked Cynthia to join my committee because I enjoy talking to her and because I know she is skilled at identifying the most important questions before her. I have; she did.

I thank Andrew Murray, Reg Kelly, and Rob Edwards, the members of my orals committee in addition to Ira, for the exam itself, in which the basic strategy that led to identification of *PRM1* was first discussed in detail. I also thank Andrew for his continued discussions on a wealth of topics, including my career plans.

I thank John Sedat and Thea Tlsty, my rotation mentors in addition to Peter, for making my first year at UCSF so enjoyable and stimulating. I wish I could have worked jointly in all the labs in which I rotated, and I am grateful to have learned so much from

them in the short time we worked together. I also thank Thea for her comments on my manuscript and her continued support.

I thank my colleagues in the Walter lab, in particular Gustavo Pesce, an outstanding teacher and friend; Pablo Aguilar, who has elevated cell fusion from my personal eccentricity to a legitimate lab project and whose carefulness and thoughtfulness will benefit that project as much as they have benefited me personally; Alex Engel, whose work continuing the project and promoting it among newcomers gives me great hope that it will grow and succeed; Chris Patil, my rotation mentor; Silke Nock, my baymate and source of great personal support; Tomas Aragon, my other baymate and co-founding member of the Max and Tomas Electric Bluegrass Jamboree; Sebastian Bernales, my most recent baymate; Hannah Cohen, the first rotation student to work with me; Muluye Liku, the second rotation student to work with me; Claudia Rubio, the third rotation student to work on cell fusion; Maria Victoria Dinglasan, whose cheer and diligence have helped sustain me when I was grouchy and lazy; and Teresa Donovan, whose wisdom and resourcefulness I have tried not to overtax, and which thankfully are matched only by her caring and patience.

I thank my classmates and fellow students, in particular Ellie Heckscher, whose friendship I have relied on; Carrie Adler, who is fun; Zemer Gitai, like me but smarter; Jesse Gray, for introspection; Christelle Sabatier, for sympathy mixed with pragmatism; Kanade Shinkai, for guitar lessons and deep talk; Charlie Holst, with whom I can speak in shorthand; Jeff Ubersax, my roommate; and Sarah Green, my roommate. I also thank my post-doctoral adviser Shai Shaham who, together with Peter, was generous enough to

ease my transition from UCSF to Rockefeller and to allow me to finish my thesis before I completed it.

I thank my family, in particular my parents Sharon and Jim and my brother Jesse for their support. I thank the newest member of my family, my wife Myriam, whose love is the greatest reward I could hope ever to receive.

Chapter 2 is reproduced from The Journal of Cell Biology (2000) 151:719-730 by copyright permission of The Rockefeller University Press.

The Rockefeller
University Press
1114 First Avenue, 3rd Floor
New York, New York 10021
(212) 327-7938
Fax (212) 327-8587

February 26, 2003

Dr. Max Heiman

Dear Dr. Heiman:

We will grant you permission for the print reproduction of JCB-vol:151,719-730,2000-article as referred to in your letter dated February 24, 2003.

Permission is granted for one time use only. Please write to us each time for permission concerning future editions and translations, as we do not grant blanket permissions.

We request that you also obtain permission from the author(s) and give suitable acknowledgment to the source in the following manner: Reproduced from **The Journal of Cell Biology, year, vol., pp.** by copyright permission of The Rockefeller University Press.

Sincerely yours,

THE JOURNAL OF
CELL BIOLOGY

Lynette N. Henry
Permissions Coordinator

Cell fusion studied in yeast mating

Maxwell G. Heiman

ABSTRACT

Cell fusion occurs throughout development, from fertilization to organogenesis. The molecular mechanisms driving plasma membrane fusion in these processes remain unknown. While yeast mating offers an excellent model system in which to study cell fusion, all genes previously shown to regulate the process act at or before cell wall breakdown, i.e., well before the two plasma membranes have come in contact. Using a new strategy in which genomic data is used to predict which genes may possess a given function, we identified *PRM1*, a gene that is selectively expressed during mating and that encodes a multispanning transmembrane protein. Prm1p localizes to sites of cell-cell contact where fusion occurs. In matings between *Δprm1* mutants, a large fraction of cells initiate zygote formation and degrade the cell wall separating mating partners but then fail to fuse. Electron microscopic analysis reveals that the two plasma membranes in these mating pairs are tightly apposed, remaining separated only by a uniform gap of about 8 nm. Thus, *PRM1* is the first gene demonstrated to act at the step of plasma

membrane fusion during yeast mating. We used the *Δprm1* mutant as a sensitized background in which to identify other genes important for cell fusion. We isolated mutations in *KEX2* and *LEM3* that impair fusion on their own and display more severe phenotypes in a *Δprm1* background. Kex2p is a well-characterized Golgi-resident protease. It acts with Kex1p, a second protease, and a *Δkex1* mutant also displays a cell fusion defect. In *Δkex2* x WT matings, more than 80 percent of unfused mating pairs display extracellular membrane-bounded blebs at the site of cell-cell contact suggestive of a defect in membrane rearrangements during cell fusion. Lem3p is a transmembrane protein that co-localizes with Prm1p at the site of cell-cell contact. In *Δprm1 Δlem3* matings, fewer than 10 percent of mating pairs successfully fuse. These three genes thus provide the frst molecular handles on the process of cell-cell fusion during yeast mating.

TABLE OF CONTENTS

LIST OF TABLES

LIST OF FIGURES

CHAPTER 1

CHAPTER 2

CHAPTER 3

CHAPTER 4

CHAPTER 1

Introduction

BACKGROUND

Membrane fusion is the joining of two greasy bilayers across a saltwater sea. For it to succeed, the core fusion machinery must accomplish three feats (Fig. 1-1). First, it must squeeze out intervening water and overcome the repulsive surface charges of the membranes to bring the bilayers together at their outer faces. Second, it must allow the hydrophobic lipid interiors of the membranes to make contact, forming a hemifusion intermediate. Third, it must resolve this intermediate so that a new topology arises (Jahn and Grubmuller, 2002).

In principle, these three steps of membrane fusion can drive either the fusion or fission of compartments depending only on whether the fusing bilayers are continuous initially. However, it is controversial whether fusion and fission are really mechanistically comparable, chiefly because compartment fission offers the opportunity to form a ring around the region of the bilayers that will fuse whereas in compartment fusion that is topologically impossible. The formation of contractile actin rings in cytokinesis, dynamin-dependent rings in vesicle budding, and FtsZ-containing rings in bacterial division highlight this important difference (Margolin, 2003; Robinson and Spudich, 2000; Sever et al., 2000). In any case, here we will consider only bilayer fusion that serves to merge two previously distinct compartments.

The most detailed description of membrane fusion in this context comes from studies of vesicle and viral fusion (Hernandez et al., 1996). In the case of a vesicle fusing with a target organelle, a cytoplasmic complex assembles through coiled-coil interactions between a transmembrane SNARE protein on the vesicle and one on the target membrane (Weber et al., 1998). This coiled-coil complex lies parallel to the membrane surface, and

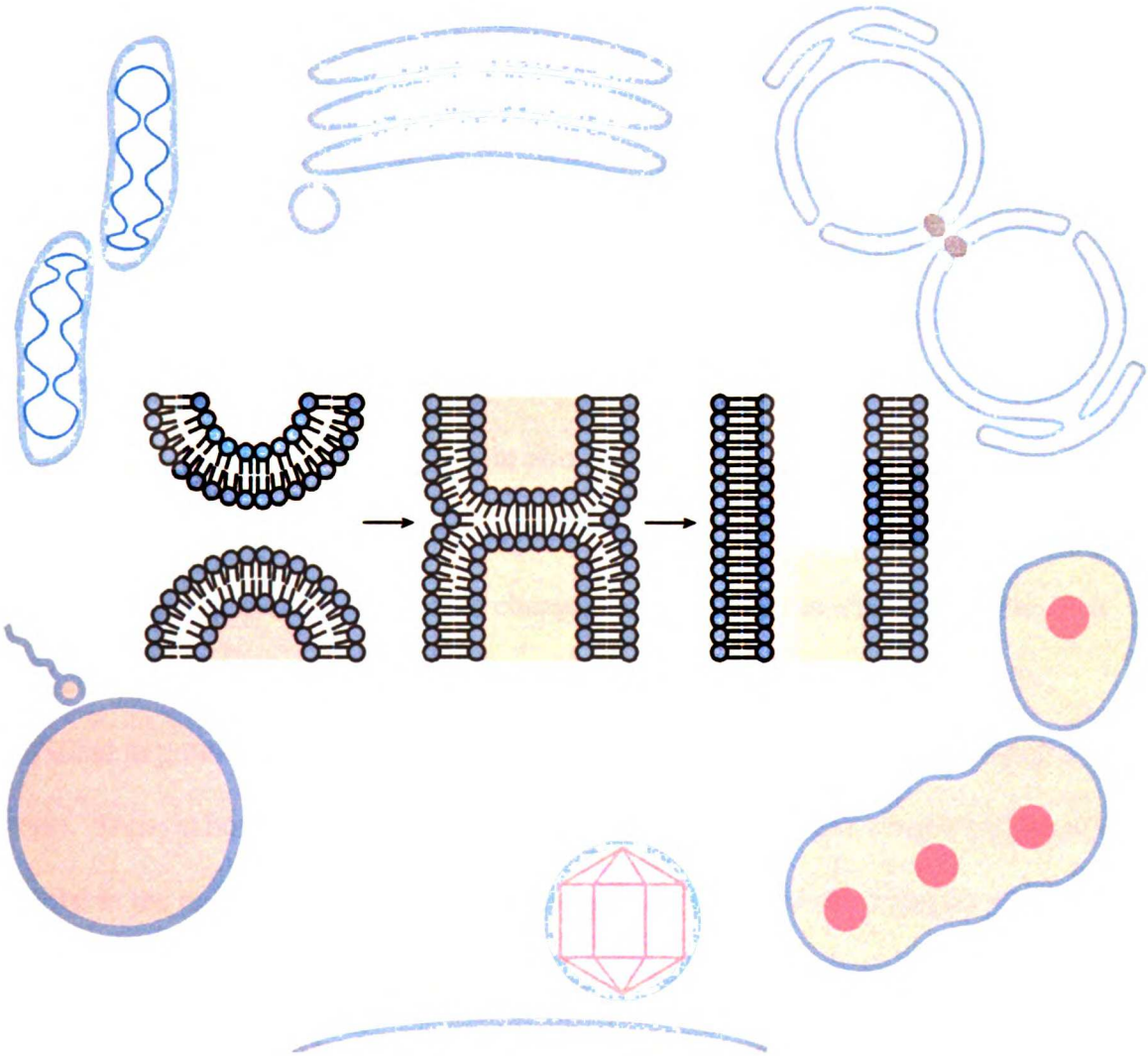

Figure 1-1

Six classes of membrane fusion

Three classes of intacellular fusion, top, and three classes of extracellular fusion, bottom, all must accomplish a common feat, the joining of lipid bilayers to merge previously distinct compartments, center. Clockwise from top left: mitochondrial fusion, vesicle-organelle fusion, nuclear fusion, syncytia formation, viral-cell fusion, and fertilization.

it is thought that the formation of the coiled coil winches the outer faces of the bilayers together to initiate the fusion reaction. By comparison, in viral fusion an extracellular complex assembles consisting of a transmembrane protein like hemagglutinin on the virus that inserts into the target membrane of the host cell (Skehel and Wiley, 2000). This protein contains internal coiled-coil regions and it is thought that conformational rearrangements of these domains bring the bilayers into close proximity and initiate fusion (Hughson, 1995). Hemagglutinin also contains structures required for the resolution step of membrane fusion, and mutant proteins lacking the transmembrane domain or bearing specific amino acid changes lead to stable hemifusion (Kemble et al., 1994; Qiao et al., 1999). SNAREs and hemagglutinin have both been shown to be sufficient to promote fusion in minimal systems (Hernandez et al., 1996; Weber et al., 1998). Thus, in both vesicle and viral fusion, a coiled-coil structure lying between and parallel to the membranes initiates fusion and also is capable of resolving the fusion intermediate. A large number of regulatory factors are superimposed on the core fusion machinery to govern the timing and tropism of fusion (Skehel and Wiley, 2000; Whyte and Munro, 2002).

An important question now is whether the coiled-coil mechanisms defined for vesicles and viruses can explain all instances of membrane fusion. Here we examine several examples of membranes that fuse without known SNAREs, and we present the factors in each system that could act as regulators or components of new coiled-coil fusases or that may constitute novel types of fusion machines.

SNARE-LESS FUSION INSIDE THE CELL: MITOCHONDRIA, CHLOROPLASTS, AND NUCLEI

Unlike the two-bilayer fusion of vesicles and organelles within the secretory pathway, fusion between mitochondrial tubules or between nuclei involves the rearrangement of four lipid bilayers (Fig. 1-1). For mitochondria, fusion of the outer mitochondrial membrane on its cytoplasmic face is followed by fusion of the inner mitochondrial membrane in the intermembrane space. For nuclei, fusion of the outer nuclear envelope or ER membrane on its cytoplasmic face is followed by fusion of the inner nuclear envelope in the ER lumen. Considering these special requirements for membrane fusion it is not surprising that specialized fusion machinery would govern them.

Mitochondria

Mitochondria act like prokaryotic hitchhikers picked up along the road of evolution by eukaryotic cells, conducting affairs according to their own customs. They use a different genetic code; they insist on carrying a circular genome expressed by coupled transcription and translation; and their protein import machinery resembles that of the bacterial membrane. However, while membrane fusion in prokaryotes has not been described, the fusion of mitochondria occurs in many species and cell types. At this point, no factors required specifically for mitochondrial inner membrane fusion are known, but several factors have been identified that facilitate outer membrane fusion by apposing membranes or initiating lipid mixing, or by regulating the machinery that does.

The first protein shown to control mitochondrial fusion emerged from studies of a developmentally regulated fusion event in spermatogenesis of the fruit fly (Hales and Fuller, 1997). In early spermatids, mitochondrially derived structures aggregate near the nucleus, wrap about each other, and fuse to form a multilayered super-mitochondrion which will ultimately power the motion of the mature sperm flagella. Viewed in cross-section this structure appears in its early stages like an onion. A genetic screen for spermatogenesis defects identified a mutant that failed to complete mitochondrial fusion and thus produced immotile sperm (Hackstein, 1991). While its spermatid mitochondria undergo apparently normal aggregation, at the stage of fusion they appear disorganized, like a fuzzy onion. Cloning of the *fuzzy onion* gene revealed it to encode an ideal candidate for the mitochondrial fusase (Hales and Fuller, 1997). Fzo is expressed only in the male germ line, its expression turning on just prior to mitochondrial fusion, and turning off just following fusion (Hales and Fuller, 1997). Fzo localizes to mitochondria as they undergo fusion (Hales and Fuller, 1997). Most importantly, *fzo* mutants display a phenotype suggestive of failed mitochondrial fusion (Hales and Fuller, 1997). An even clearer mitochondrial fusion defect appears in yeast mutants carrying a disruption of the homologous gene, *FZO1*. Upon shifting a temperature-sensitive *fzo1* mutant to the non-permissive temperature, the mitochondria which in yeast normally form a reticulum of tubules undergoing constant fusion and fission instead fragment to many small spherical structures (Hermann et al., 1998; Rapaport et al., 1998). Using an *in vivo* fusion assay available in yeast which assays mixing of mitochondria from two mating partners carrying mitochondria labelled in red and green, it was shown directly that mitochondria lacking Fzo1p could not undergo fusion (Hermann et al., 1998).

In addition to its expression profile and mutant phenotype, Fzo has a structure tantalizingly evocative of a new fusase (Fig. 1-2). Fzo family proteins share a large cytoplasmic N-terminal region containing a GTPase domain and one or two coiled-coil domains; two transmembrane segments flanking a loop that contacts the mitochondrial inner membrane; and a cytoplasmic C-terminal region containing an additional coiled-coil domain (Fritz et al., 2001; Hales and Fuller, 1997). These structural features entice the imagination when considering how Fzo may mediate fusion. First, junctions between the outer and inner mitochondrial membranes are known to serve as sites for fusion and mutations that disrupt the binding of Fzo1 to the inner mitochondrial membrane render it unable to promote fusion (Fritz et al., 2001). Second, the presence of a GTPase suggests the ability of Fzo to use energy from nucleotide hydrolysis to undergo a conformational change. Such a conformational change could promote bilayer fusion, as the conformational changes in hemagglutinin promote fusion or alternatively the GTPase could regulate the assembly of the coiled coils as Rab proteins regulate SNAREs. Third, the potential for forming coiled coils recalls the model for SNARE-mediated membrane fusion and suggests that binding of Fzo on one mitochondrial tubule to Fzo on another tubule could lead to assembly of a coiled coil between them that would initiate outer membrane mixing.

A critical question is whether Fzo interacts with itself in such a *trans* complex. Fusion is reduced if only one of the fusing tubules lacks Fzo1p, suggesting a homotypic interaction between fusion machineries (Hermann et al., 1998). Studies of the human homolog of Fzo showed that its N-terminal and C-terminal coiled-coil regions can bind each other: an N-terminal fragment containing the first coiled-coil domain localizes to

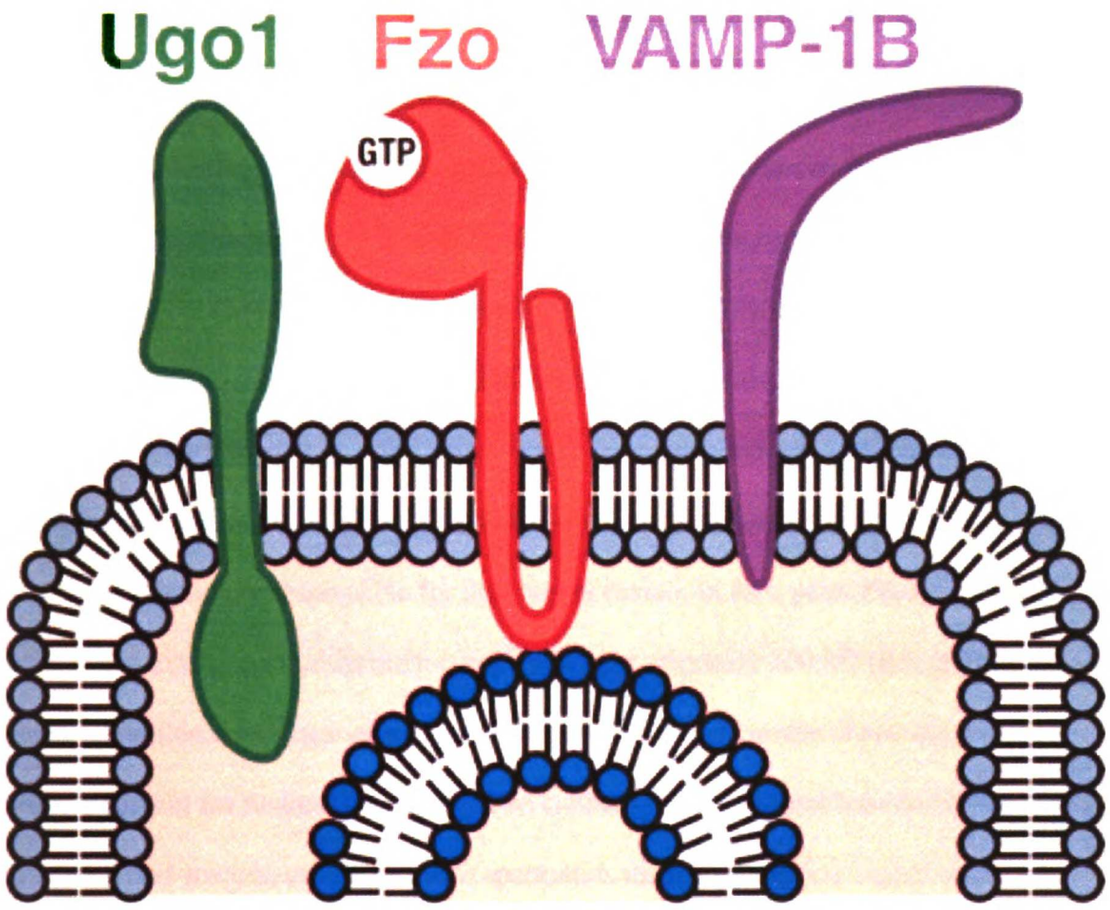

Figure 1-2

Mitochondrial fusion

Ugo1 is a transmembrane protein of the outer mitochondrial membrane involved in fusion. Fzo is a transmembrane protein of the outer membrane that makes contact with the inner membrane, and this contact is required for its role in fusion. Fzo1 has a cytoplasmic GTPase domain and coiled coils that may assemble intra- or inter-molecularly. VAMP-1B is a SNARE localized to the mitochondrial membrane but has not been shown to affect fusion.

mitochondria only when co-expressed with a mitochondrial-resident C-terminal fragment that contains the second coiled-coil domain (Rojo et al., 2002). Such an interaction could occur intermolecularly between Fzo molecules on partner tubules or intramolecularly within a single Fzo molecule. However, although the GTPase activity is required for Fzo1 to promote fusion, overexpression of a GTPase-dead allele of Fzo1p does not have a dominant effect as would be expected if an Fzo1p-Fzo1p complex formed (Hales and Fuller, 1997; Hermann et al., 1998). This result indicates a model in which Fzo does not use its coiled-coil domains directly to bring mitochondria together, but rather forms part of a larger machinery responsible for this step of fusion. In fact, yeast Fzo1p is a 98 kD protein that exists in a multiprotein complex of approximately 800 kD (Rapaport et al., 1998). Additional evidence of downstream factors comes from the observation that Fzo is not sufficient for fusion. *Drosophila* Fzo cannot rescue the mitochondrial fusion defect of a yeast *fzo1* mutant, and *Drosophila* spermatids display the "fuzzy onion" phenotype in the absence of Fzo despite the presence of another family member, Dmfn, in those cells (Hermann et al., 1998; Hwa et al., 2002). Finally, another mitochondrial transmembrane GTPase in yeast, Mgm1p, acts as a regulator rather than mediator of membrane fusion. While *mgm1* mutants display a mitochondrial fusion phenotype, this defect is overcome by the additional loss of Dnm1p, a third mitochondrial transmembrane GTPase (Wong et al., 2000). Whether Fzo acts directly to bring membranes together or indirectly to regulate such a complex will become clear only after the remaining components of the fusion machinery come to light.

One of those components has recently been identified. Using a clever genetic screen built upon their characterization of Fzo1p, Sesaki and Jensen isolated a new

mitochondrial membrane protein in yeast that is required for mitochondrial fusion and that they named Ugo1p (*ugo* means "fusion" in Japanese) (Sesaki and Jensen, 2001). Mutants lacking Ugo1p display a fragmented mitochondrial phenotype similar to mutants lacking Fzo1p, although with differences in the size, number, and distribution of the fragments suggestive of a distinct role for Ugo1p (Sesaki and Jensen, 2001). Using the yeast mating assay it was shown directly that *ugo1* mutant mitochondria cannot undergo fusion (Sesaki and Jensen, 2001). Ugo1p has a single predicted transmembrane segment, localizes to mitochondria and behaves biochemically as an integral membrane protein of the outer mitochondrial membrane (Fig. 1-2) (Sesaki and Jensen, 2001). Thus, it is in the correct position to bind to Fzo1p in *cis* to form a fusion machine; to bind to Fzo1p in *trans* to form a fusogenic bridge between mitochondrial tubules; or serve as a downstream fusion machinery regulated by Fzo1p. These models can now be distinguished using the powerful yeast mating assay to measure fusion directly in a variety of mutant backgrounds. For example, if Fzo1p and Ugo1p act in *cis* then in a *fzo1* x *ugo1* mating, fusion should fail completely. Conversely, a *fzo1 ugo1* x WT should produce a milder defect, comparable to *fzo1* x WT. If Fzo1p and Ugo1p act in *trans*, opposite results are predicted. To improve these assays, the confounding effect of wild-type protein synthesis in the fused mating pair can be avoided using gene shut-off techniques.

Besides Fzo1p and Ugo1p, another potential fusogen localizes to mitochondria – the v-SNARE VAMP-1 (Fig. 1-2). Shockingly, this secretory pathway fusase makes its way into the mitochondrial membrane in the guise of an alternately spliced isoform, VAMP-1B (Isenmann et al., 1998). Replacement of the fifth and final exon of the coding

sequence of the endosomal and plasma membrane resident VAMP-1A generates a sequence that codes for VAMP-1B, a protein with a shorter transmembrane region followed by charged rather than polar amino acids (Isenmann et al., 1998). These alterations suffice to redirect VAMP-1B to mitochondria (Isenmann et al., 1998). A v-SNARE in the mitochondria could promote events other than mitochondrial fusion, such as the exchange of calcium or lipids with the ER, and the function of VAMP1-B remains unknown. The only clues are its mitochondrial localization and its expression in a wide variety of cell types, unlike the brain-specific profile of its secretory pathway isoform. It is intriguing to note that 6 of the mere 239 genes in *S. cerevisiae* known to contain introns are v-SNAREs and the potential for alternate splice forms in some of them exists.

The discovery of mitochondrial fusion mutants has now reached a critical mass where a combination of genomics and genetics will rapidly isolate new factors. Using a collection of yeast strains carrying a disruption of every known gene, Dimmer and colleagues screened visually for mitochondrial morphology defects and found about a dozen mutants that display fragmented mitochondria, including mutants in *TOM7*, which acts in mitochondrial protein import (Dimmer et al., 2002). Mutants in *SSC7,* which acts in a separate aspect of mitochondrial protein import and folding, were found independently to have fragmented or aggregated mitochondria (Kawai et al., 2001). Notably, a similar phenomenon occurs with the protein import machinery of the ER affecting nuclear fusion, described below. Traditional forward genetics also promises to reveal additional mitochondrial fusion factors with increasing speed. Sesaki and Jensen built on the observation that an *fzo1* mutant remains respiratory-competent only if the mutation is generated in a background already lacking Dnm1p to screen for additional

mutants that behave this way. This type of screen, essentially an enhancer and suppressor screen, can be adapted to screens in *Drosophila* in order to find factors upstream or downstream of Fzo. Additionally, an unbiased screen for mitochondrial fusion mutants should be developed. One can envision a screen based on yeast strains bearing complementary mutations in the mitochondrial genome being mated so that recombination restores respiratory competence to the progeny in a mitochondrial-fusion-dependent manner. Finally, a major untapped approach lies in biochemical characterization of mitochondrial fusion. Some questions, like "What is the consequence to mitochondrial fusion of locking Fzo in a GTP-bound state?," may even now be answerable in a permeabilized cell system. Ultimately, though, only the establishment of a cell-free *in vitro* system will answer whether Fzo, Ugo1p, VAMP-1B or others can perform the herculean task of rearranging four lipid bilayers to fuse two compartments, a true mitochondrial fusase.

Chloroplasts

The wealth of knowledge accrued over the last five years concerning mitochondrial fusion contrasts starkly with the paucity of data about chloroplast fusion. Like mitochondria, chloroplasts behave as intracellular symbionts adhering to the laws of a prokaryote while residing in a eukaryotic cell. But, chloroplasts contain three membranes rather than two – an outer membrane, an inner membrane, and within that a thylakoid membrane. Thus, for complete chloroplast fusion not four but six bilayers must merge, first uniting the volumes of the intermembrane spaces, then the volumes of the stroma, and finally the volumes within the thylakoid membranes. In fact, such an amazing feat

occurs. Using the unicellular alga *Chlamydomonas reinhardtii*, Baldan and colleagues mated a mutant defective in photosystem I to a mutant defective in photosystem II in the absence of new chloroplast protein synthesis (Baldan et al., 1991). The restoration of photosynthesis reported on the successful fusion of thylakoid membranes and, presumably, of the surrounding outer and inner chloroplast membranes as well. Additionally, electron microscopic examination revealed the structural fusion of the mating partners' organelles. *Chlamydomonas* offers many of the genetic advantages of yeast – in fact, the first tetrad analysis was performed with *Chlamydomonas* – and because *Chlamydomonas* can live by fermentation, respiration, or photosynthesis, the function of the chloroplast is dispensable making it an ideal model system (Lefebvre and Silflow, 1999). By mating complementary photosynthesis-deficient *Chlamydomonas* strains and screening for mutants unable to generate photosynthesis-competent progeny, one might discover the machinery responsible for chloroplast fusion.

Nuclei

The fusion of nuclei presides over the wedding of two genomes, the ultimate function of sex. The structural details of nuclear fusion, also called karyogamy, have come into view in beautiful electron microscopic studies of Japanese medaka and sea urchin zygotes (Iwamatsu and Kobayashi, 2002; Longo and Anderson, 1968). The availability of protocols for assembling sea urchin pronuclei *in vitro* offers the promise of biochemically isolating components that drive nuclear fusion (Cameron and Poccia, 1994). Genetic screens in the filamentous fungi *Neurospora crassa* and *Podospora anserina* and the ciliate *Tetrahymena thermophila* have begun to reveal how nuclei in these organisms

dance their amazing ballets (Berteaux-Lecellier et al., 1995; Cole and Soelter, 1997; DeLange and Griffiths, 1980). In *Neurospora* for example, out of a cytoplasm hosting a veritable ballroom dancefloor of nuclei, a given nucleus pairs with a nucleus of the opposite mating type; the pair removes itself from the crowd; and then the pair fuse (Thompson-Coffe and Zickler, 1994). Already, a scaled-down version of the problem as presented in the mononucleate yeasts *S. cerevisiae* and *Schizosaccharomyces pombe* has yielded a large parts list of molecules acting in nuclear fusion.

In budding yeast following fusion of haploid mating partners, nuclei congress via the movement along microtubule tracks of nuclear-envelope-embedded cytoskeletal structures called spindle pole bodies (SPBs) (Rose, 1996). The kinesin family protein Kar3p mediates this congression; specific components within the SPB are also required (Rose, 1996). A special structural arrangement of the nucleus may accompany this movement: in filamentous fungi at this stage the SPB suddenly reacts with DNA stains; in *S. pombe* the telomeres bind the SPB; and we have observed that in *S. cerevisiae* the nucleolus consistently localizes to the trailing quadrant of the nucleus (Chikashige et al., 1997; Thompson-Coffe and Zickler, 1994). Following nuclear congression, the nuclei fuse. A set of ER membrane proteins with exposed cytoplasmic domains are required for efficient karyogamy. They include Sec63p, a single-transmembrane protein with large lumenal and cytoplasmic domains; Sec71p, a single-transmembrane protein with a large cytoplasmic domain; and Sec72p, a peripheral membrane protein on the surface of the ER (Ng and Walter, 1996) (Fig. 1-3). These proteins interact with each other as part of the post-translational translocation complex that imports proteins into the ER, and have also been implicated in import of ER proteins through the co-translational SRP-dependent

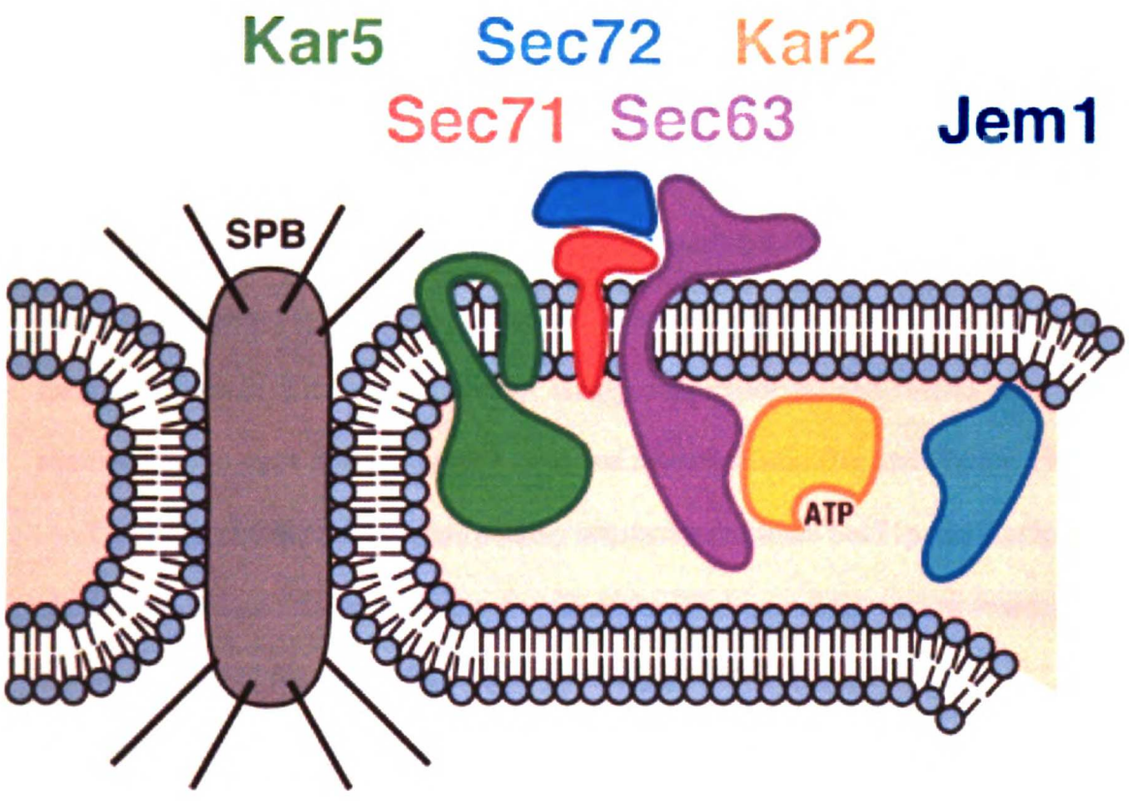

Figure 1-3

Nuclear fusion

Kar5 is a transmembrane protein required for nuclear fusion that has a large lumenal domain, associates with the spindle pole body (SPB), and may directly bind Sec7. Sec71, Sec72, and Sec63 form a complex with well-characterized roles in the translocation of proteins into the ER, and are all involved in nuclear fusion. Sec63 has a lumenal DnaJ domain that binds Kar2, a DnaK ATPase also involved in protein translocation and nuclear fusion. Another lumenal DnaJ protein, Jem1, plays a more downstream role in nuclear fusion.

translocation complex (Johnson and van Waes, 1999; Young et al., 2001). Their role in nuclear fusion, however, seems to constitute a separate function. Other mutants that impair translocation do not affect karyogamy (Ng and Walter, 1996). Moreover, studies of various temperature-sensitive alleles of these genes have shown that the severity of the translocation defect at varying temperatures does not correlate with the severity of the karyogamy defect (Brizzio et al., 1999). Lastly, suppressor mutants restore efficient translocation to these mutants yet fail to rescue nuclear fusion (Ng and Walter, 1996).

Two lines of evidence indicate a likely interaction between Sec71p and Kar5p, a pheromone-induced transmembrane protein of the ER required for nuclear fusion. First, a pair of alleles of the genes displays an interaction termed unlinked noncomplementation, such that while a heterozygote of either single mutant displays a wild-type phenotype, the double heterozygote displays a mutant phenotype (Kurihara et al., 1994). This phenomenon sometimes indicates that the mutant proteins interact to form a "poison" subunit of a complex, preventing the wild-type products in the cell from functioning. Second, mutant Sec71p affects Kar5p synthesis or stability, causing the amount of Kar5p protein to dramatically decrease while its mRNA level remains normal (Brizzio et al., 1999). Commonly, mutation of one protein in a complex will destabilize the entire complex. Combining these arguments, Sec71p may be recruited to a mating-specific karyogamy complex through interaction with the pheromone-induced Kar5p. In this model, mutant Sec71p does not bind wild-type Kar5p, leading to instability of that protein in the mutant. However, mutant Sec71p does bind mutant Kar5p, creating a stable but inactive complex that interferes with the wild-type fusion machinery. A Sec71p-Kar5p complex would be mating specific, regulated by the pheromone-induced

expression of Kar5p, and since Kar5p localizes to the SPB where nuclear fusion initiates, it would have the correct subcellular localization to mediate karyogamy (Beh et al., 1997). The cytoplasmic face of the complex would consist primarily of Sec71p and associated factors because Kar5p has a very short cytoplasmic tail (Beh et al., 1997) (Fig. 1-3). The Kar5p homolog Tht1p from *S. pombe* bears an additional cytoplasmic tail with a terminal "WWD" motif required for karyogamy and in this case the Kar5p homolog could play a more direct role in association of outer nuclear membranes (Tange et al., 1998). In both species Kar5p has a substantial lumenal region containing potential coiled-coil domains that could mediate rearrangements of the SPB or, following fusion of the outer membranes, could initiate fusion of the inner nuclear membranes (Fig. 1-3). Mutants in the *S. pombe* homolog of Kar5p contain unfused nuclei with distinct SPBs, yet as these nuclei begin a series of developmentally programmed oscillations they appear coupled in their movements, as if a bridge had formed near the SPBs linking the two nuclei (Tange et al., 1998). Indeed, just such bridges have been observed ultrastructurally linking nuclei in mutants of Kar5p in *S. cerevisiae* (Brizzio et al., 1999). Thus Kar5p likely acts after stable association of the ER membranes near the SPBs.

The karyogamy proteins of the outer membrane also interact with a soluble lumenal protein required for nuclear fusion. Kar2p, a chaperone and ATPase of the Hsp70 DnaK family and an abundant protein in the ER lumen, binds to a lumenal DnaJ domain on Sec63p (McClellan et al., 1998) (Fig. 1-3). During protein import into the ER, Kar2p interacts with polypeptides in the lumen as they transit the translocation pore, cycling on and off them in conjunction with Sec63p and thus using the energy of ATP hydrolysis to ratchet proteins across the ER membrane (Jensen and Johnson, 1999). Kar2p can also

use the energy of ATP to assist in the renaturation of misfolded proteins (Simons et al., 1995). It is unclear how either of these activities might drive membrane fusion, or whether Kar2p can act in a yet undiscovered way. The alleles of Kar2p most strongly deficient in karyogamy are not the alleles that most strongly affect translocation efficiency (Brizzio et al., 1999). Kar2p may therefore not act in its traditional roles during karyogamy. Kar2p may interact not only with the DnaJ domain of Sec63p but also with a soluble DnaJ protein in the ER lumen, Jem1p (Nishikawa and Endo, 1997; Nishikawa and Endo, 1998) (Fig. 1-3). Mutants in Jem1p arrest during karyogamy with large membranous bridges containing lumens that connect the unfused nuclei (Brizzio et al., 1999). This intermediate suggests a defect at a step following outer nuclear membrane fusion, and consistent with that idea, *jem1 kar5* double mutants display only the upstream fusion block seen in *kar5* (Brizzio et al., 1999). Overexpression of Kar2p can partly overcome the defect of a *jem1* mutant, suggesting a functional relationship between these proteins (Brizzio et al., 1999). Kar2p therefore has the opportunity to act twice in karyogamy – once with the Sec63p complex to facilitate outer membrane fusion and again with Jem1p to facilitate a later step in karyogamy.

In order to more precisely delineate the roles of each of these proteins, an *in vitro* ER fusion assay has come into use (Brizzio et al., 1999; Kurihara et al., 1994; Latterich et al., 1995). In this assay ER microsomes and nuclear envelope are isolated from two vegetatively growing strains. One set of microsomes expresses an ER lumenal enzyme; the other set is loaded with a substrate for that enzyme. Upon membrane fusion the enzyme gains access to the substrate and at the end of the reaction the amount of substrate processed by the enzyme serves as a reporter for the success of membrane

fusion. This assay shows that Sec71p, Sec72p, Kar5p, Kar2p and Jem1p all act directly in membrane fusion, even though membranes were isolated from cells not treated with pheromone (Brizzio et al., 1999; Kurihara et al., 1994; Latterich et al., 1995). Apparently, even the very low basal level of Kar5p expressed in non-mating cells is important for membrane fusion in this assay. Membranes lacking active Sec63p show no defect in this assay (Brizzio et al., 1999). Despite the ultrastructural evidence that Jem1p acts at a later step in nuclear fusion, in this assay it appears that Jem1p serves a constitutive role in fusion of the outer nuclear membrane (Brizzio et al., 1999). Additional characterization showed that the activity in the assay depends on the ER t-SNARE Ufe1p and its ATP-dependent cytoplasmic chaperone Cdc48p (Latterich et al., 1995). Neither *ufe1* mutants nor *cdc48* mutants display karyogamy defects. Thus it appears that the karyogamy complex functions not only during nuclear fusion but surprisingly may also assist Ufe1p and Cdc48p to fuse ER membranes during vegetative growth.

How could these proteins – Sec63p, Sec71p, Sec72p, Kar5p, Kar2p, and Jem1p – all of which have links to the protein translocation apparatus, participate in membrane fusion? A trivial explanation, that the true fusase depends on these proteins for its insertion into the membrane, is rendered unlikely by lack of correlation between the severity of translocation defects and karyogamy defects. It is appealing to imagine that the mechanisms established for translocation of proteins across membranes could also be used for the steps of bilayer apposition, mixing, and resolution required in membrane fusion. Accordingly, if one views a translocon as essentially a motor that pulls proteins across membranes then its activity could be modified to pull membranes together.

Suppose a transmembrane protein in the outer nuclear membrane of one nucleus were translocated by a machinery on the outer nuclear membrane of an adjoining nucleus. As the ratcheting action of Kar2p pulled upon it, fluctuations in the membranes that decreased the volume separating them would be trapped, ultimately driving the bilayers together. Alternatively, the ability of these proteins not to perform translocation but to control the opening and closing of a transmembrane pore may constitute the relevant activity. The proteolipid pore through which lipid mixing occurs has been suggested in studies of vacuole fusion to derive from alignment of a proton channel in the membrane of one vacuole with a proton channel in another vacuole (Peters et al., 2001). Building from this idea, a fusion pore may stand preassembled in the ER membrane. Upon becoming aligned with a corresponding pore in the opposite ER membrane, both pores could open, allowing lipid flow between them, and then dissociate to create a continuous lipidic pore. Many of the karyogamy complex components identified thus far have well-established roles in sealing unoccupied translocons to prevent leakage from the ER, unsealing the translocon in response to a signal from the cytoplasmic face of the membrane, and coordinating the rearrangements and dissociation of the translocon that allow hydrophobic transmembrane segments to slip in amongst lipids and completed translocation products to diffuse freely in the membrane. Clearly, each of these functions if applied not to the translocon but rather to a fusogenic pore would serve a critical role in ER membrane fusion.

SNARE-LESS FUSION OUTSIDE THE CELL: SYNCYTIUM FORMATION AND FERTILIZATION

The fusion of cells on the extracellular faces of their plasma membranes to form a syncytium or a zygote requires a set of fusases that point outward to the environment rather than inward to the cytoplasm. In this sense cell-cell fusion has as its closest correlate the fusion of a virus with a host cell mediated by a protein like hemagglutinin. The basic question then is whether a cell-cell fusion machine constitutes an inside-out set of SNAREs, a viral-like fusase, or an altogether novel apparatus for fusing membranes.

Syncytium formation

Syncytia unite the identities and couple the activities of the cells that compose them, and create the space to assemble powerful cytoskeletal meshworks, as in muscle fiber. Syncytia formation holds important medical implications, extending the promise of gene therapy for muscle disease by the delivery of healthy fusion-competent myoblasts but also being responsible for spontaneous loss of pregnancy in cases where maternal antibodies target the placenta due to the exposed phosphatidylserine associated with cell-cell fusion in that tissue (Potgens et al., 2002). The identification of the cell fusion machinery may therefore assist human health as well as shed light on a basic problem in membrane fusion. In vertebrates the primary syncytial tissues are placenta, muscle, and the osteoclasts and giant multinucleated cells derived by macrophage and monocyte fusion (Potgens et al., 2002). Syncytia formed by cell fusion have been described in other species, including sea urchin and leech (Hodor and Ettensohn, 1998; Isaksen et al.,

1999). In the nematode *Caenorhabdhitis elegans* one-third of the somatic cells develop as syncytia (Shemer and Podbilewicz, 2000).

The syncytial cells of the placenta, called syncytiotrophoblasts, have adapted a viral fusase directly for cell-cell fusion. These cells express syncytin, an envelope protein of an endogenous human retrovirus (Blond et al., 2000; Mi et al., 2000) (Fig. 1-4). Several retroviruses have left their marks on the human genome, and fifteen genes similar to syncytin are predicted to populate human chromosomes (Mi et al., 2000). Syncytin, in particular, has come under control of its host. It is expressed subject to strict developmental regulation, detectable only in placenta and weakly in testes (Mi et al., 2000). A cell line derived from a placental tumor expresses syncytin during conditions that induce syncytia formation (Mi et al., 2000). Adding anti-syncytin antibodies to these fusogenic cultures reduces fusion by 50% (Mi et al., 2000). Furthermore, expression of syncytin in cultured fibroblasts suffices to induce fusion, converting them to syncytia (Mi et al., 2000). Thus, expression of syncytin is physiological, necessary and sufficient for cell-cell fusion. In placenta, therefore, the cell-cell fusion machinery does not merely resemble that of a virus; it *is* that of a virus.

ADAM proteins bear several viral-like traits and are involved in fusion of myoblasts and monocytes. ADAMs are transmembrane proteins at the cell surface with large extracellular domains which, like hemagglutinin, undergo proteolytic activation and in some cases contain a hydrophobic motif that could act as a fusion peptide (Evans, 2001; Huovila et al., 1996). However, as described below with regard to sperm-egg fusion, it now appears that ADAMs act primarily in cell adhesion. The interaction of the adhesion molecules CD47 and MFR, two proteins with immunoglobulin-like domains, is

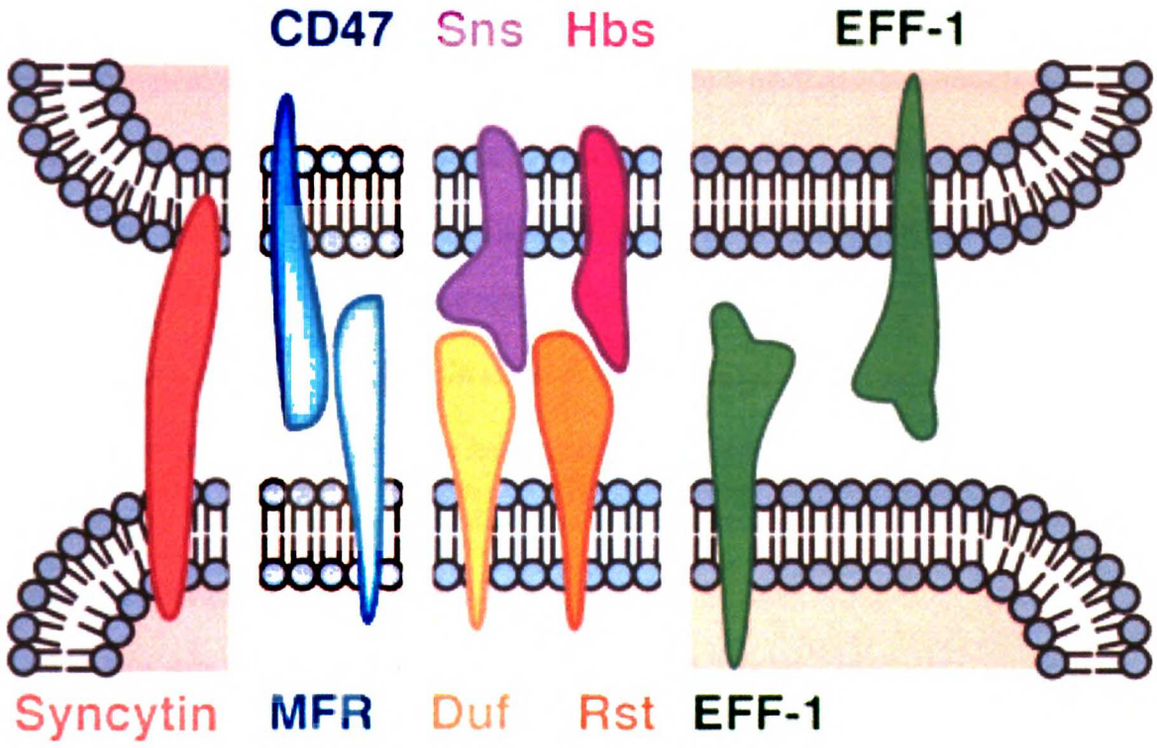

Figure 1-4

Syncytia formation

Different cell types use different machinery for cell-cell fusion. Placental cells express syncytin, a viral fusase captured by the mammalian genome. Osteoclasts require MFR and CD47, two Ig-containing proteins that interact in *trans*, for fusion. A host of membrane proteins have been identified in myoblast fusion, including the Ig-containing proteins Duf, Rst, Hbs, and Sns whose interactions and expression pattern have been well-characterized. Hypodermal fusion in *C. elegans* requires the novel transmembrane protein EFF-1.

required for macrophage fusion (Han et al., 2000) (Fig. 1-4). Another set of Ig-domain-containing proteins – Duf/Kirre, Rst/IrreC, Sns and Hbs – mediates the interaction of myoblasts during fusion in *Drosophila* (Dworak and Sink, 2002; Taylor, 2000) (Fig. 1-4). The pairing of ADAMs with integrins, CD47 with MFR, and the Ig-like myoblast proteins with each other could bring membranes into proximity, perhaps as close as 5 nm, but this distance remains a canyon in terms of membrane fusion. Genetic analyses of myoblast fusion in *Drosophila* have led to candidates to participate in the fusion machine that bridges this final gap, but also raised new possibilities about the importance of adhesion molecules at a late step in fusion.

The fine structure of myoblast fusion in *Drosophila* has been carefully documented (Doberstein et al., 1997). A specialized myoblast termed a founder cell emits an attractive signal to non-founder fusion-competent myoblasts, which then migrate toward it (Dworak and Sink, 2002; Taylor, 2000). Founders can fuse only with fusion-competent myoblasts and vice versa; each class of cell cannot fuse with its own kind. Upon making contact, the cells build a prefusion complex (Doberstein et al., 1997). Vesicles in each cell align one-to-one just beneath the plasma membranes, in perfect button rows (Doberstein et al., 1997). Fusion of these vesicles at the surface accretes an electron-dense plaque bridging the plasma membranes (Doberstein et al., 1997). The distance between apposed membranes at this point is approximately 10 nm (Doberstein et al., 1997). Eventually, numerous fusion pores appear leading ultimately to cell fusion. Mutants acting at each step have been identified. A mutant named *blown fuse* forms paired vesicles but does not produce the electron-dense plaques or fuse pores (Doberstein et al., 1997). The *blow* gene encodes a cytoplasmic protein with no known homologs,

unlikely for topological reasons to participate directly in the fusion reaction (Doberstein et al., 1997). Blow could serve as a cytoplasmic scaffold on which the fusion machinery assembles, such that in the mutant the fusase is delivered to the surface but is not anchored, diffuses away, and does not produce dense staining. Another mutant, a gain-of-function allele of a Rac protein, generates normal electron-dense plaques but not fusion pores (Doberstein et al., 1997). Rac proteins regulate actin dynamics and for that reason as well as topologically are ill-suited fusase candidates. Rearrangements of actin are vital to fusion – a mutant in Titin, another actin organizer, also displays fusion defects – but it is difficult to envision actin fusing membranes directly (Menon and Chia, 2001). Conceivably actin assembly could act as a "pushase," forcing plasma membranes together from the inside, but this model does not fit with the structure of the prefusion complex. The *rac* mutant is difficult to dismiss because its phenotype seems snatched from a dream about what one expects of a fusase mutant. Models for the role of Rac in fusion may emerge from ultrastructural studies of the recently constructed *rac1, rac2* loss-of-function mutant which also has impaired myoblast fusion (Hakeda-Suzuki et al., 2002). Since the gain-of-function Rac mutant does seem to affect the ultimate step of fusion it could serve as fodder for an enhancer or suppressor screen to identify other genes that act at this step.

One gene in particular has been shown to act at a similar step. A mutant in Sns, one of the transmembrane Ig-like proteins, also forms extensive electron-dense plaques yet fails to fuse membranes (Bour et al., 2000; Doberstein et al., 1997). Sns is part of a cohort of Ig-domain-containing proteins that includes two related proteins on founder cells, Duf/Kirre and Rst/Irrec, and two related proteins on fusion-competent myoblasts, Sns and

Hbs (Dworak and Sink, 2002; Taylor, 2000) (Fig. 1-4). Duf/Kirre and Rst/IrreC act redundantly, and Sns and Hbs oppose each other (Artero et al., 2001; Ruiz-Gomez et al., 2000; Strunkelnberg et al., 2001). Duf/Kirre and presumably Rst/IrreC can bind Sns and Hbs (Dworak et al., 2001). In current models, soluble forms of Duf/Kirre and Rst/IrreC direct the migration of fusion-competent myoblasts toward the founder cells. How can the fusion phenotype of the *sns* mutant be reconciled with the cell migration phenotypes of *hbs* and *duf/kirre, rst/irrec* mutants? One possibility is that these proteins act both early and late, first directing cell migration and then participating in construction of the prefusion complex. Consistent with this hypothesis, in the mutants that display cell migration phenotypes appropriate partners sometimes make contact by chance yet fail to fuse (Ruiz-Gomez et al., 2000). Furthermore, at sites where fusion will occur, Duf/Kirre binds to a cytoplasmic adapter, Rols7/Ants, which recruits Titin and could thereby influence late steps in fusion (Chen and Olson, 2001; Menon and Chia, 2001; Rau et al., 2001). However, a *rols7/ants* mutant fails to assemble prefusion complexes showing this factor acts at a very early step (Rau et al., 2001). One problem with interpreting this literature is a lack of conensus in nomenclature: a single gene may be referred to by up to three names, depending on the lab studying it, and in one case, for historical reasons, either of two genes may be referred to by the same name, depending on when the work was published (Paululat et al., 1997; Paululat et al., 1999). To make matters more complicated, different labs have assayed different genes or different alleles of the same gene at different developmental stages, in different tissues, and with different levels of morphological resolution, sometimes reaching opposite conclusions. A side-by-side

ultrastructural comparison of each adhesion mutant would be helpful in determining what role they play in forming the prefusion complex.

Other candidates for the fusion machinery exist. First, Rost is a transmembrane protein expressed only on founder cells, and inhibition of Rost produces a defect in which myoblasts contact founder cells but do not fuse (Paululat et al., 1997). Second, mutations in *singles bar*, a hydrophobic protein that could act close to membrane fusion, also block myoblast fusion after the step of cell-cell interaction (Ruiz-Gomez et al., 2000); N. Brown, personal communication). Third, experiments with cultured mouse myoblasts have shown fusion to depend on CD9, a tetraspanin implicated in a late step of sperm-egg fusion and homologs of which exist in *Drosophila* (Tachibana and Hemler, 1999). Ultimately, a complete manifest of the proteins specific to founder myoblasts and to fusion-competent myoblasts should be generated, possibly by using markers like Sns and Duf/Kirre to purify founder or non-founder myoblasts and then subject them to whole-genome microarray transcript analysis.

Because the problem of distinguishing adhesion from fusion has caused trouble in many studies of cell fusion, an advantage is held in systems where extensive cell-cell contact precedes membrane fusion, making it easier to assay these steps independently. In the hypoderm of *C. elegans,* forty-three cells fuse to produce 9 syncytia, and cells preparing to fuse are joined by a well-characterized network of adhesion junctions which stays in place until plasma membrane vesiculation a few minutes after fusion (Mohler et al., 1998; Shemer and Podbilewicz, 2000). By selecting fusion mutants that maintain a morphologically well-differentiated epithelial sheet with structurally normal adhesion junctions, Mohler et al. biased a genetic screen for mutants acting downstream of cell-cell

contact (Mohler et al., 2002). This approach led to the identification of the transmembrane protein EFF-1 (Mohler et al., 2002) (Fig. 1-4). In mutants lacking EFF-1, the cell-cell junctions appear normal as visualized by a fluorescent junctional marker, yet every epithelial cell fusion fails, as well as fusion in other tissues (Mohler et al., 2002). EFF-1 is expressed in the cells that fuse, at the time of fusion, and consists of a cytoplasmic domain that varies between isoforms, a transmembrane segment, and a large extracellular domain (Mohler et al., 2002). This extracellular domain contains a putative viral-like fusion peptide (Mohler et al., 2002). The recent establishment of methods for culturing *C. elegans* cells *in vitro* will allow future experiments to address whether EFF-1 expression by one cell is sufficient for fusion to any neighboring cell or whether specific cognate interactions between fusing partners must form (Christensen et al., 2002).

Fertilization

Sperm-oocyte fusion presents the same problem, topologically speaking, as syncytium formation, but with strict regulatory mechanisms to ensure that each oocyte fuses with only a single sperm. Additional complexity arises from the fact that the sperm must transit the female reproductive system, penetrate the layer of cumulus cells that surrounds the oocyte and dissolve the zona pellucida that protects the oocyte before binding to and fusing with the oocyte plasma membrane (Evans and Florman, 2002; Talbot et al., 2003). In writing, these steps seem clear and distinct. In practice, however, it has been surprising how many of the key molecular players act at multiple steps and,

conversely, how many of the single steps depend on several molecules acting in redundant fashion.

For example, the ADAM family proteins on sperm initially emerged as prime candidates to mediate the step of sperm-oocyte fusion (Evans, 2001; Huovila et al., 1996). ADAM-1 and ADAM-2 form a heterodimer, while ADAM-3 is thought to exist independently (Cuasnicu et al., 2001) (Fig. 1-5). Each of these proteins can bind to specific oocyte integrins that associate with CD9, an oocyte membrane protein required for fusion (Evans, 2001) (Fig. 1-5). Furthermore, ADAM-1 contains a predicted amphipathic helix similar to viral fusion peptides, and synthetic peptides derived from it mediate liposome-liposome fusion *in vitro* (Blobel et al., 1992; Martin and Ruysschaert, 1997; Muga et al., 1994). Pre-incubating sperm with an antibody that binds ADAM-2 causes a reduction in sperm-oocyte fusion of about 75%, and pre-incubating oocytes with a peptide derived from ADAM-2 blocks fusion almost completely (Myles et al., 1994; Primakoff et al., 1987). Despite these indications that ADAM proteins mediate sperm-oocyte fusion, knockout mice lacking ADAM-2 have defects at almost every step *but* fusion. ADAM-2-defective sperm failed to migrate into the oviduct in 5 out of 6 animals examined; 100-fold fewer sperm bind to the zona pellucida of oocytes in *in vitro* assays; and 8-fold fewer sperm bind to the plasma membrane of zona-denuded oocytes (Cho et al., 1998). However these sperm exhibit a comparatively mild 2-fold decrease in sperm-oocyte fusion (Cho et al., 1998). Likewise, ADAM-3-defective sperm display dramatically decreased binding to the zona pellucida, but fuse fine to zona-denuded oocytes (Nishimura et al., 2001). Thus if ADAMs play a direct role in sperm-oocyte fusion as earlier evidence indicates, they must act redundantly with other fusases.

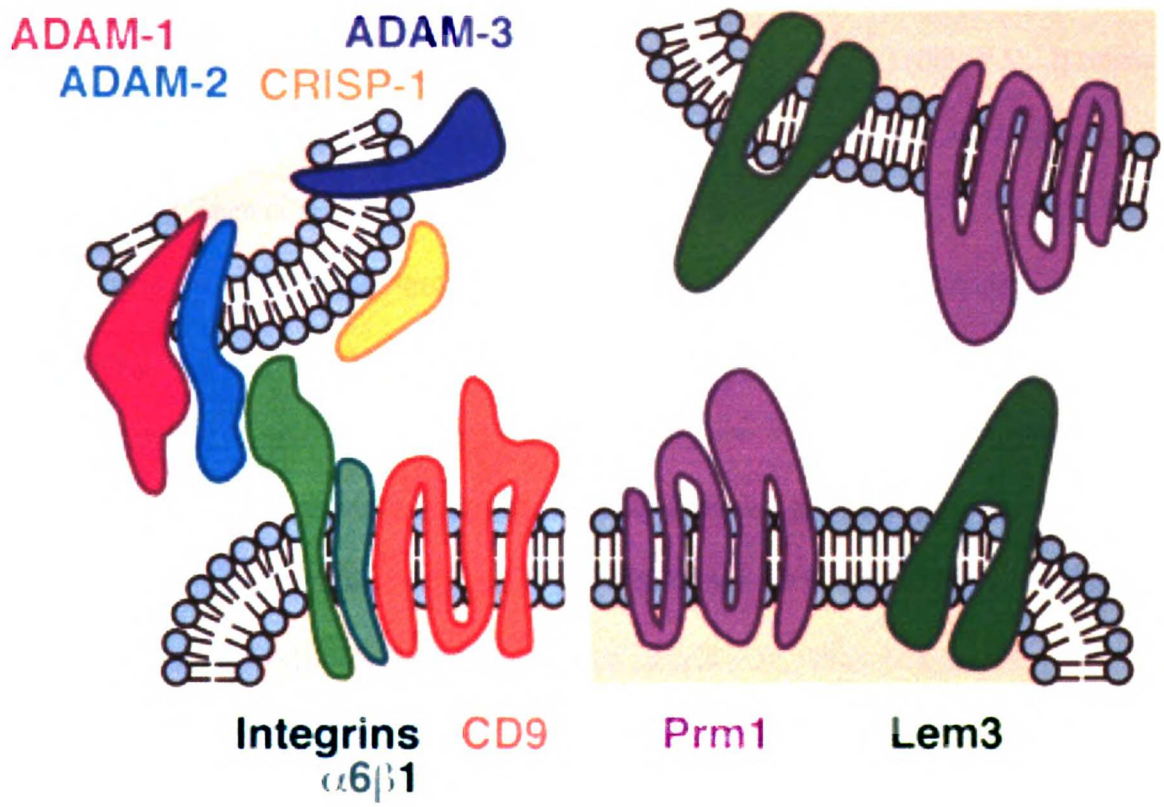

Figure 1-5

Fertilization

ADAM proteins on the sperm, top left, can bind integrins in the egg plasma membrane, bottom left. Integrins associate in *cis* with CD9, which is required for fusion. The sperm protein CRISP-1 is also required for fusion. Yeast mating, right, serves as a model system for fusion of haploid gametes to form a diploid zygote. The mating-specific plasma membrane protein Prm1 cooperates with consitutively-expressed Lem3 to facilitate fusion. An additional unidentified protein that undergoes proteolysis by Kex2 in the Golgi is hypothesized to also act during fusion.

One other candidate for a sperm-resident fusase is CRISP-1, an epididymal protein deposited on sperm as they transit that organ (Cuasnicu et al., 2001) (Fig. 1-5). It binds to the plasma membrane of the oocyte specifically in those regions that are fusion-competent (Cohen et al., 2001; Cohen et al., 2000; Ellerman et al., 2002). Pre-incubating sperm with anti-CRISP-1 antibody reduces sperm-oocyte fusion by about 80%, and pre-incubating oocytes with soluble CRISP-1 blocks fusion almost completely (Cohen et al., 2001; Cohen et al., 2000; Ellerman et al., 2002). In these respects CRISP-1 resembles the ADAMs. The next test will be whether CRISP-1-defective sperm display fusion defects and, if not, whether combining that mutation with mutations in the ADAM proteins can reveal a combined role in fusion.

On the oocyte membrane, CD9 is the premier fusion molecule to date. CD9 is a member of the four-transmembrane tetraspanin family of proteins implicated in organizing multimerized protein complexes, or "webs," in membranes (Hemler, 2001). Consistent with this hypothesis, the second extracellular domain of CD9 binds a partner in oocyte membranes and when pre-incubated with oocytes this fragment blocks sperm-oocyte fusion (Zhu et al., 2002). In contrast, this domain does not bind sperm and pre-incubation with sperm has no effect (Zhu et al., 2002). Antibodies against CD9 also block fusion when pre-incubated with oocytes, although in some cases a defect in sperm-oocyte binding is observed as well (Chen et al., 1999; Zhu et al., 2002). Most importantly, oocytes from mice with disruptions of CD9 are normal for sperm-oocyte binding but display severe defects in sperm-oocyte fusion, with only about 5% of oocytes fusing compared to 95% in the wild-type(Kaji et al., 2000; Le Naour et al., 2000; Miyado et al., 2000).

CD9 binds integrins including oocyte α6β1 which in turn binds sperm ADAMs (Almeida et al., 1995; Miyado et al., 2000) (Fig. 1-5). Yet disruption of the α6 integrin gene yields oocytes that bind and fuse sperm normally, and remain sensitive to disruption of CD9 (Miller et al., 2000). Thus, a beautiful model is killed by ugly facts. While binding data suggests a model in which CD9 multimerizes α6β1integrin in the oocyte membrane which in turn binds sperm through the ADAM proteins triggering ADAM-1 to initiate fusion, genetic disruptions do not support the idea. ADAM-1 is not functional in primates (Cho et al., 2000); ADAM-2 and ADAM-3 knockouts do not have severe fusion defects; and α6 integrin is not required for fusion. Competition experiments show CD9 may bind other integrins to mediate fusion (Zhu and Evans, 2002). Since CD9 is also expressed in the female reproductive tract and sperm lacking ADAM-2 fail to reach the oviduct, the CD9-α6β1-ADAM complex may be more relevant to sperm migration than fusion (Chen et al., 1999). However, it is crucial to remember that each of these proteins is one member of a large family. Other tetraspanins are expressed in the oocyte and the reproductive tract; other integrins are present in the oocyte; and there are multiple ADAMs on sperm as well as other potentially fusogenic molecules such as CRISP-1. Neither the absence of a "knockout" fusion phenotype nor the presence of unrelated phenotypes prove that a factor does not drive sperm-oocyte fusion, since the problem of genetic redundancy cannot be discounted.

This lesson has been borne out in studies of fertilization in the model system of yeast mating. In yeast mating, two haploid gametes of opposite mating types fuse to form a diploid zygote. The haploid cells signal to each other via pheromones, leading to cell cycle arrest, polarized growth in the direction of the mating partner and changes in cell

wall structure to form a mating pair. Next, the cell wall is dissolved at the cell-cell interface and plasma membranes come together and fuse to form a diploid zygote. Genetic screens to find mutants defective in this process yielded mutants at every step except plasma membrane fusion (Berlin et al., 1991; White and Rose, 2001). Now, it appears that tremendous genetic redundancy at the step of plasma membrane fusion helped to conceal such mutants.

Prm1p, the first protein shown to act at plasma membrane fusion, was identified by reverse genetics rather than a traditional mutant screen (Heiman and Walter, 2000). We reasoned that the machinery that fuses cells probably includes a transmembrane protein expressed specifically during mating, and we wrote a data mining program called Webminer (http://webminer.ucsf.edu) to identify such proteins. Prm1p is predicted to be a four- or five-transmembrane protein (Fig. 1-5). It is not present in vegetatively growing cultures but Prm1p is expressed in both mating types in response to pheromone (Heiman and Walter, 2000). It localizes to the tip of the mating projection, where cell fusion occurs (Heiman and Walter, 2000). In mating pairs lacking Prm1p, about 50% of the mating pairs fuse, compared to about 95% in wild-type (Heiman and Walter, 2000). In some of the mating pairs that fail to fuse, we observed by electron microscopy that the cell wall had been degraded apparently normally and plasma membranes were apposed with an 8 nm gap between them, but failed to fuse (Heiman and Walter, 2000). This phenotype had never before been seen. Thus, Prm1p acts at the step of plasma membrane fusion during yeast mating. It does not contain any characterized protein domains, although its overall structure evokes comparison to CD9. Significantly, though, Prm1p is not required for cell fusion – about half the mating pairs fuse without it. This genetic

redundancy may explain why Prm1p mutants were not identified in earlier screens, and suggests a recurring motif that extends to mammalian fertilization.

To identify the remaining machinery capable of fusing cells in the absence of Prm1p, we screened for enhancers of the *Δprm1* x *Δprm1* phenotype and identified mutations in Kex2p. Kex2p is a Golgi-resident protease of the furin family. In oocytes, furin processes zona pellucida proteins; in yeast, Kex2p processes several cell wall proteins. Furin also processes the viral protein hemagglutinin to activate it for fusion; conceivably, Kex2p could activate a similar fusogenic molecule. Further characterization showed that loss of Kex2p produces a mild cell fusion defect in a wild-type background and a severe cell fusion defect in the absence of Prm1p. Ultrastructural analysis showed that mating pairs defective in Kex2p have extracellular membrane inclusions embedded in the cell wall. Even when mutations in Prm1p and Kex2p are combined, about 15% of mating pairs still fuse.

We undertook another iteration of our enhancer screen to eliminate any remaining fusion machinery. We identified Lem3p, another transmembrane protein localized to the site of cell fusion, and Erg4p, a protein involved in the synthesis of ergosterol, the fungal equivalent of cholesterol (Fig. 1-5). The site where cell fusion occurs in yeast is rich in ergosterol, possibly organizing protein complexes into lipid rafts. A GPI-anchored protein, presumably also raft-associated, is required on oocytes for fusion competence as well (Coonrod et al., 1999a; Coonrod et al., 1999b). Lem3p acts on lipids, helping to maintain the proper distribution of specific phospholipids on each leaflet of the membrane bilayer (Kato et al., 2002). Redistribution of specific phospholipids from one

bilayer to the other could alter local curvature of the plasma membrane, supplying the initial distortion of the membrane required in many models of membrane fusion.

There are at least three explanations for the subtlety of knockout phenotypes, in yeast and mammals. First, the real fusases may simply not have been found, in which case α6β1 integrin, ADAM proteins, Prm1p, and others are all accessory factors that act early to prepare the membranes for fusion but that do not act during fusion itself. Second, these proteins may comprise part of the fusion machinery but exhibit functional redundancy with others. This redundancy could take the form of direct substitution, as of one integrin for another, or of functional overlap, for example Prm1p may adhere membranes tightly but this job may also be done by a Kex2p substrate. Third, the secret may be in the lipids. In the hemagglutinin/SNARE model of membrane fusion a single protein complex is responsible for diffusionally isolating a patch of membrane, pulling membranes into close proximity, inducing high local curvature on the membrane, creating a proteolipid channel bridging the membranes, and finally dispersing to allow free lipid diffusion and thus membrane merger. These activities could be distributed over several proteins during fertilization. CD9 and raft-based proteins can isolate membrane patches; integrin-ADAM interactions can tightly associate membranes; and proteins like Lem3p might in theory alter membrane curvature enough to promote fusion without a proteolipid channel intermediate. This model still does not explain why no single mutation has been found that blocks fertilization absolutely.

CONCLUSIONS

The crystal structures of a SNARE complex and of hemagglutinin opened our eyes to basic similarities in membrane fusion machinery (Sutton et al., 1998; Wilson et al., 1981). In a beautiful convergence of cytoplasmic and extracellular face fusion, cellular and viral strategies, it seemed that the fundamental question of membrane fusion was solved. The assembly of coiled coils anchored to each membrane pulls the membranes so tightly together that fusion ensues.

Does all cytoplasmic-face fusion mimic SNAREs? Mitochondria, chloroplasts, and nuclei require the fusion of 4 or even 6 bilayers. Hints of SNARE-like function are present in mitochondria – one SNARE is found in the membrane, and some mitochondrial fusion molecules have SNARE-like structures. Nuclei, however, have a completely different kind of machinery in their membranes required for fusion and this machinery suggests an altogether different mechanism for forming a proteolipidic pore.

Does all extracellular-face fusion mimic viruses? In placenta, almost surely it does. But other syncytia require other proteins, and so far fusing cells have not led to fusing paradigms. Rather, cell fusion may have evolved independently in different organs and organisms. In sperm-oocyte fusion and related model systems, work has gone on so long with no single factor absolutely required for fusion that one begins to wonder whether an altogether different kind of fusion may occur.

A great challenge for the next decade will be to learn whether the membrane fusion structure of SNAREs and viral fusases is universal or whether the systems enumerated here may offer fundamentally new insights into the basic problem of membrane fusion.

CHAPTER 2

Prm1p, a pheromone-regulated multispanning membrane protein, facilitates plasma membrane fusion during yeast mating

INTRODUCTION

The question at the heart of membrane fusion is how to unite the hydrophobic lipid cores of two bilayers across a gulf of water. An answer has emerged from work on the fusion of viruses with host cells and the fusion of transport vesicles with plasma membrane and organelles. In these systems a fusion protein, or fusase, drives the reaction. For influenza virus the fusase is the hemagglutinin protein; for vesicles the fusase includes the SNARE complex (Hernandez et al., 1996; Weber et al., 1998). Although hemagglutinin and SNAREs differ in composition – hemagglutinin is a single viral surface protein capable of inserting directly into the host cell plasma membrane, whereas the SNARE complex assembles from subunits associated with different bilayers – their final structures bear remarkable similarities (Weber et al., 1998). In each case, the assembled fusase has domains inserted into each of two apposing bilayers and, between these domains, a remarkably stable coiled coil (Harbury, 1998; Hughson, 1995). According to current models, the energetics of forming this coiled coil are so favorable that they outweigh the cost of pulling together the negatively charged sheets of phosphate head groups and squeezing out the water in between, thus initiating bilayer fusion (Ramalho-Santos and de Lima, 1998; Weber et al., 1998).

Although this relatively detailed mechanistic model accounts well for fusion by viruses and within the secretory pathway, it leaves unexplained a large and important class of membrane fusion—that of cell fusion. Cell fusion occurs between sperm and egg

during fertilization, during development in syncytial tissues such as muscle where myoblast precursor cells fuse into a long tube that will differentiate into a muscle fiber, and in processes such as phagocytic engulfment of cells or debris by macrophages where widely separated regions of the immune cell's plasma membrane must fuse to complete engulfment (Hernandez et al., 1996; Shemer and Podbilewicz, 2000). In each of these cases, a pair of plasma membrane bilayers fuses from the extracellular side. Do these cells therefore express a special kind of SNARE with a topology more like a viral fusase?

If so, it has not yet been found. The closest proteins identified so far are the ADAMs, integral membrane proteins that contain a peptide similar to the portion of hemagglutinin that inserts into a host cell's plasma membrane (Blobel et al., 1992; Huovila et al., 1996). During fertilization, ADAMs on the sperm bind to $\alpha 6\beta 1$ integrins on the egg with the help of another egg membrane protein, CD9 (Almeida et al., 1995; Chen et al., 1999). Blocking this interaction or removing CD9 inhibits sperm-egg fusion (Chen et al., 1999; Le Naour et al., 2000; Miyado et al., 2000). As none of the proteins in this complex are known to contain coiled coils, how this structure might generate the force required to bring membranes close enough for fusion remains a mystery.

In order to identify novel proteins that mediate cell fusion, we turned to the model system of yeast mating, in which two haploid cells fuse to produce a diploid. The mating reaction proceeds, briefly, as follows. Haploids exist as one of two mating types, **a** or α, which secrete a pheromone (**a**-factor or α-factor, respectively) that cells of the opposite mating type can detect. When the pheromone concentration reaches a certain level, the mating reaction initiates. The first steps of mating include a cell cycle arrest, remodeling of the cell wall, and polarization of mating partners towards each other. When mating

partners make contact, the cell walls knit together to form a continuous outer layer. At this point the mating partners are firmly attached but each is still surrounded completely by cell wall, the plasma membranes having not yet come in contact and the cells of course not yet having fused. Cells at this stage are said to have formed a "mating pair" or "prezygote". To complete formation of a zygote, the cell wall separating the partners must be degraded, plasma membranes must come in contact and fuse, and finally the haploid nuclei must merge into a single diploid nucleus.

A number of genetic screens have identified mutants defective in these steps by looking for cells that can form mating pairs but not diploids. All of the mutants, however, arrest in the mating reaction at either the step of cell wall breakdown or nuclear fusion (Berlin et al., 1991; White and Rose, 2001). Although these classes of genes have provided insight into cell polarization, cell wall reorganization, control of osmotic stability, and organelle positioning and dynamics, the genes that mediate the actual lipid bilayer fusion step that follows the proper juxtapositioning of plasma membranes have remained elusive. We have exploited the recently accumulating wealth of gene expression data to search for proteins that may govern the fusion of plasma membranes.

RESULTS

A new strategy for identifying genes that regulate cell fusion

We devised a strategy to identify mating-specific genes that may have escaped earlier genetic screens due to functional redundancy within or between mating partners. Such redundancy often produces a weak phenotype which can be difficult to detect. For example, in the case of the redundant genes *FUS1* and *FUS2*, a *fus2* mutant displays little mating defect unless both mating partners also have deficiencies in *FUS1* (Trueheart et al., 1987). To avoid overlooking functionally redundant genes in our search, we employed a reverse genetic strategy that did not depend initially on the strength of the mutant phenotype. Specifically, we asked, "What pheromone-induced membrane proteins have not yet been studied?"

To address this question, we compiled already-published databases of gene expression data and gene properties, restructured them in a common format, and wrote a program to search this composite database. We used the program, called Webminer (see Methods), to examine gene expression profiles of cells arrested in G1 by treatment with the pheromone α-factor. These genomic expression data sets were originally collected in the course of another group's study of cell-cycle transcription and made available on-line ((Spellman et al., 1998), http://genome-www.stanford.edu/cellcycle/). We re-interpreted the data in order to identify a number of strongly pheromone-induced proteins. As a second criterion, we demanded that potential target proteins have at least one hydrophobic domain, indicative of secretory or membrane proteins.

Specifically, we set an arbitrary cut-off to select genes which are induced more than three-fold by mating pheromone. This criterion identified a set of 54 candidate open reading frames (ORFs) out of the 6,116 ORFs assayed in the genomic expression dataset (Fig. 2-1). We next assigned a score to every ORF to reflect its likelihood of encoding a membrane protein. To calculate these values, we wrote a program that scans predicted protein sequences in windows of 19 amino acid residues and assigns a hydrophobicity, or H, value to each window based on its amino acid composition. The hydrophobicity values we used are based on the empirically observed frequency of each amino acid's presence in known transmembrane domains (Boyd et al., 1998). The highest H-value among all of a protein's windows has been defined as that protein's MaxH (Boyd et al., 1998). In most organisms, the MaxH values of all proteins fall into a bimodal distribution with a trough at 28.5 (Boyd et al., 1998). Lower values represent the set of cytosolic proteins (e.g., Tub1p, α-tubulin, has a MaxH of 22.5), and higher values represent membrane proteins (e.g., Hxt1p, a hexose transporter, has a MaxH of 30.9). In *S. cerevisiae* the bimodal distribution of MaxH values is present, but the overlap between the two sets is considerable. As a result, many known membrane proteins have MaxH values less than 28.5. We therefore set a less stringent threshold, by considering all ORFs with MaxH values greater than 25 to be possible membrane proteins, yielding a set of 2,524 ORFs. This parameter narrowed our pool of 54 candidates to 20 genes, which we henceforth refer to as PRM genes (***p***heromone-***r***egulated ***m***embrane proteins).

Of these 20 genes, ten have previously assigned functions (Fig. 2-1). Intriguingly, the identification of all ten genes can be rationalized in light of roles they have in mating:

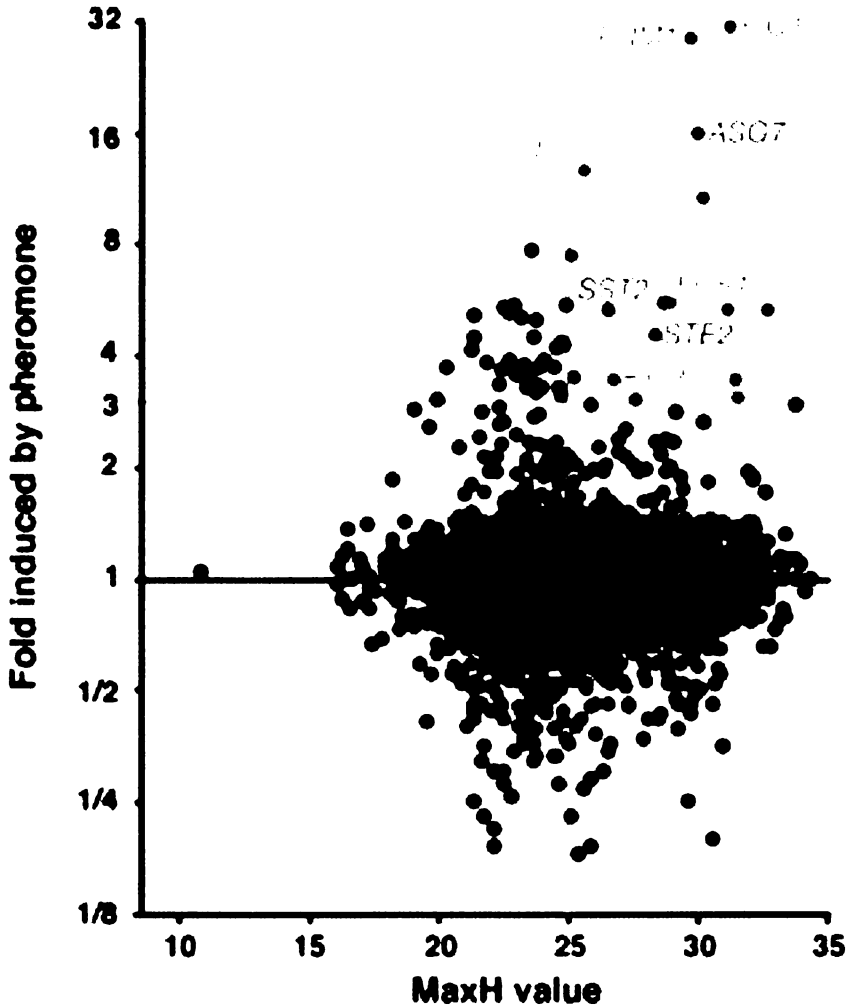

Figure 2-1

Identification of pheromone-induced putative membrane proteins by data mining

Dots represent the transcriptional induction in response to mating pheromone (y-axis) and likelihood of coding for a membrane protein (x-axis) of all 6,116 ORFs. ORFs induced more than three-fold with a MaxH score greater than 25 were investigated further. Green, mating-type specific. Orange, cell wall remodelling. Blue, involved in cell fusion. Red, uncharacterized PRM genes.

• four genes are involved in cell fusion (including the prototypical fusion genes *FUS1* and *FUS2;* (Trueheart et al., 1987) (Fig. 2-1, blue),

• three genes are involved in cell-wall synthesis and remodeling (including *AGA1* and *AGA2*, which encode the mating agglutinins; (Cappellaro et al., 1991)) (Fig. 2-1, orange),

• and three genes are involved in other functions relevant to mating (including *STE2*, which encodes the **a**-specific pheromone receptor;(Jenness et al., 1983)) (Fig. 2-1, green).

The remaining ten ORFs had not been studied (Table 2-1; Fig. 2-1, red). Based on the successful identification of other membrane proteins involved in mating, they have a high likelihood of also being players in the process. We describe here the characterization of the most highly induced ORF, *YNL279w*, which we call *PRM1*.

Prm1p is a conserved fungal protein with five putative transmembrane domains

The predicted *S. cerevisiae* Prm1p has clearly identifiable homologs in other fungi, such as *C. albicans* (Contig 5-2425, position 7551 to 5680), *S. pombe* (GenBank: 7630122), and *K. lactis* (GenBank: AJ229977, (Ozier-Kalogeropoulos et al., 1998)) (Fig. 2-2A), but contains no recognizable motifs to hint at its function.

Prm1p has five conserved regions that, based on their hydrophobic character, are likely to span the membrane (Fig. 2-2A, overlined). These putative transmembrane domains would divide the protein into two segments of about 175 residues each on one side of the membrane and two 50 - 100 amino acid segments on the other side of the

Table 2-1

Characteristics of the PRM genes

Gene	ORF	Pheromone induction[1]	Predicted protein size[2]	Predicted transmembrane segments (TMs)[2]	Notes
PRM1	*YNL279W*	31-fold	661 aa	5 TMs	Probable coiled-coil[3]
PRM2	*YIL037C*	11-fold	656 aa	4 TMs	Probable coiled-coil[3]
PRM3	*YPL192C*	8-fold	133 aa	1 TM	
PRM4	*YPL156C*	6-fold	284 aa	1 TM	
PRM5	*YIL117C*	5-fold	318 aa	1 TM	
PRM6	*YML047C*	5-fold	352 aa	2 TMs	
PRM7	*YDL039C*	4-fold	115 aa	1 TM	
PRM8	*YGL053W*	4-fold	237 aa	2 TMs	
PRM9	*YAR031W*	3-fold	298 aa	3 TMs	
PRM10	*YJL108C*	3-fold	383 aa	5 TMs	

[1](Spellman et al., 1998); http://genome-www.stanford.edu/cellcycle/

[2](Costanzo et al., 2000); http://www.proteome.com

[3]Predicted using (Singh et al., 1999); http://theory.lcs.mit.edu/vmf

Figure 2-2

Comparison of Prm1p sequences from *S. cerevisiae*, *C. albicans*, and *S. pombe*

(A) Chemically similar, aligned amino acids are shaded. In the *S. cerevisiae* sequence, predicted transmembrane domains are overlined and potential glycosylation sites are boxed. **(B)** Schematic of proposed topology for Prm1p. All consensus glycosylation sites (*S. cerevisiae*) are marked with **Y**. The intensity of shading indicates the degree of sequence similarity between the three yeast homologs: the sequence is divided into 40 blocks, each 15 amino acids in length, and each block is shaded according to the number of conserved residues contained in a 45 amino acid window centered on it. Overall percent identity between sequences: *S. cerevisiae* and *C. albicans*, 20% identical; *S. cerevisiae* and *S. pombe*, 22% identical.

A

```
                                                                1
S. cerevisiae  MSGFKCYLQLGDRLSQINLNKYTLVLLLAMLKLLFFSKSIQHAIEVSETYILSNCYSIDS
C. albicans      MFRNYLNLPEILTQVYLNKYAILLILILIKLILLETSILDNLNLVLLD-----NSICD
S. pombe         MASSYLSLAARLSQCNISPNSLCCLYILMQFFLFTKDLNTKIGDFVNDEQATCNYIQE

                                                                                2
S. cerevisiae  LYSKMTDNTPHYLGIMGNYLIEKGMEETVKATLETLSLIVYASEGLVNFAIDLYLGTYAC
C. albicans    NGEI-----QPVLNTV-HYMIVDSLQTLEAAGIVSIILTLKVIKQLALFFIELFFGTYIC
S. pombe       KVDILLDSPSLIANAA-VRVAKDGIQSTVKIILSGISDSLIAAENVFIFFIEFSYGTYLC

               1
S. cerevisiae  LIVSAVDGTVDVATNITEKLISLVNDTVSSVANELDTGLNDISKIINKVIKAASKVENFF
C. albicans    LLNAALKGSTEVALDASEGVIRAVNATVVSATNDIESALKGLSLIINDLVTGFNAIKNMF
S. pombe       LIQLAIDGILDAVADVGEEIGTAVNDTLHAIADEIEDTVSSLNEVFQSAEDSLEKVASWL

S. cerevisiae  TGDDDDSNMTSSIKSVNLTISALMNLYIPSSINDKLEELSAKTPDFAQVKNTTKNLISVP
C. albicans    TGSKSDPTQYQNKINITLGDLKSKIMIPSEVLTKLDNFKNSSLYGLSQLGNGTQTIVSTP
S. pombe       GEDINLP-------NVSIPEIQSLRNFTLSSSYDTEFEKLKAGVNFDSAINATKAAISKP

S. cerevisiae  FNEVRKNIKAVNASNIIGDTSVLYVPPVSLDNSTGICSSNQSEILAFYSILGHVLKTATV
C. albicans    FELAIKKLNTW-KLSYNFTTGA-----PSPINFREECLKDWSKLKDVQTDLAKLVEKISK
S. pombe       FSSARNLILEK-VSNYSFDTSM-----VSSPNKTHVVVCSTDDLTAISSFILSSIYKIRK

                    3
S. cerevisiae  VCITVLICFAVGAMAPVAWNEIKLNRRLCGMRDHYMLSRQDSYTSFSSENTHELKDPFRD
C. albicans    NLFIGLVLAMVGSILYVSYIQNRHNRR----------MDKFISETGID--KEVQFRNQY
S. pombe       VVIISLLIIIAGLFLISSIYEINKNCRI----RHKAFLLDEHIRSNKFEDTRDLISYIES

S. cerevisiae  PPIQNGQYDVIASYQQCFQTANNTRIAGNMTNLVTFGKSPENIDPKTKQKIENVVAYMTSE
C. albicans    NIYNNFLIYTIVKRMGIE----------LNERTIWMLSFWFSK
S. pombe       PISWNLKYFISALPLPCF----------LSVQLRNFITYIFHP

                          4
S. cerevisiae  RALCVLGIGLLGILVCICQFVMIALLKHKISHSLTSNDGDGVQNLLKSSTAVDIENQMSL
C. albicans    ISRNVFFFGIMGVVSVVAQYILLNSVQ-----SSMNNHIKSFDITSNSTSM----SASTI
S. pombe       PAAMILFISCTSFISGILQLVLLNNIRE--DGSVISALAQNSFHKVESALA----NVSVA

S. cerevisiae  NSVQTNKYINTTETNINQEVFGNINTTTLSVNNTVATMISDIDTTLADVFNGTLLYNPMK
C. albicans    YLRDMNTYIDDTQDKLNQELFSGIKEISVSLNSTIVEFLDKLNETLSDIFGSTPLAGPIN
S. pombe       NANSTNQIILKNQENINNNMFGSIHNTTLSLNSTLNTFMNELNSSMTSAFGDTFLASTVQ

S. cerevisiae  TVVGCAIENKLYTIEKAMTNIHDKAQLHIPRINGTQIKQALAKQTDNSTI--PTASSTSA
C. albicans    TVVYCTIGRKLEKVEKGLTNMNDNLNINIPSISRDI-EDGLSHMTF--------LQPQSVL
S. pombe       NVMNCLLYRKIENFEEVLTNVYNKSHIELPLLPTDILSKSIDNQTIYSSLYSSLNSSNST

                                                                    5
S. cerevisiae  ATENLLENLVNDMREGLLKILRAYHRITLGELTVALV-ILAVNLVQLPIALVILRLRLRK
C. albicans    ARANKIIDLYRKSILLELYISLGLLGVNLFQIFVGSATLTIRYWNSTRQGNNSYAISSPH
S. pombe       VSFSQIFDRVEKSVISELNFSFLFFLLNLLICAFGLIGVLSSNLKSLFLSLLDLVIPNPK

S. cerevisiae  ATFD
C. albicans    ELSEQEKQVYGYPLSHPLIDGKDLTTSSSFYPTTEEKLK
S. pombe       ENITLPVQSLAFPVTKSCRPPPIPPRESHVYDFQNFQYEEDDCIDYKRSLGLISLSSDLA

S. pombe       IDIPISPAIISDIQFNSITTESEETTYLLKEKQDRY
```

B

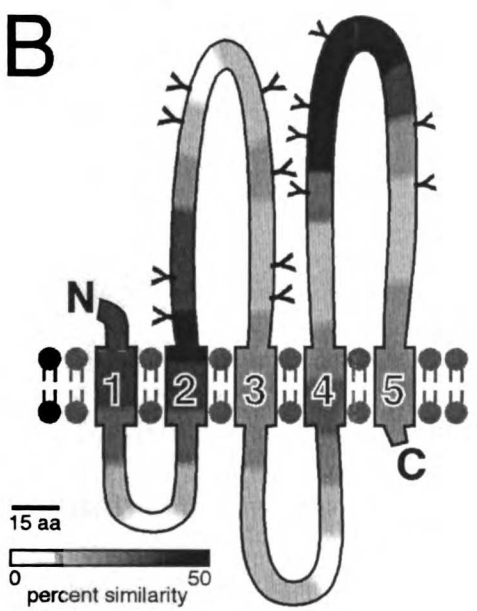

membrane (Fig. 2-2B). Together, both of the larger segments harbor 14 potential N-glycosylation sites (Fig. 2-2A and B, boxed and Y symbol, respectively), whereas the smaller ones have none. The large segments display the greatest sequence similarity between the three homologs, with about two-thirds of the residues conserved. Intriguingly, these segments are identified as potential coiled-coil-forming regions by LearnCoil-VMF, a program designed to recognize viral fusases (Singh et al., 1999). However, it is unlikely that a coiled-coil structure could assemble within a region of the protein that is anchored on both sides by transmembrane segments. The predicted overall picture of Prm1p, then, is that of a multispanning integral membrane protein presenting a large, evolutionarily conserved face on one side of the membrane and a smaller, less conserved face on the other (Fig. 2-2B).

Pheromone rapidly activates Prm1p expression in both mating types

To characterize Prm1p, we constructed strains carrying a fusion gene that appends an HA-epitope tag to the protein's C-terminus (Prm1p-HA). We then assayed cells under mating or control regimes for the expression of Prm1p-HA by resolving total cell lysates with SDS-PAGE and visualizing Prm1p-HA by immunoblot.

Vegetatively growing cells did not express Prm1p-HA at detectable levels (Fig. 2-3, lane 1) but initiated expression within five minutes after addition of α-factor (Fig. 2-3, lane 2). After 20 min of pheromone treatment, the Prm1p level reached a maximum and persisted at steady state (Fig. 2-3, lanes 5 - 7).

Figure 2-3

Expression profiles of Prm1p

(A) A strain of mating type **a** bearing a chromosomal copy of *PRM1-HA* (lanes 1-7 and 9), or a wild-type control strain (lane 8) was treated with 10 μg/ml alpha factor for 0 to 30 min, pelleted, and lysed by bead beating. Extracts were resolved by SDS-PAGE on a 12.5% gel and immunoblotted using an anti-HA antibody. For lane 9, the extract was treated with endoglycosidase H before analysis by SDS-PAGE. **(B)** The following strains were mixed: control wild-type strains of mating types **a** and α (lane 10); an **a** strain bearing *PRM1-HA* and an untagged strain of the same (lane 11) or the opposite (lane 12) mating type; an α strain bearing *PRM1-HA* and an untagged strain of the same (lane 13) or the opposite (lane 14) mating type. These mixtures were rotated for 30 min at 30°C, pelleted, lysed, and the extracts were analyzed as above. The 73 kD form of Prm1p, presumably corresponding to the primary, unglycosylated translation product is indicated with the *arrowhead.* The glycosylated forms of Prm1p migrating as a broad band centered at 115 kD are indicated with the *bracket.* A 15 kD putative proteolytic fragment is indicated by the *asterisk.* **(C)** The *PRM1* promoter sequence, beginning 250 nucleotides upstream of the translational start codon is shown. Pheromone response element consensus sequences are underlined.

A

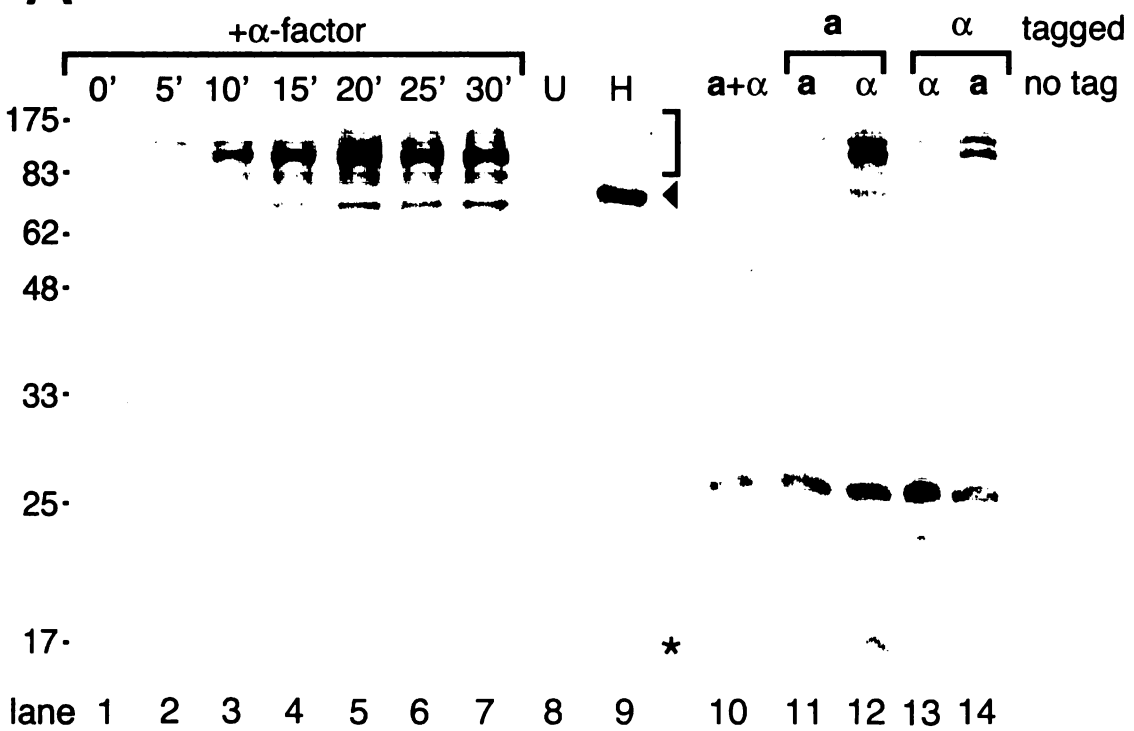

B

-250 TTTCACGGGA TTTTCGTTTA GGTGAAAATA AAATGAACGA CAGAGCATGC

-200 AGAGTCCGGG TAATACATAT GTTTCAATAC TGTTTCAATA CTGTTTCAGA

-150 AGTGCGTCAC ATATTAATTT TAACTTATAA CTGGCCTGTT GCTGGCAAGA

-100 GGTATATATA TATGACGAAT GTGACCAACA TAAGTCCTTA AGATAATCCC

- 50 GAAATATTTG GTTAGGATGA TTCCCTTTCG AATTTGTGAA CGTTGATGAT

Western blot analysis identified Prm1p-HA (and by extension Prm1p) as several major forms: a sharp band migrating at 73 kD, the size predicted from the *PRM1-HA* open reading frame (Fig. 2-3, closed arrowhead), and a series of broad bands centered at roughly 115 kD (Fig. 2-3, bracket). These species collapsed to a single band of about 73 kD after treatment with endoglycosidase H, indicating that the larger bands are heterogeneously glycosylated (Fig. 2-3, lane 9). The presence of extensive oligosaccharide addition confirms our prediction that Prm1p is initially integrated into the membrane of the endoplasmic reticulum and, based on the proposed topology in Fig. 2-2B, suggests that Prm1p may display its two large conserved segments on the lumenal or extracellular side of the membrane.

In addition to the newly synthesized and glycosylated forms, we also reproducibly observed a weaker band migrating at about 15 kD, which appeared after 30 min of pheromone treatment (Fig. 2-3, lane 7, star). Based on the position of the HA epitope, this band is likely to represent a C-terminal fragment, indicating that Prm1p-HA may undergo proteolytic processing during its maturation.

Cells of both mating types induce Prm1p when challenged with partners of the opposite mating type. Cells of mating type **a** expressed Prm1p-HA when mixed with untagged α cells for 30 min but not when mixed with cells of the same mating type (Fig. 2-3, lanes 11 and 12). The converse is also true (Fig. 2-3, lanes 13 and 14): α cells expressed Prm1p-HA when mixed with untagged **a** cells but not when mixed with untagged α cells. Prm1p-HA induction in α cells was weaker than in **a** cells, perhaps due to reduced diffusion of the lipophilic **a**-factor compared to the more hydrophilic α-factor.

The speed and extent of Prm1p expression during mating probably resulted from the presence of pheromone-responsive elements (PREs) upstream of the gene's coding sequence, as is true for many other mating-specific genes. The promoter of *PRM1* contains three head-to-tail repeats closely matching the consensus PRE, TGTTTCA(A/T) (Fig. 2-3B) (Yuan and Fields, 1991). The repeats are separated by a trinucleotide spacer TAC. These sequences appear 180 to 150 nucleotides upstream of the *PRM1* coding sequence and probably serve as binding sites for the transcription factor Ste12p, a target of the MAP kinase cascade which links gene expression to the presence of extracellular pheromone (Herskowitz, 1995).

Prm1p localizes to the site of cell fusion

As a first step towards elucidating the function of Prm1p, we asked in what cellular compartment(s) the protein resides. To this end, we constructed strains bearing a chromosomal copy of a *PRM1-GFP* fusion gene driven by its own promoter, which allowed us to detect the Prm1p-GFP gene product by fluorescence microscopy.

Prm1p-GFP first became visible after 40 min of pheromone treatment as two rings, one encompassing the nucleus and one at the cell periphery (Fig. 2-4A). This staining pattern is typical of the endoplasmic reticulum in yeast, consistent with Prm1p entering the secretory pathway.

Seventy minutes after addition of α-factor most cells have arrested in the G1 phase of the cell cycle, evidenced by their large unbudded state, and have begun to polarize.

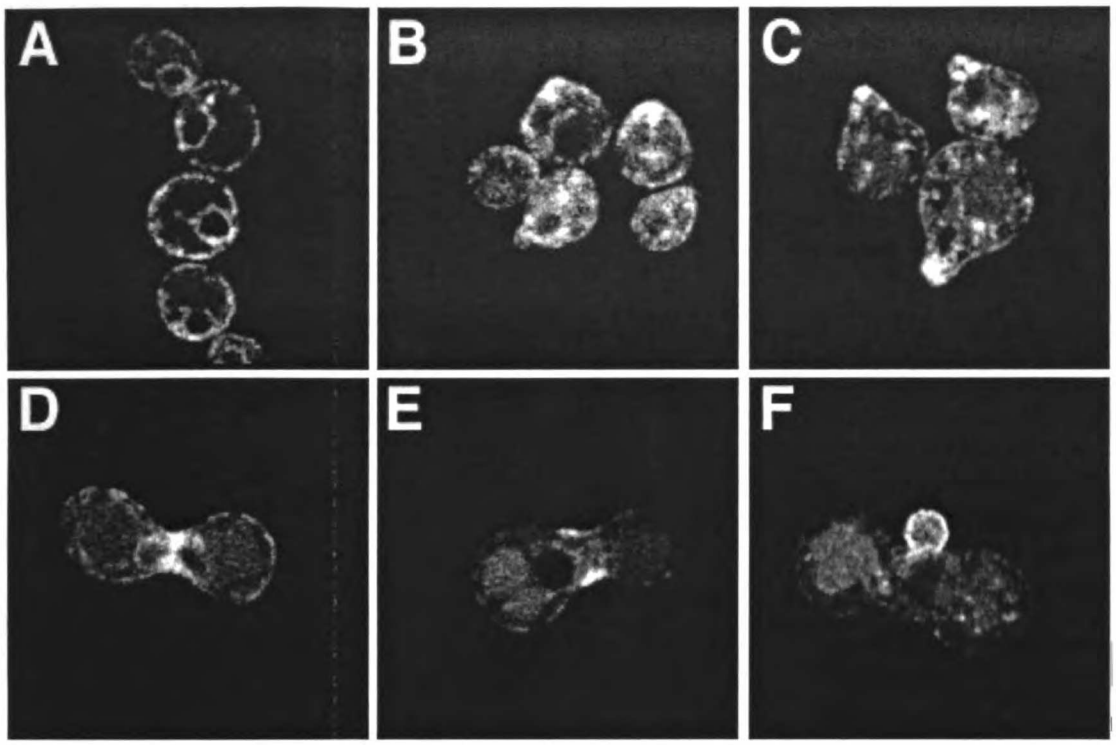

Figure 2-4

Localization of Prm1p

(A, B, C) A strain of mating type **a** bearing a *PRM1-GFP* fusion gene was treated with 10 μg/ml α-factor. Samples were taken and imaged on a confocal microscope after 40, 70, and 100 min of incubation, respectively. Apparent loss of ER staining in **B** and **C** is due primarily to differences in signal gain used to collect each image. **(D, E, F)** Strains of opposite mating types, each bearing the *PRM1-GFP* fusion gene, were mixed, concentrated, and spotted on a YPD plate. After about 2 hours at 30°C, cells were resuspended and imaged as above. Images of representative cells are shown.

Prm1p accumulated in the "potbelly" formed by this polarization in addition to its persistent staining of the endoplasmic reticulum (Fig. 2-4B).

By 100 minutes of pheromone treatment, most cells have formed mating projections, or shmoos. These shmoos would, in a more physiological setting, orient towards the greatest pheromone concentration and serve as the site where mating partners first make contact. Prm1p localized to the tip of the shmoo, where cell fusion would occur (Fig. 2-4C).

We next mixed **a** and α cells, both bearing the *PRM1-GFP* fusion gene. In such physiological mating mixes, Prm1p-GFP localized at the midpoint of recently formed mating pairs, or zygotes, where two cells have met and have initiated the steps required to degrade the intervening cell wall and fuse their plasma membranes (Fig. 2-4D). In mating pairs that have already completed this fusion step, Prm1p-GFP formed a collar around the neck of the zygote (Fig. 2-4E).

When the resulting diploid began to bud, Prm1p-GFP localized to the growing daughter (Fig. 2-4F). Since diploids no longer express Prm1p (data not shown), the protein staining the first daughter was probably inherited from the parental cells.

More than half of all mating pairs deficient in *PRM1* fail to fuse

To test whether Prm1p participates in cell fusion during mating as its expression profile and localization suggested, we constructed strains in which *PRM1* was deleted by gene replacement (see Methods). When both mating partners lacked *PRM1*, we observed morphologically aberrant mating pairs by phase contrast microscopy. The most common

aberration was the presence of a pronounced dark band at the mating pair neck, reflecting the undegraded cell wall between mating partners suggestive of a defect in cell fusion.

To monitor this phenotype more decisively, we constructed a *Δprm1* α strain expressing a soluble, cytosolic form of GFP that marks its cytoplasm. This strain allowed us to readily distinguish fused zygotes from unfused mating pairs by scoring whether GFP had spread to both cells (indicating successful cell fusion) or remained restricted to one mating partner (indicating a failure to fuse). Using this assay, we observed unambiguously that matings between *Δprm1* partners produced a mixture of fused zygotes and unfused mating pairs (Fig. 2-5, A and B).

We next quantitated the degree of the *Δprm1* fusion defect using GFP-expressing wild-type and *Δprm1* α strains. To do so, we mixed exponentially growing cultures of each of these strains with an appropriate partner strain, concentrated them on a filter, and placed the filter on a YPD plate where the cells were allowed to mate for three hours. We then fixed the cultures for microscopy. At this point, zygotes produced by wild-type control cells were abundant but most were still freshly formed, having just begun to grow their first diploid bud.

In such mating mixes between wild-type control strains, 6 percent of zygotes/mating pairs scored as unfused (Fig. 2-5C). Presumably, this baseline level reflects a kinetic intermediate in the mating reaction, and these cells would have eventually fused if the reaction were allowed to continue. Characteristically, these unfused mating pairs had a narrow neck. In contrast, when both mating partners lacked *PRM1*, 55 percent of zygotes/mating pairs were unfused, a nine-fold increase over the number observed for

Figure 2-5

***Δprm1* cells exhibit a fusion defect during mating**

(A, B) *Δprm1* **a** cells were mixed with *Δprm1* α cells expressing soluble cytosolic GFP as a reporter of cytoplasmic mixing between mating partners. This mixture was applied to a nitrocellulose filter and incubated for 3 h on a YPD plate. Fluorescent micrographs that show the GFP-stained cytoplasm of the α partner were super-positioned over bright-field images that depict the entire zygote/mating pair. **(C)** Mating mixes in which either the **a** partner, the α partner, both or neither carry a deletion of *PRM1* were prepared as described above. In all cases the α partner carried soluble cytosolic GFP. Zygotes/mating pairs were visually identified and then scored with regard to cell fusion by microscopy. Bars represent the average percent of zygotes/mating pairs that scored as unfused in four independent experiments. During each experiment, 300 zygotes/mating pairs per mating mix were counted: WT **a** x WT α, 6.2 ± 0.8 %; WT **a** x *Δprm1* α, 11.7 ± 4.0%, *Δprm1* **a** x WT α, 12.5 ± 4.0%; *Δprm1* **a** x *Δprm1* α, 54.3 ± 4.5%.

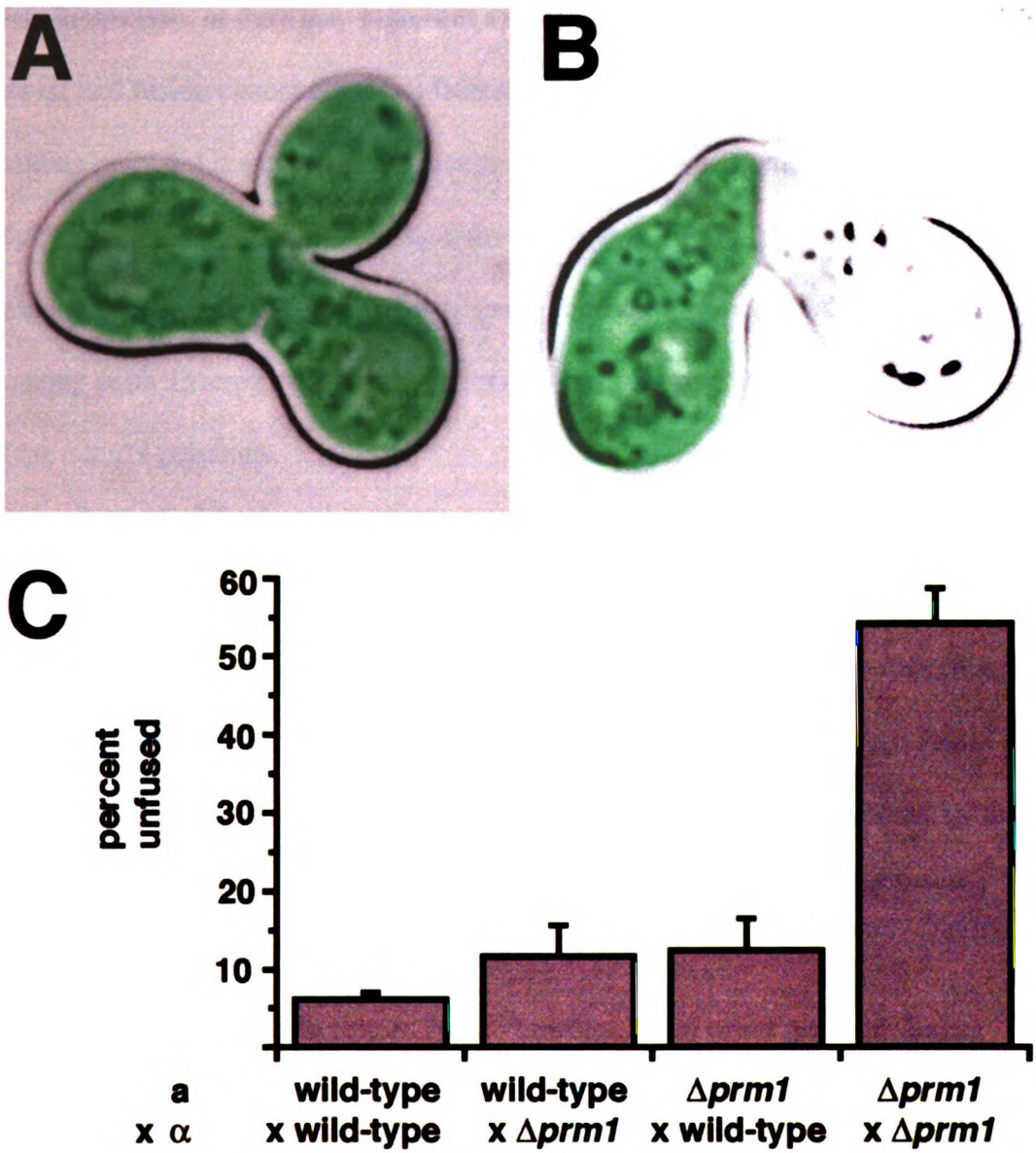
A
B
C
percent unfused
60
50
40
30
20
10
a
x α
wild-type x wild-type
wild-type x Δprm1
Δprm1 x wild-type
Δprm1 x Δprm1

wild-type strains (Fig. 2-5C). These mating pairs may reflect either a kinetic delay in the fusion reaction, or they may represent a dead end in which some step in mating has gone awry, and fusion cannot occur. At later time points the ratio of fused zygotes to unfused mating pairs did not appreciably change (data not shown), contrary to what a kinetic delay would predict. Moreover, in many of the mating pairs from a *Δprm1* x *Δprm1* mating, the neck diameter was significantly increased, indicating that these unfused mating pairs differed qualitatively from the ones observed at low frequency in the wild-type control reactions.

Is Prm1p required in both partners to promote efficient cell fusion? When one mating partner lacked *PRM1* and the other was wild-type, we consistently observed a slight but significant fusion defect, with 12 percent of all mating pairs failing to fuse (Fig. 2-5C). This defect was similar regardless of which partner carried the wild-type *PRM1* allele. These results suggest that Prm1p functions symmetrically and can perform its duty even if present in only one mating partner, albeit at a consistently reduced efficiency.

Δprm1 mutant mating pairs form "bubbles," and other strange shapes

In addition to the simple unfused phenotype shown in Figure 4B typical of all fusion mutants, we observed more unusual morphologies in *Δprm1* x *Δprm1* matings. Notably, some mating pairs displayed intercellular "bubbles," pockets of GFP-labeled or unlabeled cytoplasm from one mating partner which appeared to have invaded the other (Fig. 2-6, A - G). These bubbles appeared with approximately equal frequency in either direction: "innies" invading the α partner (Fig. 2-6, A and B), and "outies" extending from the α cell into the **a** cell (Fig. 6, C - G). Bubbles varied in size and shape, ranging from tiny

Figure 2-6

The *Δprm1* cells' failure to fuse sometimes results in intercellular "bubbles"

Mating mixes were prepared and imaged as described in the legend to Figure 2-5. Representative images are shown. **(A, B)** "Innies" intruding from the **a** cell (non-fluorescent) to the α cell (fluorescent). **(C, D, E, F)** "Outies" protruding from the α cell to the **a** cell. Note that the **a** cell in Panel D escaped G1 arrest and started budding. **(G)** A multi-lobed "outie." **(H)** An α cell, lower right, simultaneously adhered to two **a** partners. The partner on the left has begun to bud.

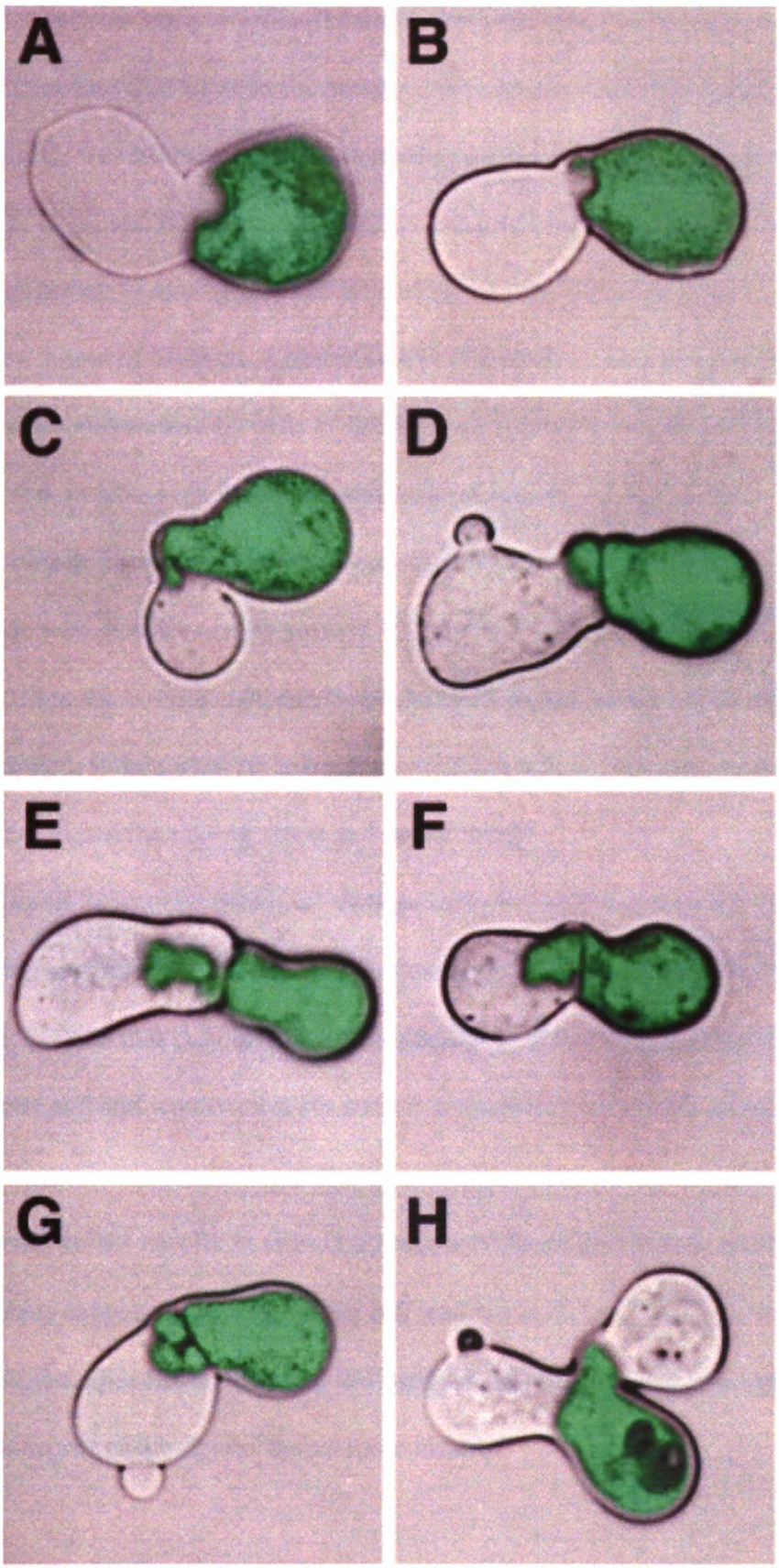
A
B
C
D
E
F
G
H

bulges in an otherwise straight cell-cell interface to large rounded pockets or, rarely, serpentine extensions that stretched across the entire length of the other mating partner.

Additionally, we observed one or both mating partners having budded a new daughter cell (Fig. 2-6, D, G, and H). Budding indicates that a cell has escaped from the G1 arrest induced by exposure to mating pheromone and has re-entered the cell cycle, committing itself to a new round of division. Apparently this release from pheromone arrest can occur even when surrounded by cells of the opposite mating type that are secreting pheromone and, in fact, even while adhered to one of them.

Lastly, some cells appeared to give up on the failed mating and, instead of budding, began to mate with another nearby partner. For instance in Figure 2-6H the GFP-expressing cell in the bottom right seemed to have attempted to mate with the partner on the left and failed. It then went on to try anew with the cell on the right, while its original mating partner exited the mating arrest and began to bud.

The ability of these cells to exit G1 or to polarize towards a new partner and re-initiate mating suggests that *Δprm1* mutants do not simply fuse more slowly than wild-type. Rather, the fact that they abandon their attempt at fusion indicates they have reached a dead end and would not form normal diploid zygotes even if given more time.

The *Δprm1* defect results in closely apposed, unfused plasma membranes

The bubbles suggested a breach of the cell wall between the mating partners, a phenotype unlike other fusion mutants. We used thin-section electron microscopy to examine this aspect of the *Δprm1* defect more closely.

Many mating pairs exhibited an apparent dissolution of their cell wall at the center of the interface between the mating partners (Fig. 2-7, A - D). In most cases we found it necessary to examine serial sections through a single mating pair to find the point where a breakthrough occurred. The region of cell wall degradation almost invariably included the center of the cell-cell interface. In some cases it appeared restricted to the center (Fig. 2-7, B and D) while in others it seemed to have spread asymmetrically to one edge of the mating pair (Fig. 2-7, A and C).

Wild-type matings involve a similar local disruption of the cell wall at the center of this interface, followed by plasma membrane fusion and continued cell wall remodeling until the cytoplasmic bridge between the cells spans the entire width of the zygote and the cell wall becomes restricted to the periphery (Gammie et al., 1998). Details of the intermediates following cell wall breakdown but preceding membrane fusion are unknown because they have not been captured by electron microscopy, presumably because these steps occur rapidly.

Δprm1 cells appeared to complete successfully the initial cell wall breakdown but then failed to perform plasma membrane fusion and continued cell wall remodeling. At the site where cell wall was removed in *Δprm1* matings, the two plasma membranes came into close apposition (Fig. 2-7). Additional membrane appeared to be added to this region equally by both partners, generating bulges that are likely to correspond to the bubbles seen by fluorescence microscopy. Thus, the volume of one mating partner must have grown while the volume of the other one shrank by the same amount. Meanwhile their surface areas must have increased coordinately.

Figure 2-7

Δprm1 cells successfully degrade their cell wall and juxtapose plasma membranes, but then fail to fuse

Mating mixes of _Δprm1_ partners were prepared as described above. The cells were then fixed, stained, and imaged by electron microscopy. Three different magnifications are shown for each image **(A - D). Left panels**: Unfused mating pairs. The fuzziest outermost layer of the depicted cells is the cell wall; the dark line underlying it is the plasma membrane. **Middle panels:** Magnification of the box from the left-side panels, showing detail of the bubble. **Right panels.** Magnification of the box from the middle panels, showing tightly juxtaposed membranes at a set distance.

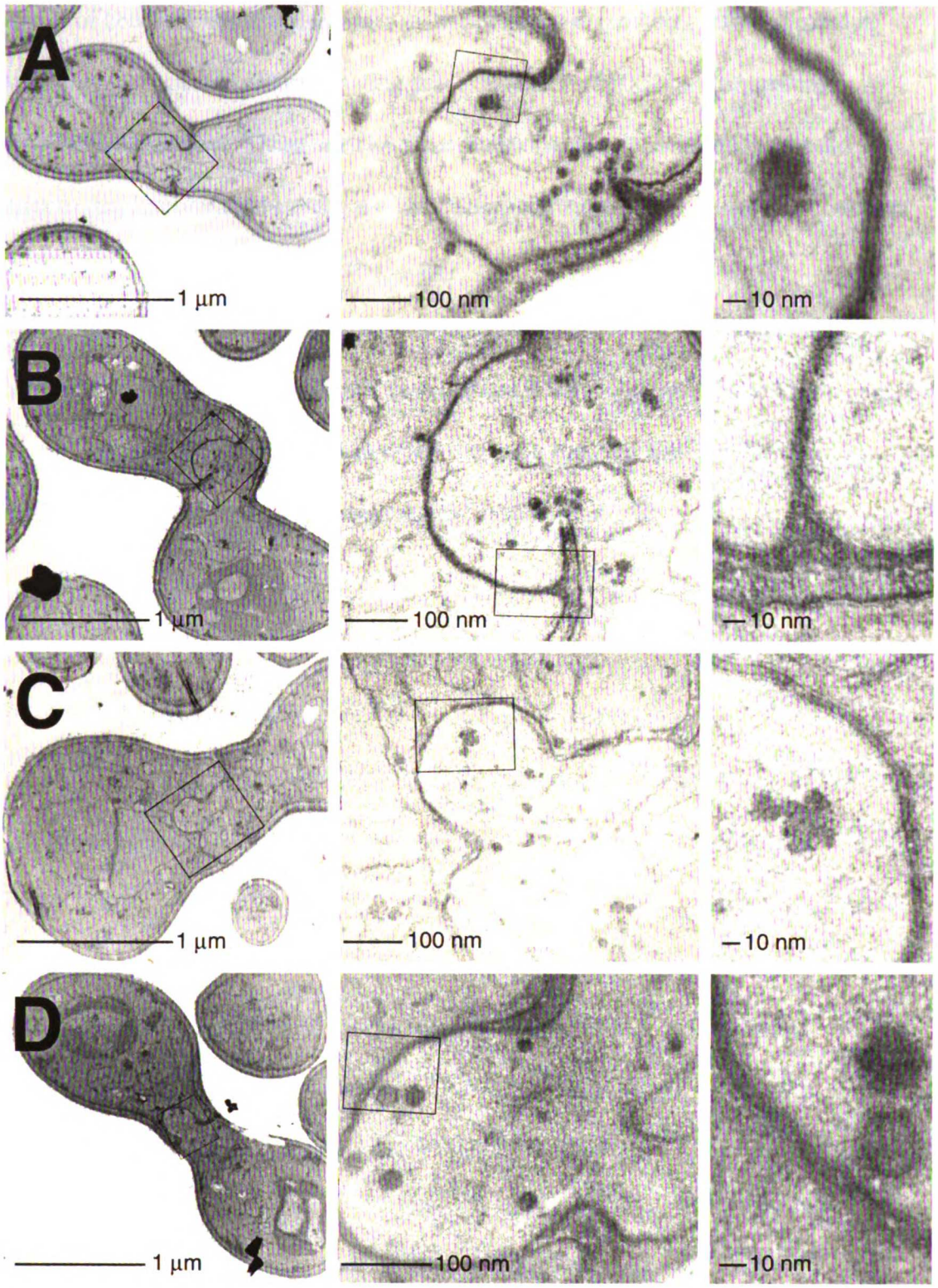
A
1 µm
100 nm
10 nm
B
1 µm
100 nm
10 nm
C
1 µm
100 nm
10 nm
D
1 µm
100 nm
10 nm

Vesicles of about 20 nm diameter were usually present in the bulge, often aligned in single-file rows oriented along a mating pair's long axis (Fig. 2-7A), suggesting cytoskeletal attachment. These vesicles were packed with a densely staining material similar to that intervening between the two mating partners. These vesicles may deliver new membrane causing growth of the bulge.

Interestingly, the juxtaposed plasma membranes of the bulge were equidistant, consistently remaining separated by a gap of about 8 nm along their entire length (Fig. 2-7). A thin layer of densely staining material was seen between them, reminiscent of membrane adherence junctions found between mammalian cells.

DISCUSSION

***PRM1* encodes a mating-specific transmembrane protein that promotes cell fusion at a very late step**

We identified a novel protein with several traits expected of a factor involved in cell fusion during mating. First, Prm1p is expressed by cells of both mating types only in response to pheromone. Second, it localizes to the tips of mating projections in shmooing cells and to the necks of mating pairs and zygotes. Third, in its apparent topology it would present two large domains to the plasma membrane of a mating partner, domains which are conserved between widely divergent fungi. Lastly, deletion of *PRM1* results in a significant defect in cell fusion, resulting in a nine-fold increase in the number of unfused mating pairs compared to wild-type matings. Thus, in some respects *PRM1* resembles many genes described already. In one key regard, though, it differs dramatically from genes found to date. The unfused zygotes produced by a *Δprm1* mating do not arrest with an intact cell wall as other fusion mutants do(Elia and Marsh, 1996; Elia and Marsh, 1998; Erdman et al., 1998; Gammie et al., 1998; Kurihara et al., 1994; Santos et al., 1997). Instead *Δprm1* mutants successfully degrade the cell wall and bring the mating partners' plasma membranes into close proximity. Nevertheless, the membranes remain unfused. This intermediate in the mating reaction has not been trapped before and defines a new step in the pathway. Upstream of membrane fusion, downstream of cell wall breakdown, Prm1p stands in a unique position to help us understand how the bilayers associate and what drives their fusion.

What does Prm1p do?

At present, we have insufficient information to distinguish among various models of how Prm1p may facilitate membrane fusion. In principle, Prm1p could either act directly at the fusion step, as a novel fusase, or indirectly, at a step upstream of fusion.

The simplest interpretation of the *Δprm1* phenotype is that Prm1p participates directly in the fusion reaction. Yet this model must be reconciled with two observations. First, mutants lacking a fusase would be expected to display an absolute mating defect. On the contrary, almost half of all *Δprm1* x *Δprm1* mating pairs still fused successfully, and, using classical plate-based mating assays that measure diploid formation among thousands of cells at a time, the *Δprm1* mating defect appeared negligible (data not shown). Thus, if Prm1p plays a direct role in membrane fusion, an alternative fusion machine (or other subunits in a Prm1p-containing complex) must exist and take over, albeit inefficiently, upon removal of Prm1p. Second, the suggested multi-membrane-spanning topology of Prm1p does not readily conform to the paradigms developed for viral or SNARE-containing fusases. In particular, full-length Prm1p offers no extracellular free ends that could easily be envisioned to function either as classical fusion peptides or to engage in coiled-coil interactions. Thus, it will be important to define the biochemistry of Prm1p in more depth: Does Prm1p associate with other subunits? Is it proteolytically processed when expressed on the cell surface (as hinted at by the preliminary observation of the C-terminal fragment in Figure 2-3A)? Proteolytic processing could generate protein fragments with a different — and in light of existing models more appealing — topology. Ultimate proof of a direct role of Prm1p in

membrane fusion, of course, would only come from a biochemical demonstration that Prm1p, possibly with associated subunits, is sufficient for lipid bilayer fusion.

The alternative notion is that Prm1p acts upstream of the fusion event, in either a signalling or a structural capacity. For instance, Prm1p could act in a pathway that senses the proximity of mating partners and responds by activating the fusion machinery. Experiments with mutants weakly deficient for pheromone production have suggested the existence of such a pathway (Brizzio et al., 1996; Elia and Marsh, 1996). Indeed, one of these mutants was noted to produce structures resembling *Δprm1* bubbles, albeit at low frequency (see Figure 3D in (Elia and Marsh, 1996)). Another possibility is that the *Δprm1* defect may be a structural problem rather than a signaling one. The densely staining matter separating plasma membranes may represent cell wall debris that a *Δprm1* mutant cannot clear. However, since any remaining cell wall debris would have to bend and thin as the bubbles grew, the membranes of large bubbles should be closer together than those of small bubbles. In fact that is not true: the gap is consistently about 8 nm wide along the entire membrane interface regardless of the bubble's size. This observation argues that the gap is occupied not by undegradable cell wall debris but by a specific structural element deposited uniformly as the bubble grows, possibly an adhesion complex fastening membranes in a pre-fusion state. Without Prm1p the adhesion complex might still assemble but function poorly. Consequently, membranes would stick together but not fuse.

Stalking the elusive fusase

We present here the results of a new kind of gene hunt, one that is likely to become increasingly prevalent as genomic databases grow. Previously the problem of membrane fusion during yeast mating had proven refractory to genetic approaches. Despite attacks from several directions and the identification of many interesting genes that act during zygote formation, *PRM1* is the first gene that clearly has some role at the level of membrane fusion. Why have mutants in this step been so difficult to find?

Most successful screens have recognized and in some way circumvented the central challenge of mating genetics. Specifically, in order to achieve an appreciable deficit in diploid formation it is usually necessary to impair a pathway not just in one cell but in both mating partners. Three kinds of strategies have solved this problem. First, some groups have taken on the formidable challenge of performing random mutagenesis in a way that generates each mutation in both mating types with complementary selectable markers (Berlin et al., 1991; Kurihara et al., 1994). This approach allowed a direct assay of the mating efficiency of any given mutant crossed to itself. This strategy has the advantage of not biasing toward a particular pathway—indeed, genes controlling not only cell fusion but nuclear fusion were found with it—but , perhaps due to its complexity, was burdened by a high background of false positive mutants which discouraged pursuing this approach to saturation.

A second approach uses a pre-existing defect in a known fusion pathway, for example *fus1 fus2* mutants (both of which genes were found serendipitously in existing lab strains), and asks for new mutants that mate poorly with the enfeebled strain but not with a wild-type strain (Berlin et al., 1991; Chenevert et al., 1994). This strategy has the

advantage of being straightforward to set up and execute, although it is probably biased towards the pathway of the starting mutation and may not effectively find components of new pathways.

Lastly, pheromone-regulated genes have been identified and then mutants in these genes assayed for mating defects. This approach was originally carried out using a randomly integrated reporter construct (Longtine et al., 1998). We have here expanded and simplified this latter approach using pre-existing genomic datasets combined with a computer-aided search for hydrophobic proteins. This technology let us begin examining candidate gene disruptions without ever doing a traditional screen. The Webminer software makes this approach readily adaptable to many studies that seek proteins expressed under certain conditions, not expressed under other conditions, and containing specific structural features.

The identification of Prm1p's role in cell fusion underscores the sensitivity of this computer-aided approach. Although the penetrance of the *Δprm1* mating defect is probably at the limit of what traditional screens can detect, by identifying a small group of candidate genes and examining individual mating pairs in which both partners carried the relevant mutation we could witness a unique phenotype that now offers an opportunity to examine the mechanisms of bilayer association and fusion in molecular detail.

METHODS

Informatics

Programs were written in the scripting language Perl. The source code for Webminer and a description of the database formats used are available at http://webminer.ucsf.edu. The *C. albicans* and *S. pombe* homologs of *PRM1* were identified by BLAST searches of the unfinished genome sequencing projects at the Stanford University DNA Sequencing Center at http://www-sequence.stanford.edu/group/candida, and the Sanger Centre at http://www.sanger.ac.uk/Projects/S_pombe/, respectively. Multiple sequence alignments were performed with MultAlin (Corpet, 1988). Transmembrane domain predictions were made using the SOSUI program at http://azusa.proteome.bio.tuat.ac.jp/sosui/ (Hirokawa et al., 1998) and then refined by discarding putative transmembrane segments not present in all homologs. Coiled coil predictions were made using LearnCoil-VMF, at http://theory.lcs.mit.edu/vmf (Singh et al., 1999).

Yeast strains and plasmids

Strains used in this study appear in Table 2-2. Gene replacements, epitope tagged constructs, and GFP fusions were generated with the PCR-transformation technique (Longtine et al., 1998): PCR was performed with unique primers and a standard set of template plasmids to generate linear DNA consisting of a pair of integration sequences targeted against *PRM1*, flanking a generic cassette. The cassette contained three copies of the HA-epitope tag, the coding sequence of GFP, or neither, and a selectable marker. Transformation of wild-type diploids resulted in insertion of this construct, such that it replaced the entire *PRM1* coding sequence or, for gene tagging, inserted in frame at its 3'

Table 2-2

The following strains were used. All were constructed in the W303 background.

MHY200	MAT**a**, *PRM1-HA:S.kluyveri HIS3*$^{+}$, *ura3-Δ99*, *leu2-Δ1*, *trp1-Δ99*, *ade2-101*^{ochre}, pRS314
MHY201	MATα, *PRM1-HA:S.kluyveri HIS3*$^{+}$, *ura3-Δ99*, *leu2-Δ1*, *trp1-Δ99*, *ade2-101*^{ochre}, pRS316
MHY153	MAT**a**, *PRM1-GFP:S.kluyveri HIS3*$^{+}$, *ura3-Δ99*, *leu2-Δ1*, *trp1-Δ99*, *ade2-101*^{ochre}, pRS314
MHY154	MATα, *PRM1-GFP:S.kluyveri HIS3*$^{+}$, *ura3-Δ99*, *leu2-Δ1*, *trp1-Δ99*, *ade2-101*^{ochre}, pRS316
MHY209	MAT**a**, *his3-Δ200*, *ura3-Δ99*, *leu2-Δ1*, *trp1-Δ99*, *ade2-101*^{ochre}, pRS314
MHY210	MATα, *his3-Δ200*, *ura3-Δ99*, *leu2-Δ1*, *trp1-Δ99*, *ade2-101*^{ochre}, pRS316
MHY198	MAT**a**, *Δprm1::S.kluyveri HIS3*$^{+}$, *ura3-Δ99*, *leu2-Δ1*, *trp1-Δ99*, *ade2-101*^{ochre}, pRS314
MHY199	MATα, *Δprm1::S.kluyveri HIS3*$^{+}$, *ura3-Δ99*, *leu2-Δ1*, *trp1-Δ99*, *ade2-101*^{ochre}, pRS316
MHY189	MATα, *his3–Δ200*, *ura3-Δ99*, *leu2-Δ1*, *trp1-Δ99*, *ade2-101*^{ochre}, pDN291
MHY191	MATα, *Δprm1::S.kluyveri HIS3*$^{+}$, *ura3-Δ99*, *leu2-Δ1*, *trp1-Δ99*, *ade2-101*^{ochre}, pDN291

end, replacing the natural stop codon. Following selection, diploids were assayed by PCR for correct insertion of the construct and then sporulated to recover haploids of both mating types that carried the integrated DNA. The plasmid pDN291, as previously described, was used to express soluble cytosolic GFP (Ng and Walter, 1996). The plasmids pRS314 and pRS316 are standard vectors containing the *TRP1* and *URA3* genes, respectively, which were used here to create a set of mating-type-specific selectable markers (Sikorski and Hieter, 1989).

Preparation of cell lysates and Western blotting

To detect expression of Prm1p-HA, 5 ml of an exponentially growing culture at optical density of 0.5 units A_{600} was either treated with 10 µl of a solution containing 5 mg/ml α-factor (Sigma, St. Louis MO) in DMSO or mixed with an equal volume of cells of the opposite mating type, also from an exponentially growing culture. When mixing cells of both mating types, the maximal gene induction was seen when both cultures had grown continuously in log phase overnight from very low density, presumably to allow accumulation of pheromone in the medium – indeed, the conditioned media of these cultures alone had detectable inducing activity (not shown). At the relevant time point after mixing, cultures were briefly spun at 4°C, and the supernatant was aspirated. The cell pellet was resuspended in 50 µl SDS-PAGE sample buffer, added to a small volume of glass beads, and lysed by continuous vortexing at 4°C for 90 s. The entire procedure took less than 4 min. The lysates were boiled for 10 min and then spun to remove insoluble debris. Alternatively, for endoglycosidase H treatment, cells were lysed as

above with the exception that sample buffer was replaced by 45 µl denaturation buffer as provided by the manufacturer (New England Biolabs, Beverly MA). Samples were then boiled 10 min, mixed with 5 µl G5 buffer as provided and 1 µl enzyme, incubated for 90 min at 37°C, and diluted 1:10 in SDS-PAGE sample buffer before loading. For Western blot analysis, lysates were run on a 12.5% SDS-polyacrylamide gel and transferred to nitrocellulose membrane using standard protocols. Membranes were blotted with a mouse monoclonal anti-HA primary antibody (HA.11, Covance, Princeton NJ) at 1:1000 dilution and a goat anti-mouse secondary antibody coupled to horseradish peroxidase (Bio Rad, Hercules CA) at 1:2000 dilution and developed with an enhanced chemiluminescence (ECL) kit (Renaissance kit, NEN, Boston MA).

Fluorescence microscopy of Prm1p-GFP

To visualize the localization of Prm1p-GFP in pheromone-treated haploids, cells were grown to log phase in defined media with twice the standard concentration of adenine to prevent accumulation of autofluorescent byproducts of adenine biosynthesis. The culture was then exposed to 10 µg/ml α-factor. Samples were taken at 40, 70 and 100 min after pheromone addition, placed on a slide, and imaged on a confocal microscope (Leica). Alternatively, to inspect Prm1p-GFP's localization in zygotes, cells of opposite mating types that each carried the *PRM1-GFP* fusion were grown to log phase, mixed in equal numbers, spotted on a YPD plate, and incubated for 2 h at 30°C. Cells were then resuspended from the plate, spotted on a slide, and imaged. Because the Prm1p-GFP signal was faint, a single medial optical section was first taken by averaging four high-intensity laser scans, which bleached most of the fluorescence. Then, a stack of eight

optical sections was collected to document the remaining fluorescence in the cells. This information was then used to deconvolve the high-intensity section, using OpenLab software (Improvision, Boston MA). Images were also smoothed and contrast-enhanced with this software.

Quantitative assay of cell fusion

Cells of opposite mating types, with the α strain expressing soluble cytosolic GFP, were grown to log phase, mixed, and vacuumed to a nitrocellulose filter. The filter was placed cell-side up on a YPD plate, and the plate incubated for 3 h at 30°C. Cells were then scraped off the filter, fixed in 4% paraformaldehyde, and incubated at 4°C overnight. This mixture was then spotted on a slide and observed with a confocal microscope (Leica). First, a field was selected randomly using transmission optics. Then, groups of zygotes and mating pairs within that field were identified by bright-field microscopy and subsequently scored as fused zygotes or unfused mating pairs by switching between bright-field and fluorescence. This procedure was continued until all the zygotes and mating pairs in the field were scored, at which point a new field was chosen and the procedure begun again. To capture images, a single optical section was taken by both bright-field and fluorescence microscopy. These images were then superimposed and contrast-enhanced.

Electron microscopy

For mating reactions, equal numbers of *Δprm1* cells of opposite mating types were mixed, spun down, spotted on a YPD plate, and allowed to mate for 3 h at 30°C. Cells

were scraped off and fixed in EM fix (1% glutaraldehyde, 0.2% paraformaldehyde, 0.04 M KPO_4 pH 7) for 5 min, spun, and incubated on ice in EM fix for 50 min. Cells were then washed twice with 0.9% NaCl, once with water, and once with 2% $KMnO_4$ (Mallinckrodt, St. Louis MO). Cells were next incubated in 2% $KMnO_4$ for 45 min at room temperature. They were then dehydrated through graded ethanol (10 min washes with 50%, 70%, 80%, 90%, 95%, 100% ethanol) and stored in a final wash of 100% ethanol overnight. To prepare for embedding, cells were washed 5 times for 10 min each with propylene oxide. For embedding, cells were stepped through graded concentrations of resin (32% Epon, 18% Araldite, 34% DDSA, 16% NMA (Ted Pella Inc., Redding CA)) mixed with propylene oxide, as follows: 2 h each with a 1:2 resin:propylene oxide mix, a 1:1 mix, a 2:1 mix, and a 3:1 mix, followed by a 1 h wash with pure resin and overnight infiltration with pure resin. The next day, cells were transferred to resin containing about 2% BDMA (Ted Pella Inc., Redding CA), incubated 4 h, and finally put in fresh resin with 2% BDMA, pelleted, and incubated at 60°C for several days for the resin to harden. Sections of about 60 nm thickness were cut, stained with lead citrate (Ted Pella Inc, Redding CA), and imaged with an electron microscope (Philips EM400).

ACKNOWLEDGMENTS

We wish to thank Mei-Lie Wong for expert training and assistance with electron microscopy and Sandra Huling for advice on sample preparation. We also thank Ira Herskowitz, Thea Tlsty, Ursula Rüegsegger, Gustavo Pesce, Arash Komeili, and Ted Powers for helpful comments on the manuscript, members of the Walter lab for their support, and Ms. Gabriela Walter-Caldera for her help in scoring fusion defects. This work was supported by grants from the NIH. MGH is a predoctoral fellow, and PW is an Investigator of the Howard Hughes Medical Institute.

CHAPTER 3

The Golgi-resident proteases Kex2p and Kex1p act in parallel to Prm1p to promote cell fusion during yeast mating

INTRODUCTION

Numerous attempts to identify the cell fusion machinery have revealed components that act at many steps in the pathway, ranging from the maintenance of osmotic integrity to the degradation of the cell wall (White and Rose, 2001). None of these genetic screens, however, identified a gene that seemed to act at the final step in cell fusion, the mixing of plasma membrane bilayers. Previously, we designed a reverse genetic approach aimed at uncovering the fusion machinery. We reasoned that the cell fusion machinery that acts during mating probably includes a transmembrane protein expressed specifically in response to mating pheromone. We began studying pheromone-regulated membrane proteins (PRM proteins) and, using a data mining program we wrote called Webminer (http://webminer.ucsf.edu), we identified the membrane protein most induced by pheromone and named it Prm1p.

Prm1p is a multispanning membrane protein not expressed under standard growth conditions but induced in both mating types in response to pheromone. It localizes to the site of cell fusion. If either mating partner lacks Prm1p then about 10% of mating pairs fail to fuse but if both mating partners lack Prm1p then about 50% of mating pairs fail to fuse. When we examined *Δprm1* x *Δprm1* mating pairs by electron microscopy we observed a morphology never before seen. In some mating pairs the cell wall had been degraded and the plasma membranes had become apposed yet failed to fuse. This result indicates that Prm1p facilitates the final step in cell fusion, that of plasma membrane fusion.

Prm1p must not constitute the complete machinery however, because even in the absence of Prm1p about half of all mating pairs still fuse. Thus, an alternate pathway

exists, one which is capable of fusing plasma membranes even in the absence of Prm1p. In this model, the loss of either the Prm1p pathway or this alternate pathway only partly impairs membrane fusion. The loss of both pathways, however, would create a severe block to membrane fusion.

RESULTS

A genetic screen for enhancers of the *Δprm1* mating defect identifies mutations in *KEX2*

To identify factors required for Prm1p-independent cell fusion, we screened for mutants that enhance the *Δprm1* x *Δprm1* mating defect. We performed random mutagenesis of a *Δprm1* MATa strain bearing a selectable marker. We plated the mutants and allowed them to form small colonies, then replica plated them to a lawn of *Δprm1* MATα cells bearing a different selectable marker. We allowed mating to occur and then replica plated to media selective for both markers, thus allowing growth only of diploids which arose during the mating. Each mutant colony from the original plate resulted on the final selective plate in a small patch with many diploid papillae emerging from it (Fig. 3-1A). The density of diploid papillae within each patch reflected the mating efficiency of the mutant which gave rise to it. Using this "replica mating" assay we screened for mutants in the *Δprm1* background which mated poorly to a *Δprm1* partner.

In addition to mutants in the PRM1-independent fusion pathway, we expected to find sterile mutants not relevant to this study. To distinguish these classes, we tested the ability of each mutant to mate to a wild-type partner. Mutants that mated very poorly to a wild-type partner were considered sterile and discarded.

To further characterize the remaining mutants, we performed a backcross to ensure that the phenotype we observed segregated as a single mutation. To our surprise, 4 out of

Figure 3-1

Replica mating strategy to isolate enhancers of *Δprm1*

(A) A *Δprm1 MATa* strain was mutagenized and plated to form colonies. Colonies were replica plated to a lawn of *Δprm1 MATα* mating partner on a YPD plate and incubated for 8 h at 30°. The mating was then replica plated to medium selective for diploids. Mutant colonies yielding a low density of diploid papillae were identified. **(B)** Patches of wild-type, *Δprm1*, and *Δprm1 Δkex2* MATa haploids were replica mated as above to a lawn of *Δprm1 MATα* mating partner. The resulting diploid papillae are shown.

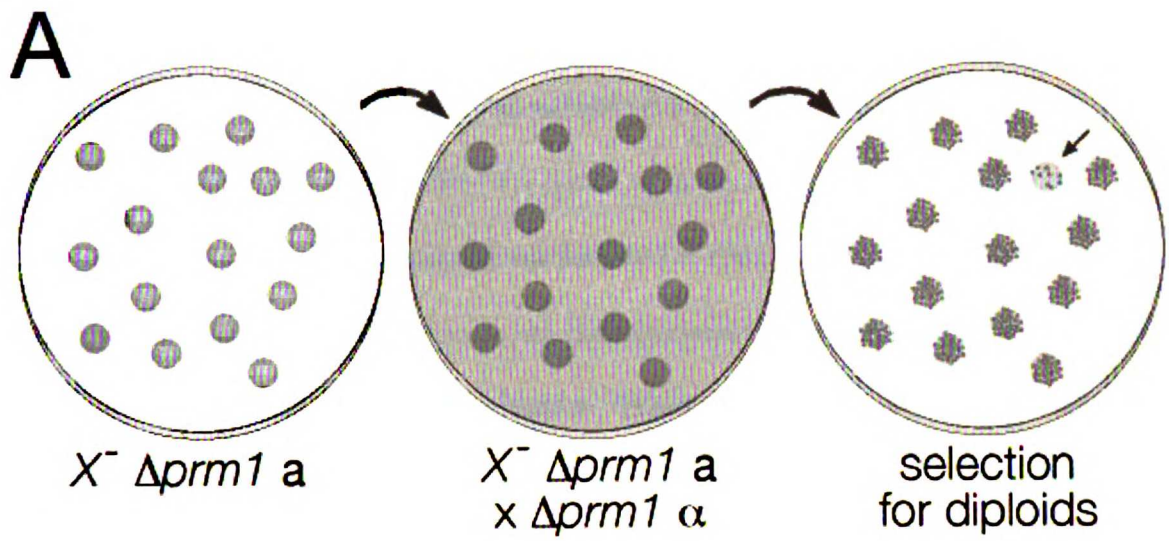
A
X⁻ Δprm1 a
X⁻ Δprm1 a
x Δprm1 α
selection
for diploids

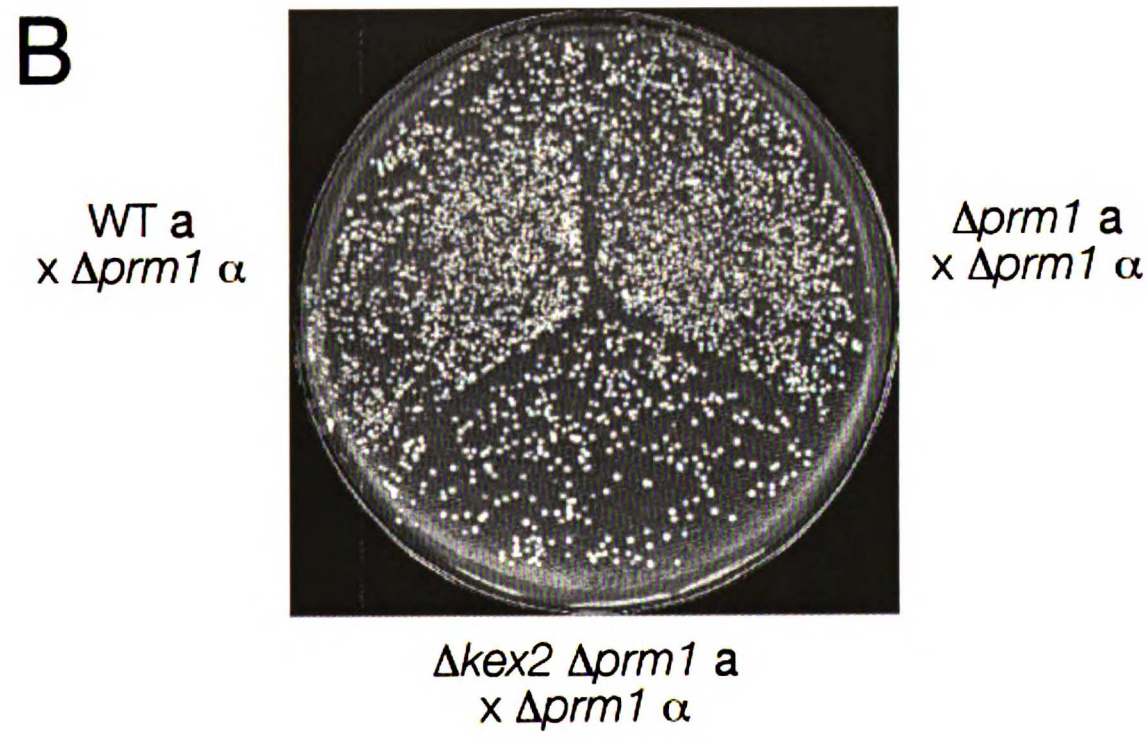
B
WT a
x Δprm1 α
Δprm1 a
x Δprm1 α
Δkex2 Δprm1 a
x Δprm1 α

10 mutants revealed a new phenotype after backcrossing. MATα progeny bearing these mutations displayed complete sterility whether mated to a wild-type or *Δprm1* partner. We assumed that a set of mutations that enhance the *Δprm1* phenotype in MATa cause sterility in MATα. Because sterility was easier to score, we used complementation cloning to isolate the gene responsible for the MATα-specific sterility in one of the mutants. The remaining mutants were not characterized further. We recovered 4 genomic fragments that restored mating to this mutant. These fragments overlapped in a region containing the coding sequence of KEX2.

Kex2p functions as a protease in the Golgi that processes several secretory pathway proteins including the α-factor mating pheromone, and therefore MATα *Δkex2* mutants are sterile (Fuller et al., 1989). In contrast, Kex2p does not process the a-factor mating pheromone and MATa *Δkex2* mutants do not have severe mating defects (Chen et al., 1997).

As expected, a MATα *Δkex2 Δprm1* mutant was sterile in our assay (not shown). In contrast, a MATa *Δkex2 Δprm1* mutant mated efficiently to a wild-type partner but poorly to a *Δprm1* partner. While we could not readily detect the weakly penetrant *Δprm1* x *Δprm1* phenotype by replica mating, the more severe phenotype of a *Δprm1 Δkex2* x *Δprm1* mating was apparent by replica mating (Fig. 1B).

Loss of Kex2p synergizes with loss of Prm1p to impair mating at the cell fusion step

To learn whether Kex2p acts to promote cell fusion, we used a quantitative cell fusion assay. Mating partners carrying deletions in PRM1, KEX2, both, or neither were mixed

and allowed to mate. One partner expressed a soluble cytoplasmic GFP to serve as a marker for cytoplasmic mixing. Mating pairs were examined by fluorescence microscopy. Mating pairs with GFP throughout their volume were considered fused, while mating pairs in which GFP remained restricted to one partner were considered unfused (Fig. 3-2A). By counting the ratio of fused to total mating pairs, we quantitated the efficiency of cell fusion. This assay differs from replica mating in that it reflects only the cell fusion step of mating rather than the entire mating process.

We observed in control matings, as seen previously, that deletion of PRM1 from both mating partners creates a substantial block to cell fusion compared to wild-type (Fig. 3-2B, compare first and last gray bars) while deletion of PRM1 from either mating partner alone produces a barely perceptible decrease in fusion efficiency (Fig. 3-2B, compare first, second, and third gray bars).

The loss of KEX2 in the MATa partner alone decreases fusion by 15% compared to wild-type (Fig. 3-2B, first pair of bars). Kex2p therefore acts at the step of cell fusion in MATa cells. Due to the role of KEX2 in α-factor processing, we could not assay MATα *Δkex2* mutants.

We observed a greater Kex2p dependency of cell fusion in matings in which both partners lacked Prm1p. The efficiency of cell fusion in *Δkex2 Δprm1* x *Δprm1* mating pairs is 70% lower than that in *Δprm1* x *Δprm1* mating pairs (Fig. 3-2B, last pair of bars). The greater Kex2p dependency in the absence of Prm1p than in wild-type is consistent with a model in which Prm1p and Kex2p act in redundant pathways to promote fusion.

The Kex2p dependency in matings in which only one partner expresses Prm1p is more complicated. *Δkex2 Δprm1* x WT matings do not differ significantly from *Δprm1* x

Figure 3-2

Δkex2 enhances the _Δprm1_ cell fusion defect

(A) *Δkex2 MATa* cells were mixed with WT *MATα* cells expressing soluble cytosolic GFP as a reporter of cytoplasmic mixing between mating partners. This mixture was applied to a nitrocellulose filter and incubated for 3 h on a YPD plate at 30°. Fluorescent micrographs showing the GFP-stained cytoplasm were super-positioned over bright-field images of the mating pairs. **(B)** Mating mixes in which mating partners carried deletions of *PRM1, KEX2*, both, or neither were prepared as described above. In all cases the MATα partner carried soluble cytosolic GFP. Mating pairs were visually identified and then scored with regard to cell fusion by microscopy. Bars represent the average percent of mating pairs that scored as fused in three independent experiments. During each experiment, 300 mating pairs per mating mix were counted. All matings are written in the form *MATa* x *MATα*: WT x WT, 98.2 ± 0.6 %; *Δkex2* x WT , 83.2 ± 2.3%; *WT* x *Δprm1*, 94.8 ± 1.4%; *Δkex2* x *Δprm1*, 43.6 ± 4.6%; *Δprm1* x WT, 95.9 ± 1.6%; *Δprm1 Δkex2* x WT, 86.3 ± 1.6%; *Δprm1* x *Δprm1*, 62.4 ± 6.8%; *Δprm1 Δkex2* x *Δprm1*, 18.5 ± 1.2%.

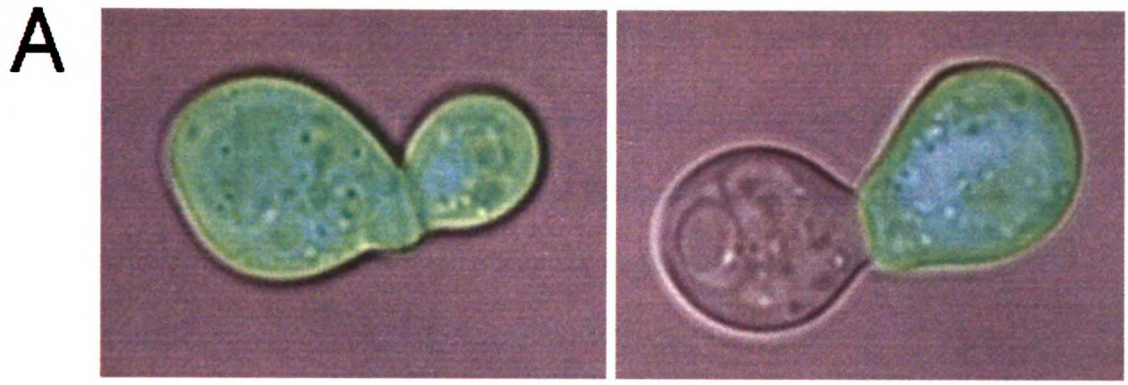
A

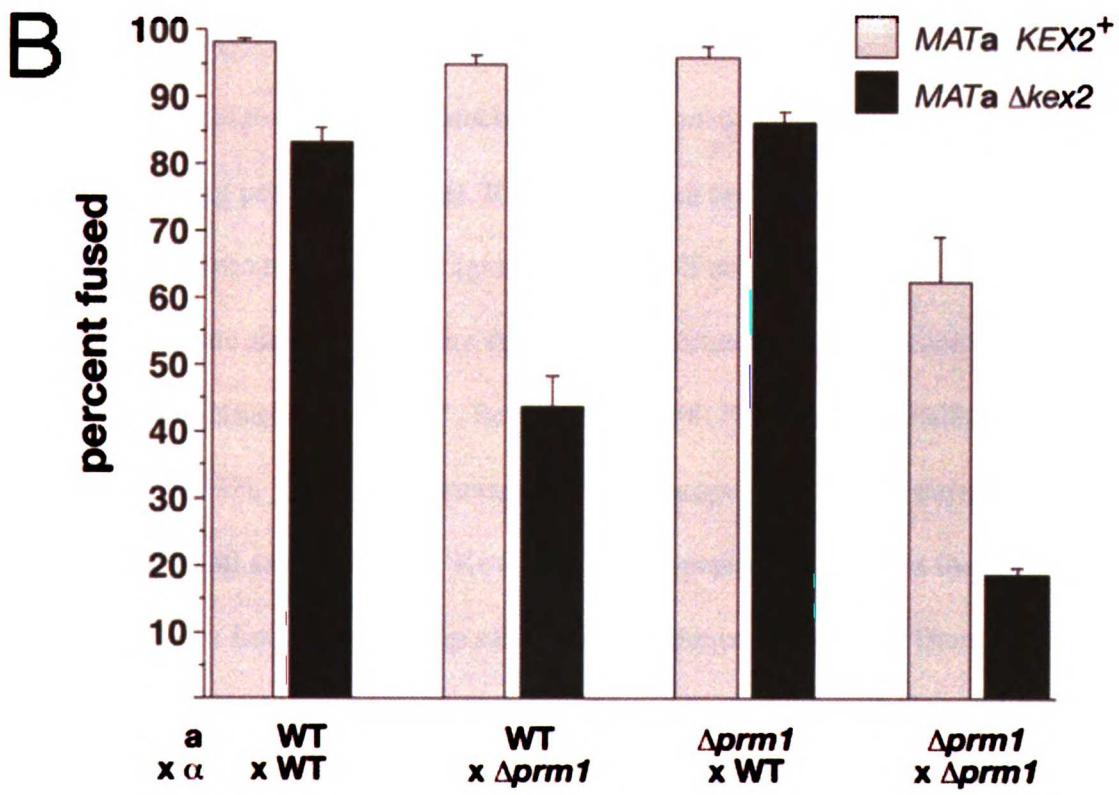
B
MATa KEX2+
MATa Δkex2
percent fused
100
90
80
70
60
50
40
30
20
10
a x α
WT x WT
WT x Δprm1
Δprm1 x WT
Δprm1 x Δprm1

WT (third pair of bars). However, *Δkex2* x *Δprm1* matings fuse with about half the efficiency of WT x *Δprm1* matings (second pair of bars). In other words, the effect of the *Δkex2* mutation is much stronger *in trans* to *Δprm1* than *in cis* to *Δprm1*. This result is not consistent with Prm1p and Kex2p acting in independent pathways, but it would be consistent with a model in which Kex2p acts both upstream and parallel to Prm1p.

The Kex2p-Kex1p processing pathway synergizes with Prm1p to promote cell fusion

Kex2p has undergone extensive biochemical and genetic characterization as part of a substrate processing pathway. In brief, Kex2p acts as an endopeptidase to cleave substrate proteins into two or more fragments (Rockwell et al., 2002). Kex2p recognizes a variety of substrate sites with varying degrees of preference, but the canonical cleavage site is the dibasic sequence "LysArg" (Bevan et al., 1998; Rockwell and Fuller, 1998; Rockwell et al., 1997). Following cleavage, a pair of exopeptidases trim the newly exposed carboxy and amino termini. Kex1p, a carboxypeptidase, removes the remaining "LysArg" sequence from many Kex2p substrates (Latchinian-Sadek and Thomas, 1993). Ste13p, an aminopeptidase, removes pairs of residues from the complementary fragment, preferring to trim "X-Ala" sequences (Anna-Arriola and Herskowitz, 1994; Julius et al., 1983).

To test whether Kex1p or Ste13p affect cell fusion, we subjected *Δkex1* and *Δste13* mutants to the same genetic analysis we used with *Δkex2* mutants. We conducted matings in which the partners lacked either Prm1p or Kex1p in all combinations, or

Prm1p or Ste13p in all combinations and assayed the resulting mating pairs for fusion using the GFP-mixing assay.

A *Δkex1* mutant displays a slight but significant fusion defect when crossed to a wild-type partner (Fig. 3-3A, first pair of bars). This defect was enhanced when we introduced a *Δprm1* mutation *in trans* but not *in cis* (Fig. 3-3A, second and third pairs of bars). Finally, the most severe defect occurred when we introduced a *Δkex1*mutation into a *Δprm1* x *Δprm1* cross, which reduces the number of successful fusions by more than half (Fig. 3-3A, last pair of bars). Overall *Δkex1* produces milder defects than *Δkex2*, but its effects on cell fusion are qualitatively the same.

In contrast, deletion of STE13 from a WT x WT mating produces no significant difference in cell fusion (Fig. 3-3B, first pair of bars). Furthermore, *Δste13* does not enhance the *Δprm1* fusion phenotype when placed *in cis* or *in trans* (Fig. 3-3B, second and third pairs of bars). When introduced into a *Δprm1* x *Δprm1* mating, the *Δste13* mutation produces almost no effect (Fig. 3-3B, last pair of bars). While a slight, possibly insignificant, lowering of successful fusion haunts the *Δste13* mutant, it does not reach the degree of either *Δkex1*or *Δkex2* and it does not synergize with *Δprm1* in any combination of matings.

Δkex2 mutants produce cytoplasmic blebs enclosed by cell wall

We characterized ultrastructurally the cell fusion intermediate at which *Δkex2* x WT matings arrest by examining fixed mating pairs using electron microscopy.

In about 80% of unfused *Δkex2* x WT mating pairs we observed bleb-like structures in the cell wall that appear disconnected from both mating partners (Figs. 3-4 and 3-5).

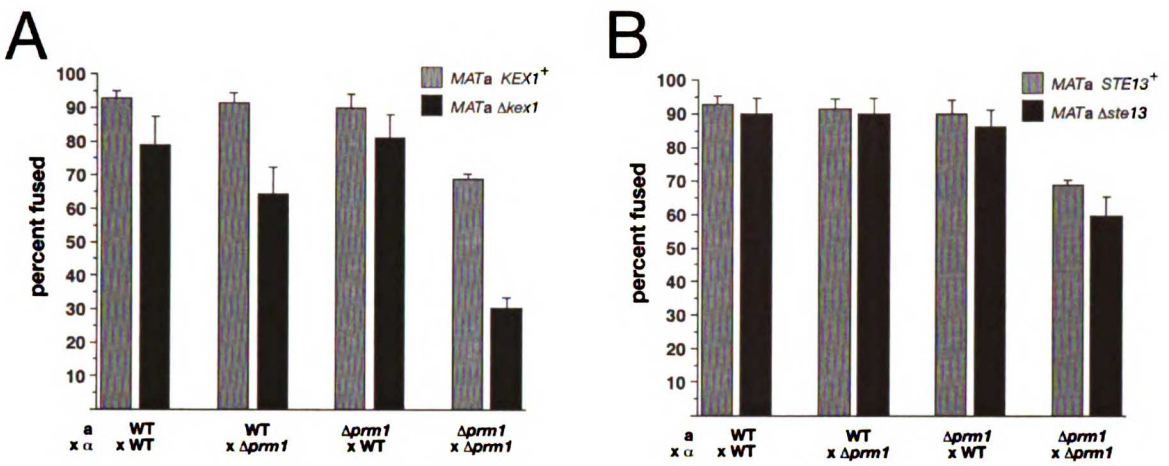

Figure 3-3

Δkex1, but not _Δste13_, enhances the _Δprm1_cell fusion defect

Mating mixes in which mating partners carried deletions of *PRM1, KEX1*, or *STE13* singly or in combination were subjected to filter matings followed by microscopic inspection of mating pairs, and fusion efficiencies were quantitated using the GFP-mixing assay as described above. All matings presented in this figure were conducted in parallel and three independent trials were performed, with 300 mating pairs per mating mix counted each time. All matings are written in the form *MATa* x *MATα*. **(A)** Matings with deletions of *KEX1:* WT x WT, 92.9 ± 2.3 %; *Δkex1* x WT , 78.8 ± 8.6%; *WT* x *Δprm1*, 91.5 ± 2.8%; *Δkex1* x *Δprm1*, 64.5 ± 7.7%; *Δprm1*x WT, 90 ± 4.2%; *Δprm1 Δkex1* x WT, 81.3 ± 6.9%; *Δprm1* x *Δprm1*, 68.7 ± 1.6%; *Δprm1 Δkex1* x *Δprm1*, 30.4 x 3.0%. **(B)** Matings with deletions of *STE13:* WT x WT, 92.9 ± 2.3 %; *Δste13* x WT , 90.1 ± 4.5%; *WT* x *Δprm1*, 91.5 ± 2.8%; *Δste13* x *Δprm1*, 90.1 ± 4.5%; *Δprm1*x WT, 90 ± 4.2%; *Δprm1 Δste13* x WT, 86.1 ± 5.2%; *Δprm1* x *Δprm1*, 68.7 ± 1.6%; *Δprm1 Δste13* x *Δprm1*, 59.7 ± 5.6%.

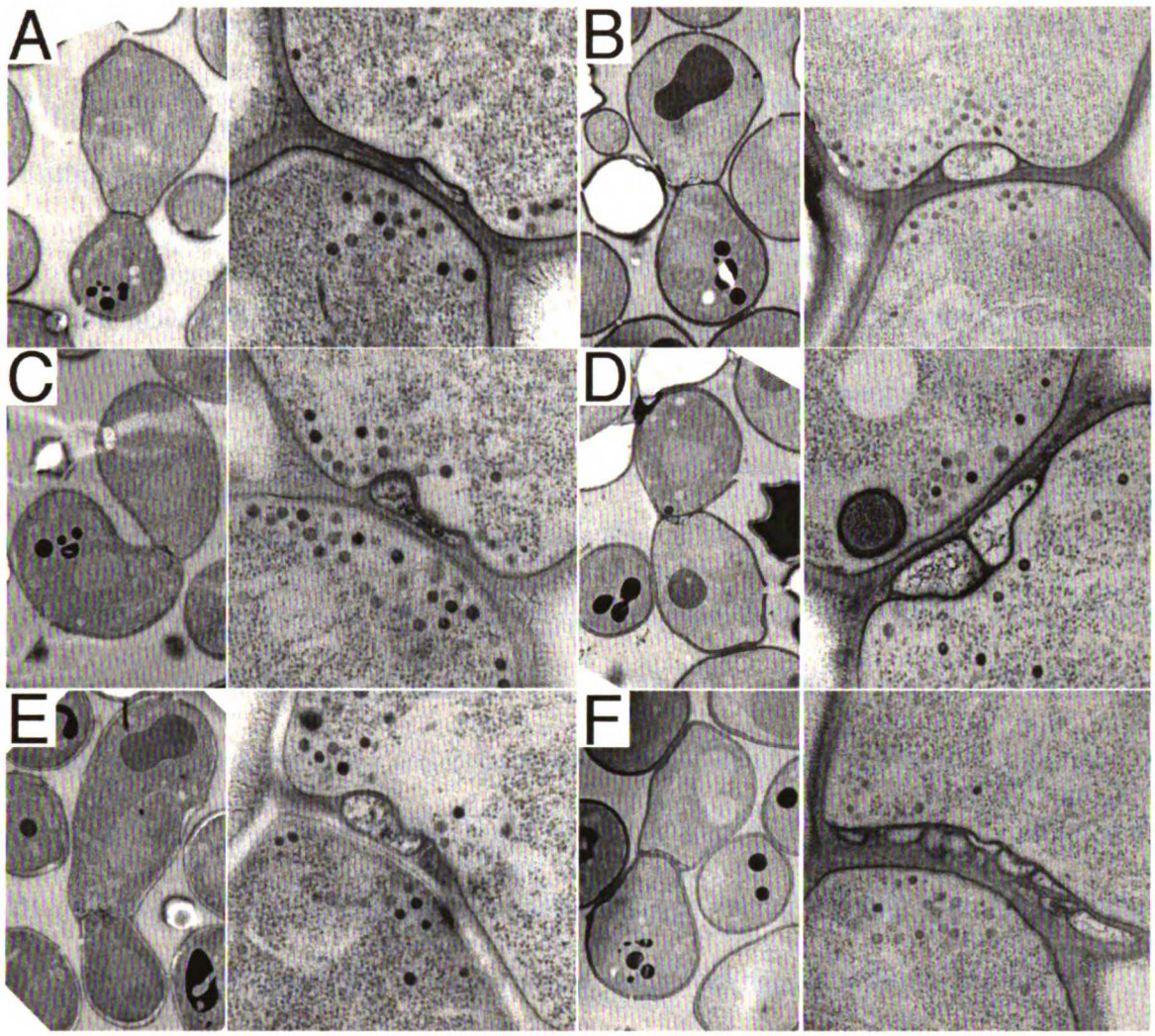

Figure 3-4

Δkex2 x WT mating pairs fail to fuse and develop extracellular "blebs"

Mating mixes of *Δkex2* x WT partners were prepared on filters as described above and incubated for about 3 h at ambient temperature. The cells were then subjected to high-pressure freezing, fixed, stained, and imaged by transmission electron microscopy. Two different magnifications are shown for each image.

The blebs are bounded by a visible lipid bilayer (see especially Figs. 3-4E, 3-5F and 3-5M; in other views the bilayer is harder to discern owing to the angle of the section relative to the plane of the bilayer). A gap of about 8 nm separates the bleb from the plasma membrane that it appears adhered to (see especially Figs. 3-4A, 3-4C, 3-4E, 3-5F, 3-5J and 3-5M). About 90% of the blebs appear preferentially linked to one mating partner, but about 10% of the blebs closely approach the plasma membrane of the other mating partner as well (see Figs. 3-4B, 3-4C, 3-5J and 3-5M). In any given section we observed numbers ranging from one bleb (see Figs. 3-4A and 3-4C), to one main bleb with others clearly above or below it (see Figs. 3-4B and 3-4E), to two blebs clearly side-by-side with their surfaces apposed (see Fig. 3-4D), to a veritable cascade of blebs spread out across the diameter of the cell-cell interface (Fig. 3-4F). About 75% of mating pairs have one to five blebs, with 5% having more and 20% having none. We never detected a clear cytoplasmic continuity between a bleb and either mating partner. The texture of the staining inside the blebs often appears fibrous, unlike the regular punctate staining of ribosomes which we observed in normal cytoplasm (see especially Fig. 3-4D).

We examined the three-dimensional structure and arrangement of blebs in more detail by serial section analysis. A representative set of serial sections appears in Figure 3-5. At one end of the series, the cell-cell interface appears restricted and secretory vesicles are sparse, indicating the sections come from a region where the cells are just beginning to make contact, off-center of the long axis of the mating pair (Figs. 3-5A and 3-5B). As the sections approach the center of the mating pair, the contact zone widens, the number of secretory vesicles increases, and a bleb appears (Figs. 3-5C and 3-5D). Moving more to the center of the cell-cell interface, the bleb broadens and appears to push slightly into

Figure 3-5

Serial section analysis of a *Δkex2* x WT mating pair

(A-K) Transmission electron micrographs of serial sections through the cell-cell interface of a *Δkex2* x WT mating pair prepared as in Fig. 3-4. **(L)** Low-magnification view of the mating pair. **(M)** High-magnification view of the bleb seen in panel F. **(N)** High-magnification view of an intracellular structure from panel G. **(O)** High-magnification view of an intracellular structure from panel I.

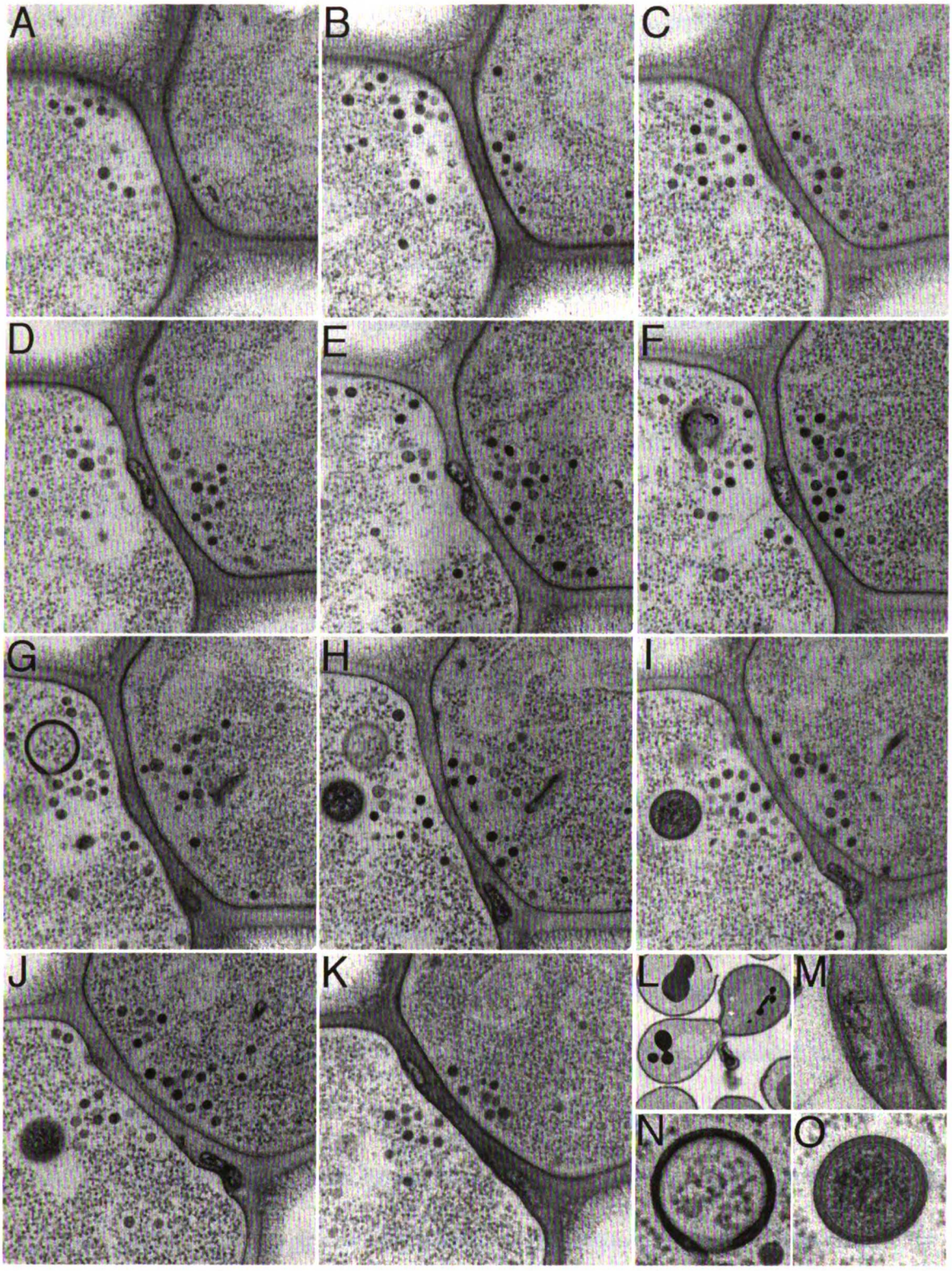
A
B
C
D
E
F
G
H
I
J
K
L
M
N
O

the mating partner on the left (Figs. 3-5E and 3-5F) before disappearing from view (Fig. 3-5G). A second bleb appears in a lower section and grows (Figs. 3-5G-K); a third and possibly a fourth bleb appear still farther (Figs. 3-5J and 3-5K). The bleb in Figs. 3-5C - 3-5F almost contacts both plasma membranes; in Fig. 3-5F (magnified in Fig. 3-5M) it appears only about 10 nm from the partner on the right.

Other structures of unknown function also appear in these images. A dark unclosed circle, seemingly vesicles in the process of fusing, begins to enclose a region of cytoplasm, reminiscent of the formation of autophagy structures (Fig. 3-5G, magnified in Fig. 3-5N). Similarly, a spherical lipid bilayer enclosed in a second bilayer with a matrix separating the two, contains dark-staining cytoplasm (Fig. 3-5I, magnified in Fig. 3-5O) and suggests a mature form of the first structure. These structures appear in sections from other mating pairs as well (see for example Fig. 3-4D).

Δprm1 Δkex2 x *Δprm1* mating pairs exhibit bubbles, blebs and an additional phenotype

We also examined the ultrastructure of *Δprm1 Δkex2* x *Δprm1* mating pairs. We observed three classes of structures in these pairs: bubbles, similar to *Δprm1* x *Δprm1* matings; blebs, similar to *Δkex2* x WT matings; and a third structure unique to *Δprm1 Δkex2* x *Δprm1* matings.

A characteristic bubble from *Δprm1 Δkex2* x *Δprm1* matings appears in Figures 3-6A and 3-6B. In this example, the mating partner on the bottom forms an extension past the midline of the mating pair and well into the space previously occupied by the mating partner on the top. The plasma membranes appear close but unfused, the cytoplasmic

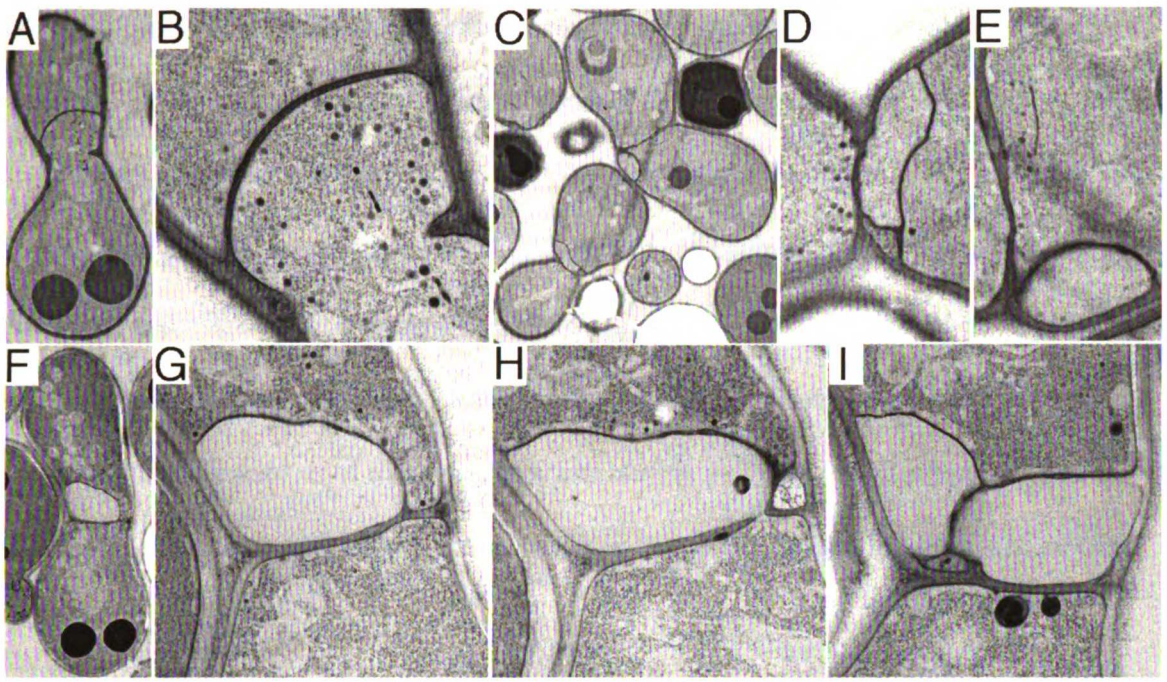

Figure 3-6

***Δprm1 Δkex2* x *Δprm1* mating pairs fail to fuse and develop a variety of structures**

Mating mixes were prepared as in Fig. 3-4. **(A, B)** A mating pair, in low- and high-magnification views, with a region of cytoplasm extending across the midline from one partner to the other. **(C-E)** Two mating pairs, in low- and high-magnification views, containing membrane-bounded inclusions with staining textures consistent with that of cytoplasm. **(F-I)** A mating pair, in low-magnification view and three serial sections in high-magnification view, with a membrane-bounded structure that extends across the midline from one partner to the other and that has that has a staining texture different than cytoplasm.

continuity between the bubble and the mating pair on the bottom is obvious, and the texture of the staining within the bubble matches that of normal cytoplasm.

Serial sections of a *Δprm1 Δkex2* x *Δprm1* bleb appear in Figure 3-7. Several blebs extend over the full length of the cell-cell interface. No cytoplasmic continuity between the blebs and either mating partner can be found, and the texture of the blebs appears fibrous unlike normal cytoplasm. Additionally, a double-bilayer-bound structure appears in the top mating partner of this pair. In some mating pairs we found structures that resembled enormous blebs (both mating pairs in Fig. 3-6C, magnified in Figs. 3-6D and 3-6E).

In addition, some *Δprm1 Δkex2* x *Δprm1* mating pairs display a unique morphology, consisting of enormous barren bubbles (EBBs). These structures appear similar to a normal *Δprm1* x *Δprm1* bubble yet lack the staining of ribosomes and vesicles that populate normal cytoplasm (Figs. 3-6F – 3-6I). These structures also lack the fibrous pattern typical of blebs. Instead, they present the appearance of empty cytoplasm, despite the presence of a clear continuity to one mating partner (see Fig. 3-6H). In one section this structure appears to involute (Fig. 3-6I).

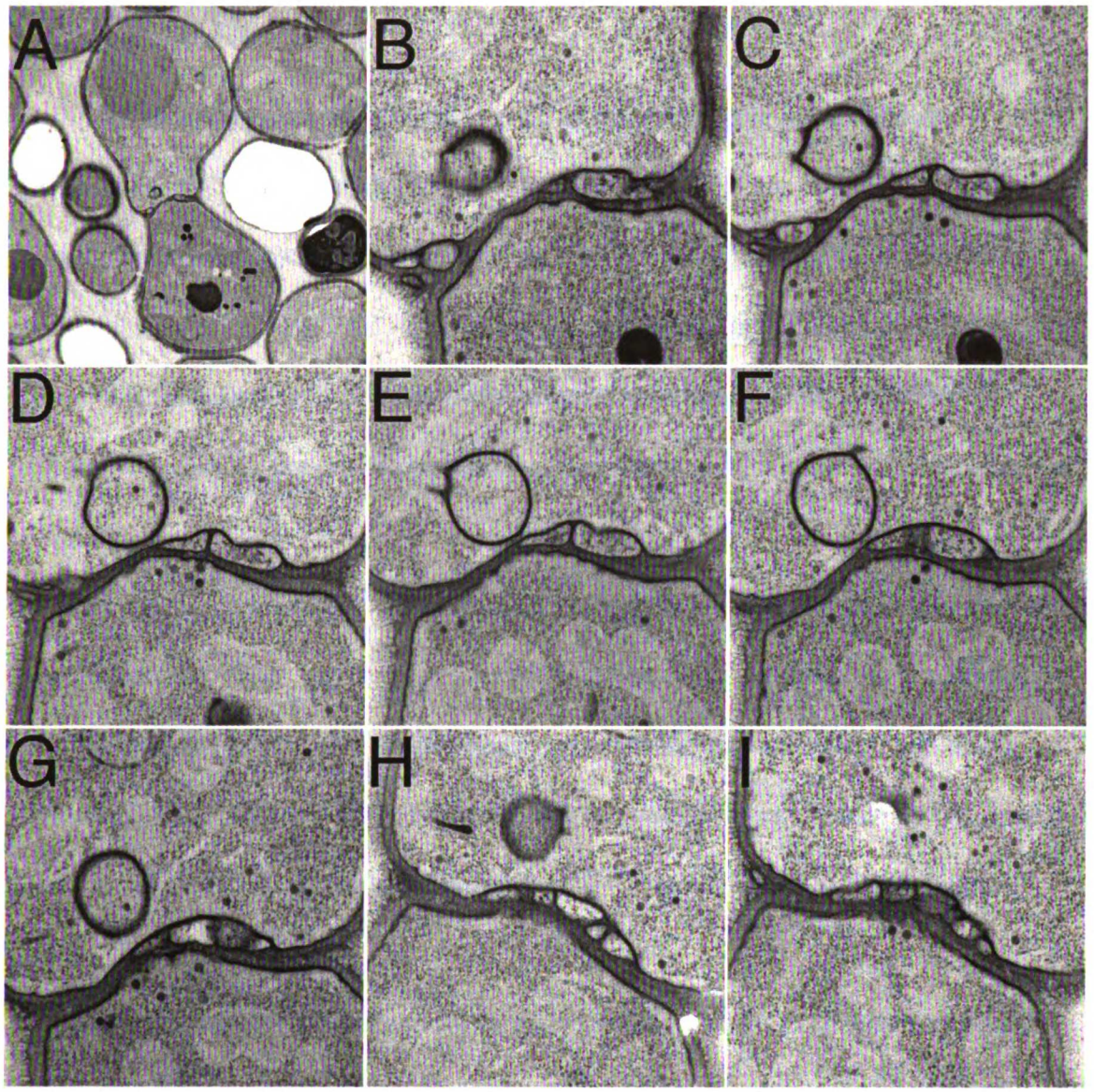

Figure 3-7

Serial section analysis of a *Δprm1 Δkex2* x *Δprm1* mating pair

(A) Low-magnification transmission electron micrograph of a *Δprm1 Δkex2* x *Δprm1* mating pair prepared as in Fig. 4. **(B-F)** High-magnification serial sections across the cell-cell interface of the mating pair shown in panel A.

DISCUSSION

KEX2 represents an additional genetic pathway leading to cell fusion

One role of Kex2p during mating is to act as a protease in the late Golgi to process the α-factor pheromone secreted by MATα cells (Rockwell et al., 2002). We present here evidence for an additional role of Kex2p in mating, acting at the step of cell fusion. This role is independent of α-factor processing because MATa cells, which do not depend on Kex2p for pheromone processing, manifest a cell fusion defect in the absence of Kex2p.

The role Kex2p plays in cell fusion most likely depends on its acting as a secretory pathway endoprotease. We could not assay "protease-dead" alleles of Kex2p because these mutants fail to leave the endoplasmic reticulum and are essentially null alleles (Gluschankof and Fuller, 1994). However, the fact that the exopeptidase Kex1p displays a similar cell fusion defect suggests that these proteases act in concert to promote cell fusion.

Efficient cell fusion depends more strongly on Kex2p and Kex1p in the absence of Prm1p. We can calculate a gene's "fusion contribution" index as the difference in fusion efficiency between matings with and without the gene (Table 3-1). Thus,

$$\frac{\text{WT x WT}}{\Delta kex2 \text{ x WT}} = \frac{98.2\% \text{ fusion}}{83.2\% \text{ fusion}} = 1.2 \text{ fusion contribution (FC) of KEX2 to a WT x WT mating}$$

In comparison, applying this formula to a *Δprm1* x *Δprm1* mating shows that KEX2 gives a 3.4 FC to a mating lacking PRM1. With this method, PRM1 itself contributes 1.5

Table 3-1

Fusion contribution (FC) of *PRM1* and *KEX2* to each mating in this study

FC of a gene to a mating is calculated as described in the text, and represents the fold decrease in percent fused mating pairs resulting from the loss of a wild-type copy of the gene in the mating. All crosses are written in the form *MATa* x *MATα*. NA, not applicable.

	PRM1 *MATa*	*PRM1* *MATα*	*KEX2* *MATa*
WT x WT	1.0	1.0	1.2
Δprm1 x WT	NA	1.5	1.1
Δkex2 x WT	1.0	1.9	NA
Δprm1 Δkex2 x WT	NA	4.7	NA
WT x *Δprm1*	1.5	NA	2.2
Δprm1 x *Δprm1*	NA	NA	3.4
Δkex2 x *Δprm1*	2.4	NA	NA
Δprm1 Δkex2 x *Δprm1*	NA	NA	NA

FC to a WT x WT mating and 4.5 FC to a *Δkex2* x WT mating. It should be noted that these figures compare loss of KEX2 in only the MATa partner with loss of PRM1 in both mating partners.

What these calculations enumerate is that the KEX2 pathway is more critical for fusion if the PRM1 pathway is impaired, and *vice versa*. This genetic behavior suggests that KEX2 and PRM1 act in redundant pathways leading to cell fusion. Moreover, it indicates that these pathways can functionally substitute for one another. Therefore the KEX2 pathway may mediate a step similar to that performed by the PRM1 pathway during cell fusion.

This analysis extends to matings where only one partner lacks PRM1. For *Δprm1* x WT, there is a 1.1 FC for KEX2; for WT x *Δprm1* there is a 2.2 FC for KEX2. Thus, KEX2 in the partner of a *Δprm1* mutant is more important for efficient fusion than KEX2 in a *Δprm1* mutant itself. One model to account for this behavior is that the KEX2 pathway promotes cell fusion independently of PRM1 but also is required for full activity of the PRM1 pathway.

Consistent with this genetic model, *Δprm1 Δkex2* x *Δprm1* mating pairs show some morphological traits of *Δprm1* x *Δprm1* matings, some traits of *Δkex2* x WT matings, and some unique phenotypes. The appearance of both bubbles and blebs in these matings supports the idea that KEX2 is not directly upstream or downstream of PRM1, because if it were then epistasis should allow only one phenotype to occur in the double mutant. Additionally, the appearance of a new phenotype provides a physical correlate to our

genetic observations that the *Δprm1 Δkex2* x *Δprm1* double mutant mating creates a phenotype more severe than simply adding the single mutant phenotypes.

Possible mechanisms by which the KEX2 pathway may promote cell fusion

Kex2p acting in its conventional role would proteolytically cleave a substrate which, in turn, promotes cell fusion. Hemagglutinin, a viral fusase, undergoes proteolysis by a Kex2p-family protease as part of its biosynthesis (Stieneke-Grober et al., 1992). Conceivably, Kex2p could cleave an analagous fusase.

Kex2p has several known substrates. In addition to α-factor, it processes killer toxin and a family of cell wall proteins (Cappellaro et al., 1998; Mrsa et al., 1997). However, the *Δkex2* mutant does not display the weakened cell wall phenotype seen by deletion of some of these cell wall proteins (not shown). Conversely, deletion of these cell wall proteins does not produce a cell fusion defect (*Δscw4 Δscw10* x *Δscw4 Δscw10*, 96% fused; *Δkex2* x WT, 87% fused). Furthermore, other cell fusion mutants that act at the step of cell wall remodeling do not show an ultrastructural morphology at all resembling *Δkex2* x WT (Gammie et al., 1998). These data, combined with the genetic arguments that the KEX2 pathway closely overlaps with the PRM1 pathway, indicate that an unknown Kex2p substrate or family of substrates promotes cell fusion.

The cytoplasmic blebs that form in a *Δkex2* x WT mating provide clues regarding at what step the Kex2p substrate acts. In many respects the blebs resemble bubbles, consistent with the genetic data that KEX2 and PRM1 act at similar steps. Like bubbles, the blebs are apposed to nearby plasma membrane by a regular gap of about 8 nm and appear to push into the space occupied by one mating partner. One mechanism for the

formation of the blebs is that a *Δprm1* x *Δprm1* like bubble forms but is then severed or pinched off from the partner that forms it (Fig. 3-8A).

Another model focuses on the vesicles that concentrate at the fusion zone in wild-type matings. The vesicles may resemble the sperm acrosome, a repository of fusogenic materials that are delivered to the surface in a burst of exocytosis. During normal acrosomal vesicle fusion, cytoplasmic fragments are excised from the sperm due to rapid exocytosis at many points along the plasma membrane (Primakoff and Myles, 2002). Such events have not been described during wild-type yeast mating, however, if in *Δkex2* x WT matings vesicle delivery is premature or misregulated it could produce the blebs observed (Fig. 3-8B).

The appearance of the closed-circle figures in cytoplasm of *Δkex2* x WT matings provides another potential source for the blebs. Delivery of these double-membrane-bounded structures to the surface would produce the blebs (Fig. 3-8C). Why these structures form and what their function is, if any, remain a complete mystery.

Identification of a Kex2p substrate relevant to fusion will begin to illuminate how the KEX2 and PRM1 pathways cooperate during cell fusion. This substrate may be difficult to identify, first, because it may be part of a set of Kex2p substrates which act redundantly to promote fusion and, second, because a null allele of the substrate may not correspond phenotypically to the unprocessed form of the substrate produced in a *Δkex2* mutant. Importantly, the severity of the *Δprm1 Δkex2* x *Δprm1* defect provides a plate mating phenotype that now allows rapid identification of additional genes in the PRM1 and KEX2 pathways in the future.

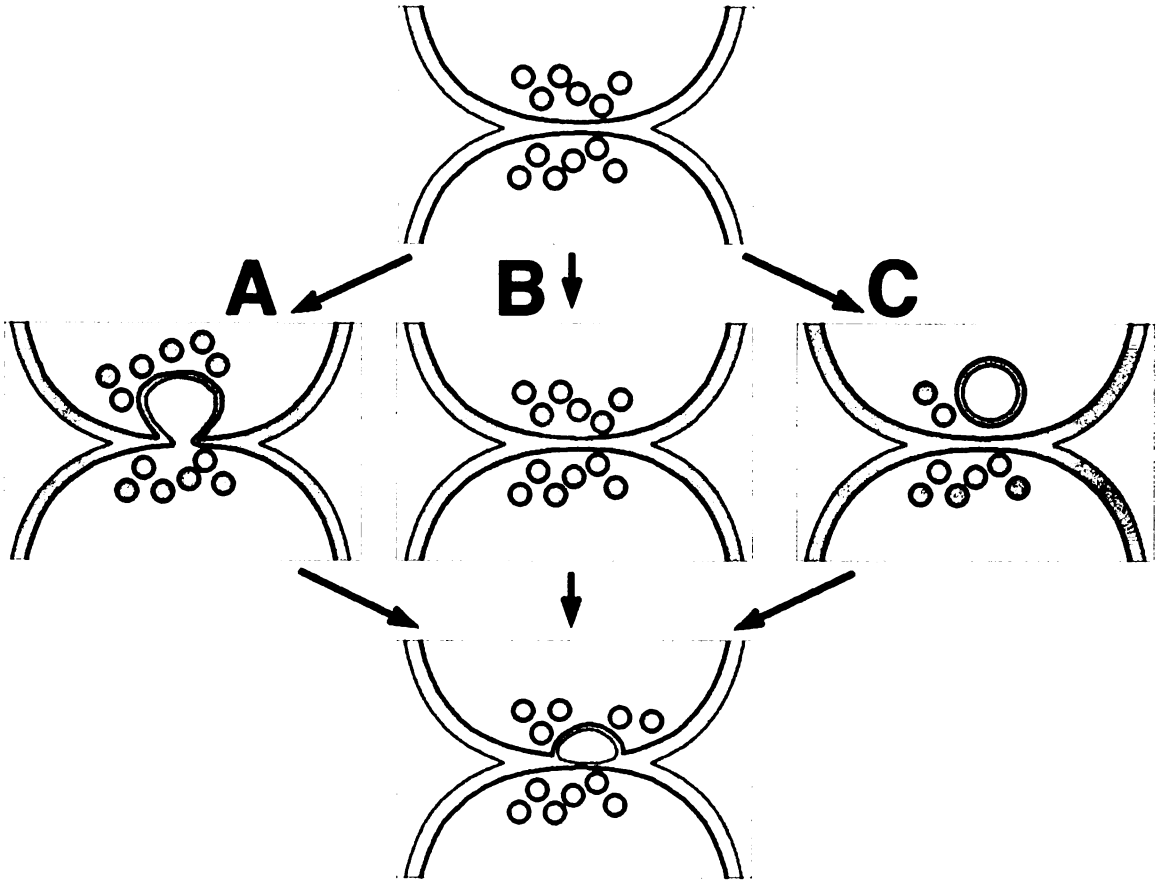

Figure 3-8

Possible models for the mechanism of bleb formation

Three possibilities for how defective attempts at cell fusion could produce membrane-bound cell wall inclusions at the cell-cell interface. **(A)** A cytoplasmic extension reaches across the midline and then is severed. **(B)** Synchronous fusion of vesicles to each other and to the plasma membrane excises a pocket of cytoplasm. **(C)** An intracellular inclusion forms and is delivered to the surface.

METHODS

Yeast strains and plasmids

Strains used in this study appear in Table 3-2. Gene replacements were generated with the PCR-transformation technique. Strains MHY398 and MHY427 were derived from KRY18, a gift of Robert Fuller (Komano and Fuller, 1995). The plasmid pDN291, as previously described, was used to express soluble cytosolic GFP and contains the *URA3* gene (Ng and Walter, 1996). The plasmid pRS314 is a standard vector containing the *TRP1* gene, and was used in conjunction with pDN291 to create a set of mating-type-specific selectable markers (Sikorski and Hieter, 1989).

Genetic screen for enhancers of *Δprm1*

Δprm1 TRP1 MATa cells were grown to log phase, and 4 A_{600} units were washed once in 10 ml 10 mM potassium phosphate pH 7.4 (Sigma), then resuspended in same. 300 µl ethyl methane sulfonate (Sigma) was added, cells were vortexed, and incubated 30 min at 30°C. At that point, 15 ml 10% sodium thiosulfate (Sigma) was added to quench the reaction. Cells were washed twice in YPD medium and allowed to recover in YPD for 90 min at 30°C to fix any mutations that were induced. Serial dilutions of this stock were plated to medium lacking tryptophan and the titer of colony forming units was calculated; meanwhile the stock was kept at 4°C. For screening, the stock was plated to 100 plates lacking tryptophan at a density of about 120 colonies per plate. Colonies were allowed to grow for 40 h at 30°C. After about 25 h, a stationary overnight culture of *Δprm1 URA3 MATα* was plated to 100 plates of YPD at 100 µl/plate and incubated at room temperature for the remaining 15 h to form lawns. These lawns were re-spread with 100

Table 3-2

The following strains were used. All were constructed in the W303 background.

MHY425	MATa, *his3-Δ200, ura3-Δ99, leu2-Δ1, trp1-Δ99, ade2-101^{ochre}*, pRS314
MHY189	MATα, *his3-Δ200, ura3-Δ99, leu2-Δ1, trp1-Δ99, ade2-101^{ochre}*, pDN291
MHY426	MATa, *Δprm1::S.kluyveri HIS3^{+}, his3-Δ200, ura3-Δ99, leu2-Δ1, trp1-Δ99, ade2-101^{ochre}*, pRS314
MHY191	MATα, *Δprm1::S.kluyveri HIS3^{+}, his3-Δ200, ura3-Δ99, leu2-Δ1, trp1-Δ99, ade2-101^{ochre}*, pDN291
MHY398	MATa, *Δkex2::TRP1, his3-Δ200, ura3-Δ99, leu2-Δ1, trp1-Δ99, ade2-101^{ochre}*
MHY461	MATa, *Δkex1::kan^{R}, his3-Δ200, ura3-Δ99, leu2-Δ1, trp1-Δ99, ade2-101^{ochre}*, pRS314
MHY462	MATa, *Δste13::kan^{R}, his3-Δ200, ura3-Δ99, leu2-Δ1, trp1-Δ99, ade2-101^{ochre}*, pRS314
MHY427	MATa, *Δprm1::S.kluyveri HIS3^{+}, Δkex2::TRP1, his3-Δ200, ura3-Δ99, leu2-Δ1, trp1-Δ99, ade2-101^{ochre}*
MHY445	MATa, *Δprm1::S.kluyveri HIS3^{+}, Δkex1::kan^{R}, his3-Δ200, ura3-Δ99, leu2-Δ1, trp1-Δ99, ade2-101^{ochre}*, pRS314
MHY447	MATa, *Δprm1::S.kluyveri HIS3^{+}, Δste13::kan^{R}, his3-Δ200, ura3-Δ99, leu2-Δ1, trp1-Δ99, ade2-101^{ochre}*, pRS314
MHY189	MATα, *his3-Δ200, ura3-Δ99, leu2-Δ1, trp1-Δ99, ade2-101^{ochre}*, pDN291
MHY189	MATα, *his3-Δ200, ura3-Δ99, leu2-Δ1, trp1-Δ99, ade2-101^{ochre}*, pDN291
MHY387	MATa, *Δscw4::S.kluyveri HIS3^{+}, his3-Δ200, ura3-Δ99, leu2-Δ1, trp1-Δ99, ade2-101^{ochre}*, pRS314
MHY388	MATα, *Δscw10::S.kluyveri HIS3^{+}, his3-Δ200, ura3-Δ99, leu2-Δ1, trp1-Δ99, ade2-101^{ochre}*, pDN291
MHY389	MATa, *Δscw4::S.kluyveri HIS3^{+}, Δscw10::S.kluyveri HIS3^{+}, his3-Δ200, ura3-Δ99, leu2-Δ1, trp1-Δ99, ade2-101^{ochre}*, pRS314
MHY390	MATα, *Δscw10::S.kluyveri HIS3^{+}, Δscw10::S.kluyveri HIS3^{+}, his3-Δ200, ura3-Δ99, leu2-Δ1, trp1-Δ99, ade2-101^{ochre}*, pDN291

μl/plate water to a dull matte appearance indicative of homogeneity. Colonies were replica plated to mating lawns and incubated for 8 h at 30°C. The plates were then replica plated to media lacking tryptophan and uracil to select for diploids. Phenotypes were scored on plates incuibates for 2 days at 30°C. We have noticed that the clarity of the phenotypes depends critically on having homogeneous lawns of the proper density.

Complementation of the *Δprm1* enhancer mutation

Because MATα-specific sterility appeared in several of the enhancer mutants, we scored for complementation of this phenotype which was easier to score. Following backcross to a *Δprm1*strain, the sterile *Δprm1 MATα* was transformed with a pRS316-based library, a generous gift of Sean O'Rourke (O'Rourke and Herskowitz, 2002). 15,000 transformants were subjected to a replica mating assay as described above, with a tester strain as partner.

Quantitative assay of cell fusion

The cell fusion assay was performed as described previously. Cells of opposite mating types, with the *MATa* strain expressing soluble cytosolic GFP, were grown overnight to log phase, 1 A_{600} unit of each were mixed, and vacuumed to a nitrocellulose filter. The filter was placed cell-side up on a YPD plate, and the plate incubated for 3 h at 30°C. Cells were then scraped off the filter, fixed in 4% paraformaldehyde, and incubated at 4°C overnight. This mixture was then spotted on a slide and observed with a confocal microscope (Leica). First, a field was selected randomly using transmission optics. Then, groups of zygotes and mating pairs within that field were identified by bright-field

microscopy and subsequently scored as fused zygotes or unfused mating pairs by switching between bright-field and fluorescence. This procedure was continued until all the zygotes and mating pairs in the field were scored, at which point a new field was chosen and the procedure begun again. To capture images, a single optical section was taken by both bright-field and fluorescence microscopy. These images were then superimposed and contrast-enhanced.

Electron microscopy

Mating reactions were performed identically to the method described for quantitative fusion assays, but at room temperature. During the mating, plates were taken to the University of California Berkeley electron microscopy lab and subjected to high-pressure freezing after about 3 h total incubation (McDonald, 1999). Samples were fixed, stained and embedded (McDonald, 1999). Sections of about 60 nm thickness were cut, post-stained with uranyl acetate and lead citrate (Ted Pella Inc, Redding CA), and imaged with an electron microscope (Philips Tecnai-F20).

ACKNOWLEDGMENTS

We would like to thank Jason Brickner for his expertise on *KEX2*, his suggestion to test *KEX1* and *STE13* for similar phenotypes, and other helpful discussions. We also thank Kent McDonald and his colleagues at the Berkeley EM lab for performing the high pressure freezing, fixing, staining, and embedding of samples for electron microscopy, and Kent for instructive discussions on preserving sample integrity. We thank Mei Lie Wong for sectioning EM samples and Mei Lie, Michael Braunfeld, and Prabha Das for instruction on using the microscope. We also thank members of the Walter lab and Herskowitz lab for helpful discussions and encouragement.

CHAPTER 4

Lem3p, a transmembrane protein at the site of cell-cell contact, is required for efficient cell fusion during yeast mating

INTRODUCTION

Previously, we identified the first protein that appears to act at the step of plasma membrane fusion during yeast mating. Prm1p, a multispanning membrane protein, is expressed specifically during mating and localizes to the site of fusion. In the absence of Prm1p, mating partners can bring their plasma membranes into apposition but in half the cases the membranes fail to fuse. We used a *Δprm1* mutant as a sensitized background in which to search for other genes controlling this step in mating. We identified Kex2p, a Golgi-resident protease, as aiding Prm1p to promote cell fusion. Presumably, Kex2p processes a secretory pathway protein as that protein traverses the Golgi, thus activating it for a role in fusion it will fulfill upon reaching the plasma membrane. This system could bear similarity to that of hemagglutinin, a viral fusogenic protein which also undergoes processing by a Kex2p-family protease (Stieneke-Grober et al., 1992).

Yet even in a *Δprm1 Δkex2* x *Δprm1* mating, about 20% of mating pairs successfully fuse. This remaining fusion activity may depend on KEX2 in the MATα partner, but this copy of KEX2 cannot be removed without rendering the strain sterile due to lack of α-factor pheromone production (Rockwell et al., 2002). To identify downstream components of the KEX2 cell fusion pathway as well as cell fusion factors that function in parallel to PRM1 and KEX2 we screened for mutants in a MATα background that mate very poorly in the absence of PRM1 and KEX2.

RESULTS

An iterated screen for cell fusion mutants identifies LEM3

In order to identify remaining cell fusion machinery in the *Δprm1 Δkex2* x *Δprm1* mating, we used a variation of the "replica mating" strategy we had employed previously to find enhancers of *Δprm1* x *Δprm1* (Fig. 4-1A). This time, we mutagenized a MATα *Δprm1* strain and replica mated the resulting colonies to a lawn of MATa *Δprm1 Δkex2* partner. Mutants mating very poorly were isolated. The ability of these mutants to mate to a wild-type partner was tested, and those that could not were considered sterile and discarded.

We focused on the five remaining mutants with the most dramatic mating defects. Four of these mutants display a strong cell fusion phenotype as scored by microscopic examination of individual mating pairs. We attempted to clone one of the mutants, which we called "B5$^-$," by complementation of the *Δprm1 Δkex2* x B5$^-$ *Δprm1* phenotype. However, the complementing plasmids that we recovered contained PRM1 rather than candidates for wild-type B5. Therefore, we took a different approach. We converted B5$^-$ *Δprm1* to a MATa background and found that mating this mutant against itself resulted in a stronger defect and furthermore that it could no longer be complemented by PRM1-containing plasmids. Therefore, we undertook complementation cloning of B5 in the B5$^-$ *Δprm1* x B5$^-$ *Δprm1* background. We recovered a complementing plasmid bearing a genomic fragment with 6 open reading frames (ORFs). We tested these ORFs

Figure 4-1

Replica mating strategy to isolate enhancers of *Δprm1Δkex2*

(A) A *Δprm1 MATα* strain was mutagenized and plated to form colonies. Colonies were replica plated to a lawn of *Δprm1Δkex2 MATa* mating partner on a YPD plate and incubated for 8 h at 30°. The mating was then replica plated to medium selective for diploids. Mutant colonies yielding a low density of diploid papillae were identified. **(B)** Patches of wild-type, *Δprm1*, and *Δprm1 Δlem3 MATα* haploids were replica mated as above to a lawn of *Δprm1Δkex2 MATa* mating partner. The resulting diploid papillae are shown.

A

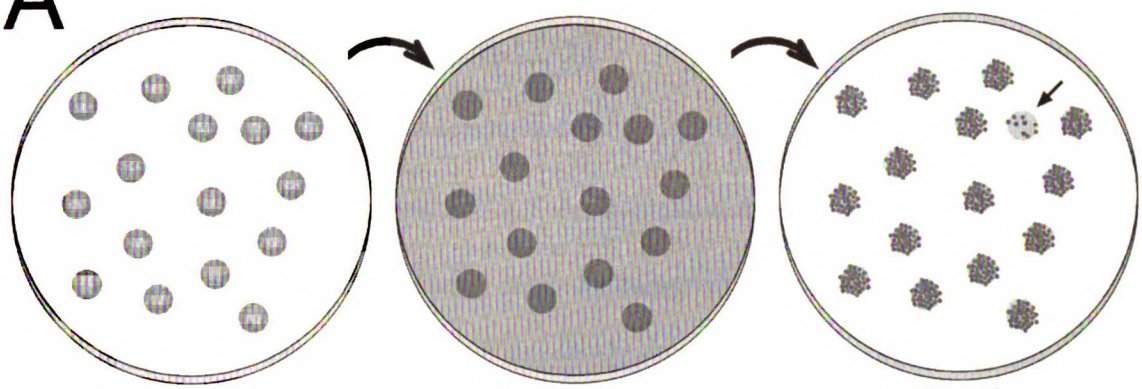

X⁻ Δ*prm1* α

X⁻ Δ*prm1* α
x Δ*prm1* Δ*kex2* a

selection
for diploids

B

Δ*prm1* Δ*kex2* a
x
WT α

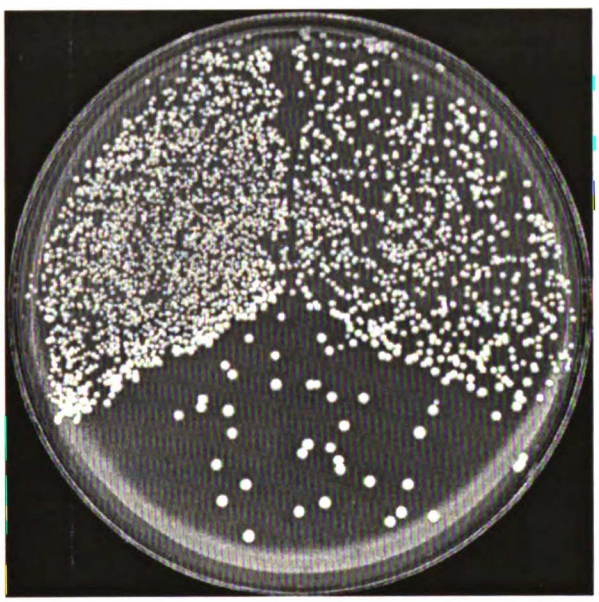

Δ*prm1* Δ*kex2* a
x
Δ*prm1* α

Δ*prm1* Δ*kex2* a
x
Δ*prm1* Δ*lem3* α

individually and by deletion from the plasmid, and found the source of the complementing activity was a gene called LEM3.

LEM3 encodes a predicted transmembrane protein. As expected, *Δlem3* mutants phenocopy the B5$^-$ mutant, and we will use the null allele *Δlem3* for the remainder of this study. Whereas *Δprm1 Δkex2* x *Δprm1* replica matings produce about 5-fold fewer diploid papillae than WT x WT, *Δprm1 Δkex2* x *Δprm1 Δlem3* replica matings produce about 100-fold fewer papillae than WT x WT (Fig. 4-1B).

Lem3p localizes to small buds and shmoo tips

A previous study has shown Lem3p to reside in the ER and plasma membrane of non-mating cells (Kato et al., 2002). To extend these studies to the context of mating, we generated a Lem3p-GFP fusion in the genome under its natural promoter, and examined its expression under both non-mating and mating conditions.

In cells grown under non-mating conditions, Lem3p-GFP localizes to small buds (Fig. 4-2A – 4-2C). This localization was not previously described. Lem3p-GFP concentrates in daughter buds with diameters less than about half the diameter of their mothers, while Lem3-GFP does not appear noticeably enriched in the plasma membrane of the mother cells or of larger buds. Lem3-GFP also appears in some newly divided cells as a streak at the presumptive bud site or, possibly, as a remnant at the site of cytokinesis (Fig. 4-2A, rightmost cell). Lem3p-GFP also marks the endoplasmic reticulum faintly, presumably reflective of recently synthesized protein.

In cells grown under conditions that mimic mating, Lem3p-GFP localizes to the tips of mating projections, or "shmoos" (Fig. 4-2D – 4-2F). Thus, Lem3p is a membrane

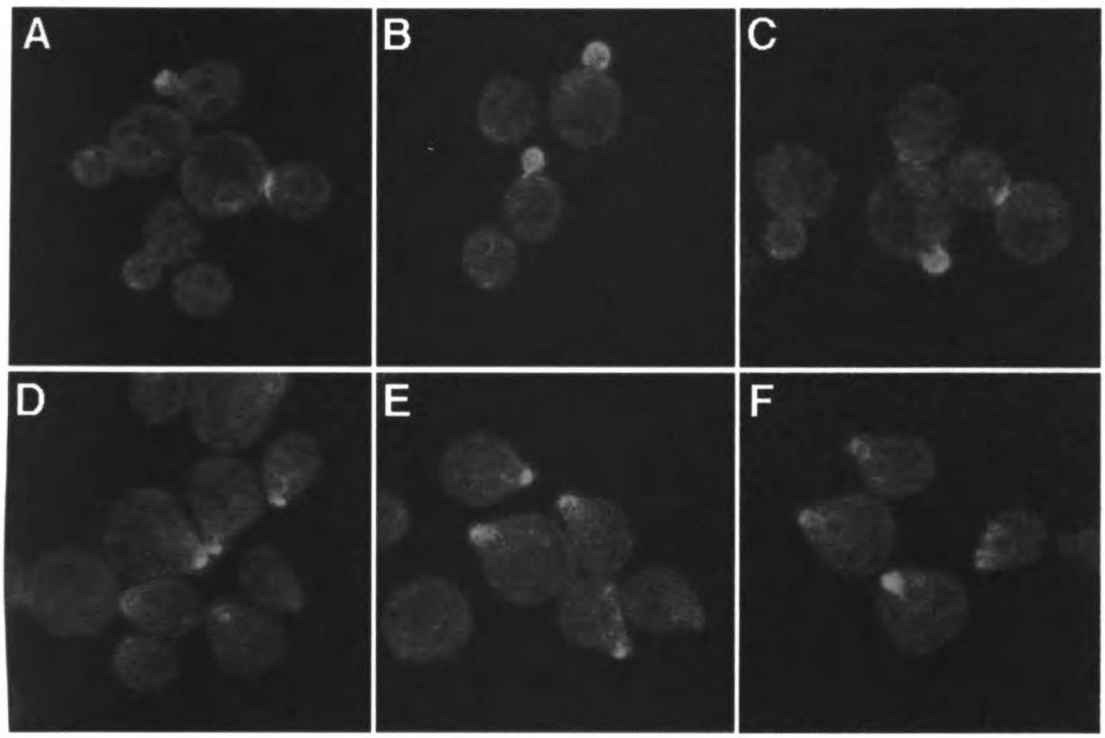

Figure 4-2

Localization of Lem3p

(A-C) A *MATa* strain bearing a *LEM3-GFP* fusion gene integrated in the genome at the LEM3 locus was taken during logarithmic vegetative growth and imaged on a confocal microscope. **(D-F)** The same strain was treated with 10 μg/ml α-factor mating pheromone for 70 min and then imaged.

protein present at the site where fusion will occur. Notably, Prm1p also localizes to daughter buds and shmoo tips.

Δlem3 and *Δkex2* display a synthetic growth defect

To further characterize the contribution to cell fusion made by LEM3, we attempted to generate double mutants between LEM3, PRM1, and KEX2 in all combinations. When we generated the *Δkex2 Δlem3* double mutant, however, we observed a strong growth defect not present in either single mutant (Fig. 4-3).

Δlem3 has previously been shown to display synthetic lethal interactions with knockouts of two genes, CDC50 and YNR048W, which encode proteins similar to Lem3p (Radji et al., 2001). The synthetic defect of *Δlem3* with *Δkex2* could be explained if Kex2p were required to process Cdc50p or Ynr048wp. However, Western blot analysis showed no change in the masses of these proteins in a *Δkex2* background compared to wild-type (not shown). We also observed no change for Lem3p itself (not shown). Thus, Lem3p and its relatives do not appear to depend on Kex2p for processing. The synthetic lethal interaction may reflect an essential function shared redundantly by the LEM3 and KEX2 pathways.

Δlem3 and *Δprm1* display a synthetic cell fusion defect

To learn whether *Δlem3* mutants affect the step of cell fusion, we employed a quantitative cell fusion assay in which we examined individual mating pairs formed by partners lacking either PRM1, LEM3, both, or neither. Because the *Δkex2 Δlem3* mutant grows very slowly, we did not include it in this assay.

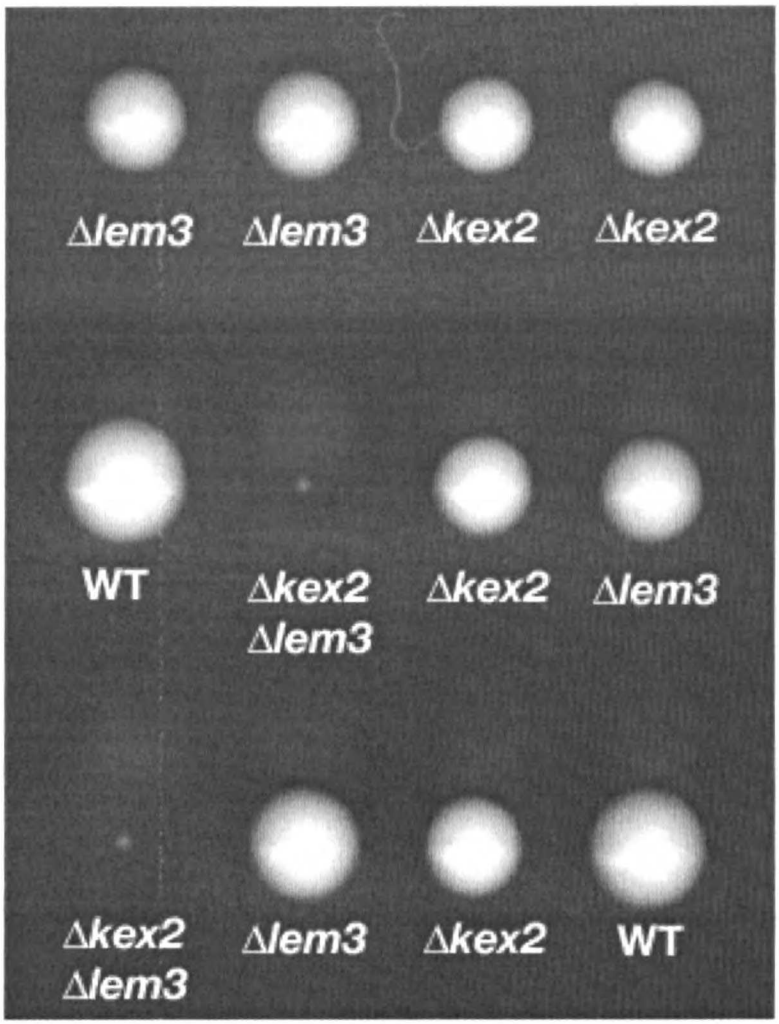

Figure 4-3

Synthetic growth defect of *Δkex2* and *Δlem3*

A *Δkex2 MATa* strain was mated to a *Δlem3 MATα* strain to construct a diploid strain bearing one copy of each deletion and one copy of each wild-type gene. This diploid strain was induced to sporulate. The resulting spore tetrads were dissected on YPD medium and incubated for about 48 h at 30° to allow each spore to form a colony. An image of the plate is shown, with spores from single tetrads arranged in rows. Subsequently, the colonies were genotyped by replica plating to media selective for markers used in the gene disruptions.

In each mating, one partner expressed soluble cytoplasmic GFP and the other did not. If cell fusion succeeded, then GFP diffused rapidly so both mating partners expressed GFP fluorescence; if cell fusion failed, then GFP remained restricted to one partner. By counting the ratio of fused mating pairs to total mating pairs, we quantitated the degree of the fusion defect produced by the lack of PRM1 or LEM3 in all combinations.

In control matings, as seen previously, the absence of PRM1 in either the MATa or MATα partner alone produced marginal effects while the absence of PRM1 in both mating partners reduced the number of fused mating pairs to about 60% (Fig. 4-4, compare crosses 1, 2, 5 and 6). By contrast, the loss of LEM3 in either mating partner alone decreased fusion to about 75%. The loss of LEM3 in both mating partners led to about 35% successful fusion (Fig. 4-4, compare crosses 1, 3, 9, and 11). Therefore, LEM3 affects mating at the step of cell fusion, and has a stronger effect than PRM1.

We next wanted to ask whether the cell fusion defects produced by *Δprm1* and *Δlem3* synergize, indicative of a shared function. We previously used a calculation in which we define a gene's "fusion contribution" to a given mating as the ratio of successful fusion with and without the gene (Table 4-1). For LEM3, then,

$$\frac{\text{WT x WT}}{\textit{Δlem3} \text{ x } \textit{Δlem3}} = \frac{\text{95\% fused mating pairs}}{\text{33\% fused mating pairs}} = \text{2.9 fusion contribution (FC) of LEM3 in a WT x WT mating}$$

Using this formula, the fusion contribution of LEM3 increases from 2.9 FC in a WT x WT mating to 10.2 FC in a *Δprm1* x *Δprm1* mating. Likewise, the contribution of PRM1

Figure 4-4

Δlem3 enhances the _Δprm1_ cell fusion defect

Logarithmically growring strains of opposite mating types bearing deletions of *PRM1*, *LEM3*, both, or neither were mixed in all combinations. In all cases, the *MATα* strain expressed soluble cytosolic GFP. This mixture was applied to a nitrocellulose filter, incubated for 3 h on a YPD plate at 30° and then fixed. Mating pairs were visually identified by microscopy and diffusion of the GFP marker was used to score successful cell fusion. Bars represent the average percent of mating pairs that scored as fused in three independent experiments. During each experiment, 300 mating pairs per mating mix were counted. All matings are written in the form *MATa* x *MATα*: WT x WT, 95 ± 1%; *WT* x *Δprm1*, 90 ± 3%; WT x *Δlem3*, 63 ± 1%; WT x *Δprm1 Δlem3*, 60 ± 2%; *Δprm1* x WT, 93 ± 2%; *Δprm1* x *Δprm1*, 61 ± 5%; *Δprm1* x *Δlem3*, 65 ± 3%, *Δprm1* x *Δprm1 Δlem3*, 36 ± 5%; *Δlem3* x WT, 74 ± 6%; *Δlem3* x *Δprm1*, 23 ± 8%; *Δlem3* x *Δlem3*, 33 ± 7%; *Δlem3* x *Δprm1 Δlem3*, 9 ± 2%; *Δprm1 Δlem3* x WT, 42 ± .4%; *Δprm1 Δlem3* x *Δprm1*, 26 ± 3%; *Δprm1 Δlem3* x *Δlem3*, 13 ± 3%; *Δprm1Δlem3* x *Δprm1 Δlem3*, 6 ± 2%.

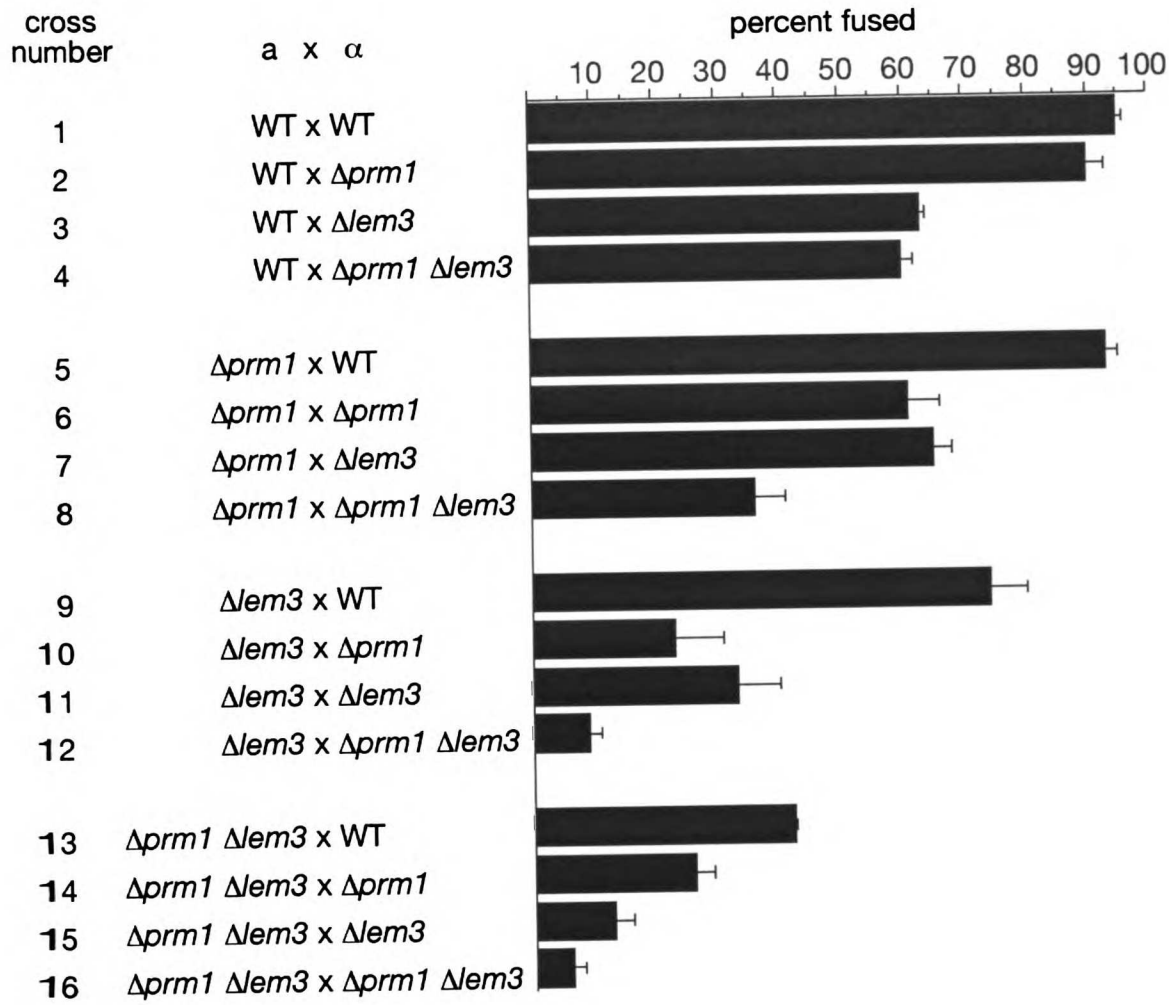
cross number
a x α
percent fused
10 20 30 40 50 60 70 80 90 100
1 WT x WT
2 WT x Δprm1
3 WT x Δlem3
4 WT x Δprm1 Δlem3
5 Δprm1 x WT
6 Δprm1 x Δprm1
7 Δprm1 x Δlem3
8 Δprm1 x Δprm1 Δlem3
9 Δlem3 x WT
10 Δlem3 x Δprm1
11 Δlem3 x Δlem3
12 Δlem3 x Δprm1 Δlem3
13 Δprm1 Δlem3 x WT
14 Δprm1 Δlem3 x Δprm1
15 Δprm1 Δlem3 x Δlem3
16 Δprm1 Δlem3 x Δprm1 Δlem3

Table 4-1

Fusion contribution (FC) of *PRM1* and *LEM3* to each mating in this study

FC of a gene to a mating is calculated as described in the text, and represents the fold decrease in percent fused mating pairs resulting from the loss of a wild-type copy of the gene in the mating. All crosses are written in the form *MATa* x *MATα*. NA, not applicable.

	PRM1 *MATa*	*PRM1* *MATα*	*LEM3* *MATa*	*LEM3* *MATα*
WT x WT	1.0	1.1	1.3	1.5
Δprm1 x WT	NA	1.5	2.2	1.4
Δlem3 x WT	1.8	3.2	NA	2.2
Δprm1 Δlem3 x WT	NA	1.6	NA	3.2
WT x *Δprm1*	1.5	NA	3.9	1.5
Δprm1 x *Δprm1*	NA	NA	2.4	1.7
Δlem3 x *Δprm1*	0.9	NA	NA	2.6
Δprm1 Δlem3 x *Δprm1*	NA	NA	NA	4.3
WT x *Δlem3*	1.0	1.1	1.9	NA
Δprm1 x *Δlem3*	NA	1.8	5.0	NA
Δlem3 x *Δlem3*	2.5	3.7	NA	NA
Δprm1 Δlem3 x *Δlem3*	NA	2.2	NA	NA
WT x *Δprm1 Δlem3*	1.7	NA	6.7	NA
Δprm1 x *Δprm1 Δlem3*	NA	NA	6.0	NA
Δlem3 x *Δprm1 Δlem3*	1.5	NA	NA	NA
Δprm1 Δlem3 x *Δprm1 Δlem3*	NA	NA	NA	NA

increases from 1.6 FC in a WT x WT mating to 5.5 FC in a *Δlem3* x *Δlem3* mating. The increased dependency on LEM3 in the absence of PRM1, and *vice versa*, indicates that these genes overlap in their function.

This synergy also occurs if only one mating partner lacks PRM1. The contribution of LEM3 increases in *Δprm1* x WT and WT x *Δprm1* matings to 7.2 FC and 10.0 FC, respectively.

However, not all combinations of *Δprm1* and *Δlem3* synergize. For example, the contribution of PRM1 to a WT MATa x *Δlem3* MATα mating is 1 FC in the MATa partner and 1.1 FC in the MATα partner, equivalent to its contribution in a WT x WT mating. However, the contribution of PRM1 to a *Δlem3* MATa x WT MATα mating is 1.8 FC in the MATa partner and 3.2 FC in the MATα partner. This mating-type specific synergy suggests a mating-type specific function for either PRM1 or LEM3.

DISCUSSION

Possible activities for Lem3p

Lem3p localizes during mating to the shmoo tip, the site where cell fusion will occur, and it is predicted to present a large extracellular loop on the cell surface. It is thus in a prime position to influence the fusion of plasma membranes. In fact, mutants lacking Lem3p frequently fail to complete the cell fusion step of mating. In the absence of Prm1p, a protein shown to affect the plasma membrane step of cell fusion, a *Δlem3* mutant becomes far less successful at fusion. This synergy suggests a cooperativity between the Prm1p and Lem3p pathways. Thus, the localization of Lem3p in the cell and the genetic behavior of a *Δlem3* mutant indicate that Lem3p may act at the plasma membrane fusion step of cell fusion.

Lem3p also acts during vegetative growth. It displays an interesting localization in non-mating conditions, becoming concentrated in the plasma membrane of the daughter bud. This localization suggests a daughter-specific function of the protein. Furthermore, in the absence of Kex2p, the loss of Lem3p provokes a large decrease in growth rate. Thus, Lem3p provides a critical function in non-mating cells which overlaps with the function of a Kex2p-dependent pathway. Lem3p also overlaps with a Kex2-dependent pathway to promote fusion. If the same Kex2p substrate is involved in both cases, it indicates that it and Lem3p share a function vital to cell fusion and to general cell health.

Previous studies have implicated Lem3p in a variety of processes. First, characterization of Cdc50p, a protein highly similar to Lem3p, indicates that Cdc50p is important for progression of the cell cycle from G1 to S and that Cdc50p may indirectly regulate transcription (Radji et al., 2001). Second, studies of Lem3p have indicated that

it can modulate transcription in a heterologous hormone-regulated gene expression system (Sitcheran et al., 2000). Third, a different study identified a *Δlem3* mutant as hypersensitive to the drug brefeldin A, suggesting impairment of membrane biogenesis or secretory function in the *Δlem3* mutant (Muren et al., 2001). Fourth, a *Δlem3* mutant appeared unable to internalize the lipids phosphatidylethanolamine (PE) and phosphatidylcholine (PC) while the transport of other lipids appeared normal (Kato et al., 2002).

If Lem3p acts transcriptionally it could send a "ready to bud!" signal from the presumptive bud site in non-mating conditions and a "ready to fuse!" signal from the shmoo tip in mating conditions. Alternatively, Lem3p may act in lipid trafficking, perhaps organizing lipids in the plasma membrane of the daughter bud during non-mating conditions and in the plasma membrane of the shmoo tip during mating conditions. The effect of Lem3p on PE and PC is especially intriguing, since transfer of these lipids away from their normal residence on the cytoplasmic leaflet of the plasma membrane bilayer could alter the curvature of the plasma membrane, an important step in bilayer fusion. Lem3p and Prm1p both associate with detergent-insoluble lipid rafts in the shmoo tip. Mutants that block raft formation also block efficient mating. The co-localization, raft association, similar phenotypes, and synergistic mutant behavior of Lem3p with Prm1p suggest that Lem3p with its single large extracellular loop may interact with Prm1p with its two large extracellular loops to form a plasma membrane complex that promotes cell fusion.

METHODS

Yeast strains and plasmids

Strains used in this study appear in Table 4-1. Gene replacements were generated with the PCR-transformation technique (Longtine et al., 1998). Strains harboring the *Δkex2* mutation were derived from Bob Fuller's strain. The plasmid pDN291, as previously described, was used to express soluble cytosolic GFP and contains the *URA3* gene (Ng and Walter, 1996). The plasmid pRS314 is a standard vector containing the *TRP1* gene, and was used in conjunction with pDN291 to create a set of mating-type-specific selectable markers (Sikorski and Hieter, 1989).

Genetic screen for enhancers of *Δprm1Δkex2*

Δprm1 URA3 MATα cells were grown to log phase, and 4 A_{600} units were washed once in 10 ml 10 mM potassium phosphate pH 7.4 (Sigma), then resuspended in same. 300 µl ethyl methane sulfonate (Sigma) was added, cells were vortexed, and incubated 30 min at 30°C. At that point, 15 ml 10% sodium thiosulfate (Sigma) were added to quench the reaction. Cells were washed twice in YPD medium and allowed to recover in YPD for 90 min at 30°C to fix any mutations that were induced. Serial dilutions of this stock were plated to medium lacking uracil and the titer of colony forming units was calculated; meanwhile the stock was kept at 4°C. For screening, the stock was plated to 100 plates lacking uracil at a density of about 120 colonies per plate. Colonies were allowed to grow for 40 h at 30°C. After about 25 h, a stationary overnight culture of *Δprm1 Δkex2::TRP1 MATa* was plated to 100 plates of YPD at 100 µl/plate and incubated at room temperature for the remaining 15 h to form lawns. These lawns were

Table 4-2

The following strains were used. All were constructed in the W303 background.

MHY425	MATa, *his3-Δ200, ura3-Δ99, leu2-Δ1, trp1-Δ99, ade2-101^{ochre}*, pRS314
MHY189	MATα, *his3-Δ200, ura3-Δ99, leu2-Δ1, trp1-Δ99, ade2-101^{ochre}*, pDN291
MHY426	MATa, *Δprm1::S.kluyveri HIS3^{+}, his3-Δ200, ura3-Δ99, leu2-Δ1, trp1-Δ99, ade2-101^{ochre}*, pRS314
MHY191	MATα, *Δprm1::S.kluyveri HIS3^{+}, his3-Δ200, ura3-Δ99, leu2-Δ1, trp1-Δ99, ade2-101^{ochre}*, pDN291
MHY398	MATa, *Δkex2::TRP1, his3-Δ200, ura3-Δ99, leu2-Δ1, trp1-Δ99, ade2-101^{ochre}*
MHY380	MATa, *Δlem3::kan^{R}, his3-Δ200, ura3-Δ99, leu2-Δ1, trp1-Δ99, ade2-101^{ochre}*, pRS314
MHY375	MATα, *Δlem3::kan^{R}, his3-Δ200, ura3-Δ99, leu2-Δ1, trp1-Δ99, ade2-101^{ochre}*, pDN291
MHY382	MATa, *Δprm1::S.kluyveri HIS3^{+}, Δlem3::kan^{R}, his3-Δ200, ura3-Δ99, leu2-Δ1, trp1-Δ99, ade2-101^{ochre}*, pRS314
MHY376	MATα, *Δprm1::S.kluyveri HIS3^{+}, Δlem3::kan^{R}, his3-Δ200, ura3-Δ99, leu2-Δ1, trp1-Δ99, ade2-101^{ochre}*, pDN291
MHY396	MATa, *LEM3-GFP:HIS3^{+}, his3-Δ200, ura3-Δ99, leu2-Δ1, trp1-Δ99, ade2-101^{ochre}*
MHY395	MATa, *LEM3-HA:HIS3^{+}, his3-Δ200, ura3-Δ99, leu2-Δ1, trp1-Δ99, ade2-101^{ochre}*
MHY397	MATa, *LEM3-HA:HIS3^{+}, Δkex2::TRP1, his3-Δ200, ura3-Δ99, leu2-Δ1, trp1-Δ99, ade2-101^{ochre}*
MHY367	MATa, *CDC50-HA:HIS3^{+}, his3-Δ200, ura3-Δ99, leu2-Δ1, trp1-Δ99, ade2-101^{ochre}*
MHY368	MATa, *CDC50-HA:HIS3^{+}, Δkex2::TRP1, his3-Δ200, ura3-Δ99, leu2-Δ1, trp1-Δ99, ade2-101^{ochre}*
MHY372	MATa, *YNR048W-HA:HIS3^{+}, Δkex2::TRP1, his3-Δ200, ura3-Δ99, leu2-Δ1, trp1-Δ99, ade2-101^{ochre}*

re-spread with 100 µl/plate water to a dull matte appearance indicative of homogeneity. Colonies were replica plated to mating lawns and incubated for 8 h at 30°C. The plates were then replica plated to media lacking tryptophan and uracil to select for diploids. Phenotypes were scored on plates incubated for 2 days at 30°C. We have noticed that the clarity of the phenotypes depends critically on having homogeneous lawns of the proper density.

Complementation of the *Δprm1Δkex2* enhancer mutation

We switched the mating type of the *Δprm1 B5⁻ MATα* enhancer mutant by transforming it with a construct that integrates a *URA3:MATa* sequences at the MAT locus, so that transformants carry a *MATα:URA3:MATa* arrangement . This strain was then grown non-selectively and plated on 5-floroorotic acid to select for loss of the *URA3* marker indicating recombination between the two MAT sequences. The resulting strains were tested individually for mating type; half of them were *MATa*. The *Δprm1 B5⁻ MATa* strain was transformed with a pRS426-based library, a gift of Sean O'Rourke, and about 7,500 transformants were subjected to replica mating assay as described above, with the *Δprm1 B5⁻ MATa* strain as partner.

Preparation of cell lysates and Western blotting

To detect expression of HA-epitope-tagged constructs, 5 ml of an exponentially growing culture at optical density of 0.5 units A_{600} was harvested, and the cell pellet was resuspended in 50 µl SDS-PAGE sample buffer, added to about 30 µl of glass beads, and lysed by continuous vortexing at 4°C for 90 s. The lysates were boiled for 10 min and

then spun to remove insoluble debris. Alternatively, for endoglycosidase H treatment, cells were lysed as above with the exception that sample buffer was replaced by 45 µl denaturation buffer as provided by the manufacturer (New England Biolabs, Beverly MA). Samples were then boiled 10 min, mixed with 5 µl G5 buffer as provided and 1 µl enzyme, incubated for 90 min at 37°C, and diluted 1:10 in SDS-PAGE sample buffer before loading. For Western blot analysis, lysates were run on a 12.5% SDS-polyacrylamide gel and transferred to nitrocellulose membrane using standard protocols. Membranes were blotted with a mouse monoclonal anti-HA primary antibody (HA.11, Covance, Princeton NJ) at 1:1000 dilution and a goat anti-mouse secondary antibody coupled to horseradish peroxidase (Bio Rad, Hercules CA) at 1:2000 dilution and developed with an enhanced chemiluminescence (ECL) kit (Renaissance kit, NEN, Boston MA).

Fluorescence microscopy of Lem3p-GFP

To visualize the localization of Lem3p-GFP, cells were grown to log phase in defined media with twice the standard concentration of adenine to prevent accumulation of autofluorescent byproducts of adenine biosynthesis. The culture was then directly imaged on a confocal microscope (Leica) or exposed to 10 mg/ml α-factor for 70 min and then imaged. Alternatively, to inspect Prm1p-GFP's localization in zygotes, cells of opposite mating types that each carried the *PRM1-GFP* fusion were grown to log phase, mixed in equal numbers, spotted on a YPD plate, and incubated for 2 h at 30°C. Cells were then resuspended from the plate, spotted on a slide, and imaged. Because the Prm1p-GFP signal was faint, a single medial optical section was first taken by averaging four high-

intensity laser scans, which bleached most of the fluorescence. Then, a stack of eight optical sections was collected to document the remaining fluorescence in the cells. This information was then used to deconvolve the high-intensity section, using OpenLab software (Improvision, Boston MA). Images were also smoothed and contrast-enhanced with this software.

Quantitative assay of cell fusion

The cell fusion assay was performed as described previously. Cells of opposite mating types, with the *MATa* strain expressing soluble cytosolic GFP, were grown overnight to log phase, 1 A_{600} unit of each were mixed, and vacuumed to a nitrocellulose filter. The filter was placed cell-side up on a YPD plate, and the plate incubated for 3 h at 30°C. Cells were then scraped off the filter, fixed in 4% paraformaldehyde, and incubated at 4°C overnight. This mixture was then spotted on a slide and observed with a confocal microscope (Leica). First, a field was selected randomly using transmission optics. Then, groups of zygotes and mating pairs within that field were identified by bright-field microscopy and subsequently scored as fused zygotes or unfused mating pairs by switching between bright-field and fluorescence. This procedure was continued until all the zygotes and mating pairs in the field were scored, at which point a new field was chosen and the procedure begun again. To capture images, a single optical section was taken by both bright-field and fluorescence microscopy. These images were then superimposed and contrast-enhanced.

ACKNOWLEDGMENTS

We would like to thank Hannah Cohen for her efforts to clone the *LEM3* mutation, design of the strategy of mating *Δprm1 B5⁻* mutants to themselves, and generation of the *Δprm1 B5⁻ MATa* strain that was ultimately used for cloning *LEM3*. We thank Pablo Aguilar for testing each ORF on the *B5⁻*-complementing plasmid individually for rescuing activity. We thank Gustavo Pesce for helpful discussions and providing mapping strains that were used in alternate strategies to clone *LEM3*. We thank the Herskowitz, O'Shea, and Madhani labs for providing strains that were to beused in other mapping strategies. We thank members of the Walter and Herskowitz labs, particularly Ira Herskowitz, for helpful discussions on cloning strategies. We thank members of the Yamamoto lab, particularly Neal Freedman and the work of Rachel Sitcheran, for providing information about *LEM3*.

CHAPTER 5

Conclusions

We have identified three proteins that promote cell fusion during yeast mating. Of the three, Prm1p is the factor most likely to act at the ultimate step of plasma membrane merger – it is expressed only during mating, it is a transmembrane protein, it localizes to the site of fusion, and in its absence membranes become apposed but do not fuse. Yet its phenotype is only weakly penetrant, meaning that its function is helpful but in most cases not necessary. Its dispensability could be because it is inherently not required or because its function is redundant with that of another factor. In either case, mutations in additional components of the fusion machinery should produce more severe phenotypes in the absence of Prm1p. We identified Kex2p and Lem3p as two such enhancers.

The clearest evidence that Kex2p and Lem3p act at the same step as Prm1p is that the loss of those factors produces much stronger phenotypes if Prm1p is absent. We have summarized this observation in the fusion contribution, or FC, of each factor, which denotes how much worse fusion becomes in the absence of a given protein. Kex2p contributes 1.2 FC to a wild-type mating but 3.4 FC to a *Δprm1* mating. The combined effects of Lem3p in both mating partners contribute 2.9 FC to a wild-type mating but about 10.2 FC to a *Δprm1* mating. These results argue against a simple "two-fusase" model where Prm1p and a redundant factor are the only fusases. Ultrastructurally as well, a *Δkex2* mating does not look like a *Δprm1* mating and indicates that we have identified multiple pathways that each play a key role in promoting cell fusion.

In a conventional model, Kex2p could biosynthetically process and thus activate a fusase. Lem3p, with its two transmembrane domains and co-localization with Prm1p, could play a direct role or could locally alter membrane curvature. We may be making a mistake, though, by thinking conventionally. If membrane fusion in yeast mating were

like viral or vesicle fusion, then a mutation that completely blocks it would most likely have surfaced in one of the many genetic screens to date. Thinking a little less conventionally, a network of protein-protein interactions may act as a fusion machine or even a "fusion web" such that loss of any few components weakens but does not destroy the meshwork. More radically, the fusase could include factors that act earlier in mating, such as mating pheromones, whose upstream roles obscure their part at the step of cell fusion. As a related hypothesis, a checkpoint could arrest cells at an earlier step of mating (like cell wall degradation) until a functional fusase assembles. Finally, fusion may not be mediated through protein-protein interactions at all but through fusogenic small molecules, like calcium (which helps to bring membranes together *in vitro*) and amphipathic molecules able to bridge the bilayers.

All this fog is wonderful or repulsive, depending on perspective. It is at the heart of what made this project exciting from its inception, the idea that membrane dynamics extend beyond the circumference of SNAREs and hemagglutinin. On the other hand, if one desires a mechanistic understanding of biology, then fuzzy meshworks and checkpoints induce only nausea. We need meaningful questions about Prm1p, Kex2p, and Lem3p in cell fusion that nevertheless do not brick us in to the conventional view of fusases: What domains of Prm1p are required for its activity? With what proteins do Prm1p and Lem3p associate? What Kex2p substrate affects fusion? Prm1p and its enhancers have given us our first molecular handles on the plasma membrane fusion step of yeast mating. With focused questions and an open mind we may now find the fusase.

APPENDIX

References

Almeida, E.A., A.P. Huovila, A.E. Sutherland, L.E. Stephens, P.G. Calarco, L.M. Shaw, A.M. Mercurio, A. Sonnenberg, P. Primakoff, D.G. Myles, and et al. 1995. Mouse egg integrin alpha 6 beta 1 functions as a sperm receptor. *Cell.* 81:1095-104.

Anna-Arriola, S.S., and I. Herskowitz. 1994. Isolation and DNA sequence of the STE13 gene encoding dipeptidyl aminopeptidase. *Yeast.* 10:801-10.

Artero, R.D., I. Castanon, and M.K. Baylies. 2001. The immunoglobulin-like protein Hibris functions as a dose-dependent regulator of myoblast fusion and is differentially controlled by Ras and Notch signaling. *Development.* 128:4251-64.

Baldan, B., J. Girard-Bascou, F.A. Wollman, and J. Olive. 1991. Evidence for thylakoid membrane fusion during zygote formation in Chlamydomonas reinhardtii. *J Cell Biol.* 114:905-15.

Beh, C.T., V. Brizzio, and M.D. Rose. 1997. KAR5 encodes a novel pheromone-inducible protein required for homotypic nuclear fusion. *J Cell Biol.* 139:1063-76.

Berlin, V., J.A. Brill, J. Trueheart, J.D. Boeke, and G.R. Fink. 1991. Genetic screens and selections for cell and nuclear fusion mutants. *Methods Enzymol.* 194:774-92.

Berteaux-Lecellier, V., M. Picard, C. Thompson-Coffe, D. Zickler, A. Panvier-Adoutte, and J.M. Simonet. 1995. A nonmammalian homolog of the PAF1 gene (Zellweger syndrome) discovered as a gene involved in caryogamy in the fungus Podospora anserina. *Cell.* 81:1043-51.

Bevan, A., C. Brenner, and R.S. Fuller. 1998. Quantitative assessment of enzyme specificity in vivo: P2 recognition by Kex2 protease defined in a genetic system. *Proc Natl Acad Sci U S A.* 95:10384-9.

Blobel, C.P., T.G. Wolfsberg, C.W. Turck, D.G. Myles, P. Primakoff, and J.M. White. 1992. A potential fusion peptide and an integrin ligand domain in a protein active in sperm-egg fusion. *Nature*. 356:248-52.

Blond, J.L., D. Lavillette, V. Cheynet, O. Bouton, G. Oriol, S. Chapel-Fernandes, B. Mandrand, F. Mallet, and F.L. Cosset. 2000. An envelope glycoprotein of the human endogenous retrovirus HERV-W is expressed in the human placenta and fuses cells expressing the type D mammalian retrovirus receptor. *J Virol.* 74:3321-9.

Bour, B.A., M. Chakravarti, J.M. West, and S.M. Abmayr. 2000. Drosophila SNS, a member of the immunoglobulin superfamily that is essential for myoblast fusion. *Genes Dev.* 14:1498-511.

Boyd, D., C. Schierle, and J. Beckwith. 1998. How many membrane proteins are there? *Protein Sci.* 7:201-5.

Brizzio, V., A.E. Gammie, G. Nijbroek, S. Michaelis, and M.D. Rose. 1996. Cell fusion during yeast mating requires high levels of a-factor mating pheromone. *J Cell Biol.* 135:1727-39.

Brizzio, V., W. Khalfan, D. Huddler, C.T. Beh, S.S. Andersen, M. Latterich, and M.D. Rose. 1999. Genetic interactions between KAR7/SEC71, KAR8/JEM1, KAR5, and KAR2 during nuclear fusion in Saccharomyces cerevisiae. *Mol Biol Cell.* 10:609-26.

Cameron, L.A., and D.L. Poccia. 1994. In vitro development of the sea urchin male pronucleus. *Dev Biol.* 162:568-78.

Cappellaro, C., K. Hauser, V. Mrsa, M. Watzele, G. Watzele, C. Gruber, and W. Tanner. 1991. Saccharomyces cerevisiae a- and alpha-agglutinin: characterization of their molecular interaction. *Embo J.* 10:4081-8.

Cappellaro, C., V. Mrsa, and W. Tanner. 1998. New potential cell wall glucanases of Saccharomyces cerevisiae and their involvement in mating. *J Bacteriol.* 180:5030-7.

Chen, E.H., and E.N. Olson. 2001. Antisocial, an intracellular adaptor protein, is required for myoblast fusion in Drosophila. *Dev Cell.* 1:705-15.

Chen, M.S., K.S. Tung, S.A. Coonrod, Y. Takahashi, D. Bigler, A. Chang, Y. Yamashita, P.W. Kincade, J.C. Herr, and J.M. White. 1999. Role of the integrin-associated protein CD9 in binding between sperm ADAM 2 and the egg integrin alpha6beta1: implications for murine fertilization. *Proc Natl Acad Sci U S A.* 96:11830-5.

Chen, P., S.K. Sapperstein, J.D. Choi, and S. Michaelis. 1997. Biogenesis of the Saccharomyces cerevisiae mating pheromone a-factor. *J Cell Biol.* 136:251-69.

Chenevert, J., N. Valtz, and I. Herskowitz. 1994. Identification of genes required for normal pheromone-induced cell polarization in Saccharomyces cerevisiae. *Genetics.* 136:1287-96.

Chikashige, Y., D.Q. Ding, Y. Imai, M. Yamamoto, T. Haraguchi, and Y. Hiraoka. 1997. Meiotic nuclear reorganization: switching the position of centromeres and telomeres in the fission yeast Schizosaccharomyces pombe. *Embo J.* 16:193-202.

Cho, C., D.O. Bunch, J.E. Faure, E.H. Goulding, E.M. Eddy, P. Primakoff, and D.G. Myles. 1998. Fertilization defects in sperm from mice lacking fertilin beta. *Science*. 281:1857-9.

Cho, C., H. Ge, D. Branciforte, P. Primakoff, and D.G. Myles. 2000. Analysis of mouse fertilin in wild-type and fertilin beta(-/-) sperm: evidence for C-terminal modification, alpha/beta dimerization, and lack of essential role of fertilin alpha in sperm-egg fusion. *Dev Biol.* 222:289-95.

Christensen, M., A. Estevez, X. Yin, R. Fox, R. Morrison, M. McDonnell, C. Gleason, D.M. Miller, 3rd, and K. Strange. 2002. A primary culture system for functional analysis of C. elegans neurons and muscle cells. *Neuron.* 33:503-14.

Cohen, D.J., D.A. Ellerman, D. Busso, M.M. Morgenfeld, A.D. Piazza, M. Hayashi, E.T. Young, M. Kasahara, and P.S. Cuasnicu. 2001. Evidence that human epididymal protein ARP plays a role in gamete fusion through complementary sites on the surface of the human egg. *Biol Reprod.* 65:1000-5.

Cohen, D.J., D.A. Ellerman, and P.S. Cuasnicu. 2000. Mammalian sperm-egg fusion: evidence that epididymal protein DE plays a role in mouse gamete fusion. *Biol Reprod.* 63:462-8.

Cole, E.S., and T.A. Soelter. 1997. A mutational analysis of conjugation in Tetrahymena thermophila. 2. Phenotypes affecting middle and late development: third prezygotic nuclear division, pronuclear exchange, pronuclear fusion, and postzygotic development. *Dev Biol.* 189:233-45.

Coonrod, S., S. Naaby-Hansen, J. Shetty, and J. Herr. 1999a. PI-PLC releases a 25-40 kDa protein cluster from the hamster oolemma and affects the sperm penetration assay. *Mol Hum Reprod.* 5:1027-33.

Coonrod, S.A., S. Naaby-Hansen, J. Shetty, H. Shibahara, M. Chen, J.M. White, and J.C. Herr. 1999b. Treatment of mouse oocytes with PI-PLC releases 70-kDa (pI 5) and 35- to 45-kDa (pI 5.5) protein clusters from the egg surface and inhibits sperm-oolemma binding and fusion. *Dev Biol.* 207:334-49.

Corpet, F. 1988. Multiple sequence alignment with hierarchical clustering. *Nucleic Acids Res.* 16:10881-90.

Costanzo, M.C., J.D. Hogan, M.E. Cusick, B.P. Davis, A.M. Fancher, P.E. Hodges, P. Kondu, C. Lengieza, J.E. Lew-Smith, C. Lingner, K.J. Roberg-Perez, M. Tillberg, J.E. Brooks, and J.I. Garrels. 2000. The yeast proteome database (YPD) and Caenorhabditis elegans proteome database (WormPD): comprehensive resources for the organization and comparison of model organism protein information. *Nucleic Acids Res.* 28:73-6.

Cuasnicu, P.S., D.A. Ellerman, D.J. Cohen, D. Busso, M.M. Morgenfeld, and V.G. Da Ros. 2001. Molecular mechanisms involved in mammalian gamete fusion. *Arch Med Res.* 32:614-8.

DeLange, A.M., and A.J. Griffiths. 1980. Meiosis in Neurospora crassa. II. Genetic and cytological characterization of three meiotic mutants. *Genetics.* 96:379-98.

Dimmer, K.S., S. Fritz, F. Fuchs, M. Messerschmitt, N. Weinbach, W. Neupert, and B. Westermann. 2002. Genetic basis of mitochondrial function and morphology in Saccharomyces cerevisiae. *Mol Biol Cell.* 13:847-53.

Doberstein, S.K., R.D. Fetter, A.Y. Mehta, and C.S. Goodman. 1997. Genetic analysis of myoblast fusion: blown fuse is required for progression beyond the prefusion complex. *J Cell Biol.* 136:1249-61.

Dworak, H.A., M.A. Charles, L.B. Pellerano, and H. Sink. 2001. Characterization of Drosophila hibris, a gene related to human nephrin. *Development.* 128:4265-76.

Dworak, H.A., and H. Sink. 2002. Myoblast fusion in Drosophila. *Bioessays.* 24:591-601.

Elia, L., and L. Marsh. 1996. Role of the ABC transporter Ste6 in cell fusion during yeast conjugation. *J Cell Biol.* 135:741-51.

Elia, L., and L. Marsh. 1998. A role for a protease in morphogenic responses during yeast cell fusion. *J Cell Biol.* 142:1473-85.

Ellerman, D.A., V.G. Da Ros, D.J. Cohen, D. Busso, M.M. Morgenfeld, and P.S. Cuasnicu. 2002. Expression and structure-function analysis of de, a sperm cysteine-rich secretory protein that mediates gamete fusion. *Biol Reprod.* 67:1225-31.

Erdman, S., L. Lin, M. Malczynski, and M. Snyder. 1998. Pheromone-regulated genes required for yeast mating differentiation. *J Cell Biol.* 140:461-83.

Evans, J.P. 2001. Fertilin beta and other ADAMs as integrin ligands: insights into cell adhesion and fertilization. *Bioessays.* 23:628-39.

Evans, J.P., and H.M. Florman. 2002. The state of the union: the cell biology of fertilization. *Nat Cell Biol.* 4 Suppl:s57-63.

Fritz, S., D. Rapaport, E. Klanner, W. Neupert, and B. Westermann. 2001. Connection of the mitochondrial outer and inner membranes by Fzo1 is critical for organellar fusion. *J Cell Biol.* 152:683-92.

Fuller, R.S., A. Brake, and J. Thorner. 1989. Yeast prohormone processing enzyme (KEX2 gene product) is a Ca2+-dependent serine protease. *Proc Natl Acad Sci U S A.* 86:1434-8.

Gammie, A.E., V. Brizzio, and M.D. Rose. 1998. Distinct morphological phenotypes of cell fusion mutants. *Mol Biol Cell.* 9:1395-410.

Gluschankof, P., and R.S. Fuller. 1994. A C-terminal domain conserved in precursor processing proteases is required for intramolecular N-terminal maturation of pro-Kex2 protease. *Embo J.* 13:2280-8.

Hackstein, J.H. 1991. Spermatogenesis in Drosophila. A genetic approach to cellular and subcellular differentiation. *Eur J Cell Biol.* 56:151-69.

Hakeda-Suzuki, S., J. Ng, J. Tzu, G. Dietzl, Y. Sun, M. Harms, T. Nardine, L. Luo, and B.J. Dickson. 2002. Rac function and regulation during Drosophila development. *Nature.* 416:438-42.

Hales, K.G., and M.T. Fuller. 1997. Developmentally regulated mitochondrial fusion mediated by a conserved, novel, predicted GTPase. *Cell.* 90:121-9.

Han, X., H. Sterling, Y. Chen, C. Saginario, E.J. Brown, W.A. Frazier, F.P. Lindberg, and A. Vignery. 2000. CD47, a ligand for the macrophage fusion receptor, participates in macrophage multinucleation. *J Biol Chem.* 275:37984-92.

Harbury, P.A. 1998. Springs and zippers: coiled coils in SNARE-mediated membrane fusion. *Structure.* 6:1487-91.

Heiman, M.G., and P. Walter. 2000. Prm1p, a pheromone-regulated multispanning membrane protein, facilitates plasma membrane fusion during yeast mating. *J Cell Biol.* 151:719-30.

Hemler, M.E. 2001. Specific tetraspanin functions. *J Cell Biol.* 155:1103-7.

Hermann, G.J., J.W. Thatcher, J.P. Mills, K.G. Hales, M.T. Fuller, J. Nunnari, and J.M. Shaw. 1998. Mitochondrial fusion in yeast requires the transmembrane GTPase Fzo1p. *J Cell Biol.* 143:359-73.

Hernandez, L.D., L.R. Hoffman, T.G. Wolfsberg, and J.M. White. 1996. Virus-cell and cell-cell fusion. *Annu Rev Cell Dev Biol.* 12:627-61.

Herskowitz, I. 1995. MAP kinase pathways in yeast: for mating and more. *Cell.* 80:187-97.

Hirokawa, T., S. Boon-Chieng, and S. Mitaku. 1998. SOSUI: classification and secondary structure prediction system for membrane proteins. *Bioinformatics.* 14:378-9.

Hodor, P.G., and C.A. Ettensohn. 1998. The dynamics and regulation of mesenchymal cell fusion in the sea urchin embryo. *Dev Biol.* 199:111-24.

Hughson, F.M. 1995. Structural characterization of viral fusion proteins. *Curr Biol.* 5:265-74.

Huovila, A.P., E.A. Almeida, and J.M. White. 1996. ADAMs and cell fusion. *Curr Opin Cell Biol.* 8:692-9.

Hwa, J.J., M.A. Hiller, M.T. Fuller, and A. Santel. 2002. Differential expression of the Drosophila mitofusin genes fuzzy onions (fzo) and dmfn. *Mech Dev.* 116:213-6.

Isaksen, D.E., N.J. Liu, and D.A. Weisblat. 1999. Inductive regulation of cell fusion in leech. *Development.* 126:3381-90.

Isenmann, S., Y. Khew-Goodall, J. Gamble, M. Vadas, and B.W. Wattenberg. 1998. A splice-isoform of vesicle-associated membrane protein-1 (VAMP-1) contains a mitochondrial targeting signal. *Mol Biol Cell.* 9:1649-60.

Iwamatsu, T., and H. Kobayashi. 2002. Electron microscopic observations of karyogamy in the fish egg. *Dev Growth Differ.* 44:357-63.

Jahn, R., and H. Grubmuller. 2002. Membrane fusion. *Curr Opin Cell Biol.* 14:488-95.

Jenness, D.D., A.C. Burkholder, and L.H. Hartwell. 1983. Binding of alpha-factor pheromone to yeast a cells: chemical and genetic evidence for an alpha-factor receptor. *Cell.* 35:521-9.

Jensen, R.E., and A.E. Johnson. 1999. Protein translocation: is Hsp70 pulling my chain? *Curr Biol.* 9:R779-82.

Johnson, A.E., and M.A. van Waes. 1999. The translocon: a dynamic gateway at the ER membrane. *Annu Rev Cell Dev Biol.* 15:799-842.

Julius, D., L. Blair, A. Brake, G. Sprague, and J. Thorner. 1983. Yeast alpha factor is processed from a larger precursor polypeptide: the essential role of a membrane-bound dipeptidyl aminopeptidase. *Cell.* 32:839-52.

Kaji, K., S. Oda, T. Shikano, T. Ohnuki, Y. Uematsu, J. Sakagami, N. Tada, S. Miyazaki, and A. Kudo. 2000. The gamete fusion process is defective in eggs of Cd9-deficient mice. *Nat Genet.* 24:279-82.

Kato, U., K. Emoto, C. Fredriksson, H. Nakamura, A. Ohta, T. Kobayashi, K. Murakami-Murofushi, and M. Umeda. 2002. A novel membrane protein, Ros3p, is required for phospholipid translocation across the plasma membrane in Saccharomyces cerevisiae. *J Biol Chem.* 277:37855-62.

Kawai, A., S. Nishikawa, A. Hirata, and T. Endo. 2001. Loss of the mitochondrial Hsp70 functions causes aggregation of mitochondria in yeast cells. *J Cell Sci.* 114:3565-74.

Kemble, G.W., T. Danieli, and J.M. White. 1994. Lipid-anchored influenza hemagglutinin promotes hemifusion, not complete fusion. *Cell.* 76:383-91.

Komano, H., and R.S. Fuller. 1995. Shared functions in vivo of a glycosyl-phosphatidylinositol-linked aspartyl protease, Mkc7, and the proprotein processing protease Kex2 in yeast. *Proc Natl Acad Sci U S A.* 92:10752-6.

Kurihara, L.J., C.T. Beh, M. Latterich, R. Schekman, and M.D. Rose. 1994. Nuclear congression and membrane fusion: two distinct events in the yeast karyogamy pathway. *J Cell Biol.* 126:911-23.

Latchinian-Sadek, L., and D.Y. Thomas. 1993. Expression, purification, and characterization of the yeast KEX1 gene product, a polypeptide precursor processing carboxypeptidase. *J Biol Chem.* 268:534-40.

Latterich, M., K.U. Frohlich, and R. Schekman. 1995. Membrane fusion and the cell cycle: Cdc48p participates in the fusion of ER membranes. *Cell.* 82:885-93.

Le Naour, F., E. Rubinstein, C. Jasmin, M. Prenant, and C. Boucheix. 2000. Severely reduced female fertility in CD9-deficient mice. *Science.* 287:319-21.

Lefebvre, P.A., and C.D. Silflow. 1999. Chlamydomonas: the cell and its genomes. *Genetics.* 151:9-14.

Longo, F.J., and E. Anderson. 1968. The fine structure of pronuclear development and fusion in the sea urchin, Arbacia punctulata. *J Cell Biol.* 39:339-68.

Longtine, M.S., A. McKenzie, 3rd, D.J. Demarini, N.G. Shah, A. Wach, A. Brachat, P. Philippsen, and J.R. Pringle. 1998. Additional modules for versatile and economical PCR-based gene deletion and modification in Saccharomyces cerevisiae. *Yeast.* 14:953-61.

Margolin, W. 2003. Bacterial division: the fellowship of the ring. *Curr Biol.* 13:R16-8.

Martin, I., and J.M. Ruysschaert. 1997. Comparison of lipid vesicle fusion induced by the putative fusion peptide of fertilin (a protein active in sperm-egg fusion) and the NH2-terminal domain of the HIV2 gp41. *FEBS Lett.* 405:351-5.

McClellan, A.J., J.B. Endres, J.P. Vogel, D. Palazzi, M.D. Rose, and J.L. Brodsky. 1998. Specific molecular chaperone interactions and an ATP-dependent conformational change are required during posttranslational protein translocation into the yeast ER. *Mol Biol Cell.* 9:3533-45.

McDonald, K. 1999. High-pressure freezing for preservation of high resolution fine structure and antigenicity for immunolabeling. *Methods Mol Biol.* 117:77-97.

Menon, S.D., and W. Chia. 2001. Drosophila rolling pebbles: a multidomain protein required for myoblast fusion that recruits D-Titin in response to the myoblast attractant Dumbfounded. *Dev Cell.* 1:691-703.

Mi, S., X. Lee, X. Li, G.M. Veldman, H. Finnerty, L. Racie, E. LaVallie, X.Y. Tang, P. Edouard, S. Howes, J.C. Keith, Jr., and J.M. McCoy. 2000. Syncytin is a captive retroviral envelope protein involved in human placental morphogenesis. *Nature.* 403:785-9.

Miller, B.J., E. Georges-Labouesse, P. Primakoff, and D.G. Myles. 2000. Normal fertilization occurs with eggs lacking the integrin alpha6beta1 and is CD9-dependent. *J Cell Biol.* 149:1289-96.

Miyado, K., G. Yamada, S. Yamada, H. Hasuwa, Y. Nakamura, F. Ryu, K. Suzuki, K. Kosai, K. Inoue, A. Ogura, M. Okabe, and E. Mekada. 2000. Requirement of CD9 on the egg plasma membrane for fertilization. *Science.* 287:321-4.

Mohler, W.A., G. Shemer, J.J. del Campo, C. Valansi, E. Opoku-Serebuoh, V. Scranton, N. Assaf, J.G. White, and B. Podbilewicz. 2002. The type I membrane protein EFF-1 is essential for developmental cell fusion. *Dev Cell.* 2:355-62.

Mohler, W.A., J.S. Simske, E.M. Williams-Masson, J.D. Hardin, and J.G. White. 1998. Dynamics and ultrastructure of developmental cell fusions in the Caenorhabditis elegans hypodermis. *Curr Biol.* 8:1087-90.

Mrsa, V., T. Seidl, M. Gentzsch, and W. Tanner. 1997. Specific labelling of cell wall proteins by biotinylation. Identification of four covalently linked O-mannosylated proteins of Saccharomyces cerevisiae. *Yeast.* 13:1145-54.

Muga, A., W. Neugebauer, T. Hirama, and W.K. Surewicz. 1994. Membrane interaction and conformational properties of the putative fusion peptide of PH-30, a protein active in sperm-egg fusion. *Biochemistry.* 33:4444-8.

Muren, E., M. Oyen, G. Barmark, and H. Ronne. 2001. Identification of yeast deletion strains that are hypersensitive to brefeldin A or monensin, two drugs that affect intracellular transport. *Yeast.* 18:163-72.

Myles, D.G., L.H. Kimmel, C.P. Blobel, J.M. White, and P. Primakoff. 1994. Identification of a binding site in the disintegrin domain of fertilin required for sperm-egg fusion. *Proc Natl Acad Sci U S A.* 91:4195-8.

Ng, D.T., and P. Walter. 1996. ER membrane protein complex required for nuclear fusion. *J Cell Biol.* 132:499-509.

Nishikawa, S., and T. Endo. 1997. The yeast JEM1p is a DnaJ-like protein of the endoplasmic reticulum membrane required for nuclear fusion. *J Biol Chem.* 272:12889-92.

Nishikawa, S., and T. Endo. 1998. Reinvestigation of the functions of the hydrophobic segment of Jem1p, a yeast endoplasmic reticulum membrane protein mediating nuclear fusion. *Biochem Biophys Res Commun.* 244:785-9.

Nishimura, H., C. Cho, D.R. Branciforte, D.G. Myles, and P. Primakoff. 2001. Analysis of loss of adhesive function in sperm lacking cyritestin or fertilin beta. *Dev Biol.* 233:204-13.

O'Rourke, S.M., and I. Herskowitz. 2002. A third osmosensing branch in Saccharomyces cerevisiae requires the Msb2 protein and functions in parallel with the Sho1 branch. *Mol Cell Biol.* 22:4739-49.

Ozier-Kalogeropoulos, O., A. Malpertuy, J. Boyer, F. Tekaia, and B. Dujon. 1998. Random exploration of the Kluyveromyces lactis genome and comparison with that of Saccharomyces cerevisiae. *Nucleic Acids Res.* 26:5511-24.

Paululat, A., A. Goubeaud, C. Damm, S. Knirr, S. Burchard, and R. Renkawitz-Pohl. 1997. The mesodermal expression of rolling stone (rost) is essential for myoblast

fusion in Drosophila and encodes a potential transmembrane protein. *J Cell Biol.* 138:337-48.

Paululat, A., A. Holz, and R. Renkawitz-Pohl. 1999. Essential genes for myoblast fusion in Drosophila embryogenesis. *Mech Dev.* 83:17-26.

Peters, C., M.J. Bayer, S. Buhler, J.S. Andersen, M. Mann, and A. Mayer. 2001. Trans-complex formation by proteolipid channels in the terminal phase of membrane fusion. *Nature.* 409:581-8.

Potgens, A.J., U. Schmitz, P. Bose, A. Versmold, P. Kaufmann, and H.G. Frank. 2002. Mechanisms of syncytial fusion: a review. *Placenta.* 23 Suppl A:S107-13.

Primakoff, P., H. Hyatt, and J. Tredick-Kline. 1987. Identification and purification of a sperm surface protein with a potential role in sperm-egg membrane fusion. *J Cell Biol.* 104:141-9.

Primakoff, P., and D.G. Myles. 2002. Penetration, adhesion, and fusion in mammalian sperm-egg interaction. *Science.* 296:2183-5.

Qiao, H., R.T. Armstrong, G.B. Melikyan, F.S. Cohen, and J.M. White. 1999. A specific point mutant at position 1 of the influenza hemagglutinin fusion peptide displays a hemifusion phenotype. *Mol Biol Cell.* 10:2759-69.

Radji, M., J.M. Kim, T. Togan, H. Yoshikawa, and K. Shirahige. 2001. The cloning and characterization of the CDC50 gene family in Saccharomyces cerevisiae. *Yeast.* 18:195-205.

Ramalho-Santos, J., and M.C. de Lima. 1998. The influenza virus hemagglutinin: a model protein in the study of membrane fusion. *Biochim Biophys Acta.* 1376:147-54.

Rapaport, D., M. Brunner, W. Neupert, and B. Westermann. 1998. Fzo1p is a mitochondrial outer membrane protein essential for the biogenesis of functional mitochondria in Saccharomyces cerevisiae. *J Biol Chem.* 273:20150-5.

Rau, A., D. Buttgereit, A. Holz, R. Fetter, S.K. Doberstein, A. Paululat, N. Staudt, J. Skeath, A.M. Michelson, and R. Renkawitz-Pohl. 2001. rolling pebbles (rols) is required in Drosophila muscle precursors for recruitment of myoblasts for fusion. *Development.* 128:5061-73.

Robinson, D.N., and J.A. Spudich. 2000. Towards a molecular understanding of cytokinesis. *Trends Cell Biol.* 10:228-37.

Rockwell, N.C., and R.S. Fuller. 1998. Interplay between S1 and S4 subsites in Kex2 protease: Kex2 exhibits dual specificity for the P4 side chain. *Biochemistry.* 37:3386-91.

Rockwell, N.C., D.J. Krysan, T. Komiyama, and R.S. Fuller. 2002. Precursor processing by kex2/furin proteases. *Chem Rev.* 102:4525-48.

Rockwell, N.C., G.T. Wang, G.A. Krafft, and R.S. Fuller. 1997. Internally consistent libraries of fluorogenic substrates demonstrate that Kex2 protease specificity is generated by multiple mechanisms. *Biochemistry.* 36:1912-7.

Rojo, M., F. Legros, D. Chateau, and A. Lombes. 2002. Membrane topology and mitochondrial targeting of mitofusins, ubiquitous mammalian homologs of the transmembrane GTPase Fzo. *J Cell Sci.* 115:1663-74.

Rose, M.D. 1996. Nuclear fusion in the yeast Saccharomyces cerevisiae. *Annu Rev Cell Dev Biol.* 12:663-95.

Ruiz-Gomez, M., N. Coutts, A. Price, M.V. Taylor, and M. Bate. 2000. Drosophila dumbfounded: a myoblast attractant essential for fusion. *Cell.* 102:189-98.

Santos, B., A. Duran, and M.H. Valdivieso. 1997. CHS5, a gene involved in chitin synthesis and mating in Saccharomyces cerevisiae. *Mol Cell Biol.* 17:2485-96.

Sesaki, H., and R.E. Jensen. 2001. UGO1 encodes an outer membrane protein required for mitochondrial fusion. *J Cell Biol.* 152:1123-34.

Sever, S., H. Damke, and S.L. Schmid. 2000. Garrotes, springs, ratchets, and whips: putting dynamin models to the test. *Traffic.* 1:385-92.

Shemer, G., and B. Podbilewicz. 2000. Fusomorphogenesis: cell fusion in organ formation. *Dev Dyn.* 218:30-51.

Sikorski, R.S., and P. Hieter. 1989. A system of shuttle vectors and yeast host strains designed for efficient manipulation of DNA in Saccharomyces cerevisiae. *Genetics.* 122:19-27.

Simons, J.F., S. Ferro-Novick, M.D. Rose, and A. Helenius. 1995. BiP/Kar2p serves as a molecular chaperone during carboxypeptidase Y folding in yeast. *J Cell Biol.* 130:41-9.

Singh, M., B. Berger, and P.S. Kim. 1999. LearnCoil-VMF: computational evidence for coiled-coil-like motifs in many viral membrane-fusion proteins. *J Mol Biol.* 290:1031-41.

Sitcheran, R., R. Emter, A. Kralli, and K.R. Yamamoto. 2000. A genetic analysis of glucocorticoid receptor signaling. Identification and characterization of ligand-effect modulators in Saccharomyces cerevisiae. *Genetics.* 156:963-72.

Skehel, J.J., and D.C. Wiley. 2000. Receptor binding and membrane fusion in virus entry: the influenza hemagglutinin. *Annu Rev Biochem.* 69:531-69.

Spellman, P.T., G. Sherlock, M.Q. Zhang, V.R. Iyer, K. Anders, M.B. Eisen, P.O. Brown, D. Botstein, and B. Futcher. 1998. Comprehensive identification of cell cycle-regulated genes of the yeast Saccharomyces cerevisiae by microarray hybridization. *Mol Biol Cell.* 9:3273-97.

Stieneke-Grober, A., M. Vey, H. Angliker, E. Shaw, G. Thomas, C. Roberts, H.D. Klenk, and W. Garten. 1992. Influenza virus hemagglutinin with multibasic cleavage site is activated by furin, a subtilisin-like endoprotease. *Embo J.* 11:2407-14.

Strunkelnberg, M., B. Bonengel, L.M. Moda, A. Hertenstein, H.G. de Couet, R.G. Ramos, and K.F. Fischbach. 2001. rst and its paralogue kirre act redundantly during embryonic muscle development in Drosophila. *Development.* 128:4229-39.

Sutton, R.B., D. Fasshauer, R. Jahn, and A.T. Brunger. 1998. Crystal structure of a SNARE complex involved in synaptic exocytosis at 2.4 A resolution. *Nature.* 395:347-53.

Tachibana, I., and M.E. Hemler. 1999. Role of transmembrane 4 superfamily (TM4SF) proteins CD9 and CD81 in muscle cell fusion and myotube maintenance. *J Cell Biol.* 146:893-904.

Talbot, P., B.D. Shur, and D.G. Myles. 2003. Cell adhesion and fertilization: steps in oocyte transport, sperm-zona pellucida interactions, and sperm-egg fusion. *Biol Reprod.* 68:1-9.

Tange, Y., T. Horio, M. Shimanuki, D.Q. Ding, Y. Hiraoka, and O. Niwa. 1998. A novel fission yeast gene, tht1+, is required for the fusion of nuclear envelopes during karyogamy. *J Cell Biol.* 140:247-58.

Taylor, M.V. 2000. Muscle development: molecules of myoblast fusion. *Curr Biol.* 10:R646-8.

Thompson-Coffe, C., and D. Zickler. 1994. How the cytoskeleton recognizes and sorts nuclei of opposite mating type during the sexual cycle in filamentous ascomycetes. *Dev Biol.* 165:257-71.

Trueheart, J., J.D. Boeke, and G.R. Fink. 1987. Two genes required for cell fusion during yeast conjugation: evidence for a pheromone-induced surface protein. *Mol Cell Biol.* 7:2316-28.

Weber, T., B.V. Zemelman, J.A. McNew, B. Westermann, M. Gmachl, F. Parlati, T.H. Sollner, and J.E. Rothman. 1998. SNAREpins: minimal machinery for membrane fusion. *Cell.* 92:759-72.

White, J.M., and M.D. Rose. 2001. Yeast mating: getting close to membrane merger. *Curr Biol.* 11:R16-20.

Whyte, J.R., and S. Munro. 2002. Vesicle tethering complexes in membrane traffic. *J Cell Sci.* 115:2627-37.

Wilson, I.A., J.J. Skehel, and D.C. Wiley. 1981. Structure of the haemagglutinin membrane glycoprotein of influenza virus at 3 A resolution. *Nature.* 289:366-73.

Wong, E.D., J.A. Wagner, S.W. Gorsich, J.M. McCaffery, J.M. Shaw, and J. Nunnari. 2000. The dynamin-related GTPase, Mgm1p, is an intermembrane space protein

required for maintenance of fusion competent mitochondria. *J Cell Biol.* 151:341-52.

Young, B.P., R.A. Craven, P.J. Reid, M. Willer, and C.J. Stirling. 2001. Sec63p and Kar2p are required for the translocation of SRP-dependent precursors into the yeast endoplasmic reticulum in vivo. *Embo J.* 20:262-71.

Yuan, Y.L., and S. Fields. 1991. Properties of the DNA-binding domain of the Saccharomyces cerevisiae STE12 protein. *Mol Cell Biol.* 11:5910-8.

Zhu, G.Z., B.J. Miller, C. Boucheix, E. Rubinstein, C.C. Liu, R.O. Hynes, D.G. Myles, and P. Primakoff. 2002. Residues SFQ (173-175) in the large extracellular loop of CD9 are required for gamete fusion. *Development.* 129:1995-2002.

Zhu, X., and J.P. Evans. 2002. Analysis of the roles of RGD-binding integrins, alpha(4)/alpha(9) integrins, alpha(6) integrins, and CD9 in the interaction of the fertilin beta (ADAM2) disintegrin domain with the mouse egg membrane. *Biol Reprod.* 66:1193-202.